U R A N I U M P L A N T I D E N T I F I C A T I O N

U S I N G C O R R E L A T I O N M E T H O D S

M Braae

Submitted in fulfillment of the requirements for the degree of M.Sc. (Eng)
Faculty of Engineering University of Cape Town

September 1974

ACKNOWLEDGEMENTS

To Mr.S.G.McLaren for his encouragement and guidance.

To Dr.G.S.Hansford and Dr.D.N.Swingler for those enlightening discussions.

To the National Institute for Metallurgy for their financial and technical support.

SUMMARY

Theory relating to identification of an uranium plant using on-line correlation techniques is described. Generation and properties of pseudo-random ternary m-sequences are discussed, particular attention being given to selection of a suitable sequence for testing a system.

The geometry and control policy of the uranium plant is outlined and existing and experimental equipment required for realizing perturbation of the plant is considered. A theoretical model of the plant is studied to detect effects that might adversely affect the experimental results.

Programs written to evaluate correlation functions and for general data handling are briefly outlined.

The pseudo-random ternary m-sequence noise is selected with reference to the plant characteristics as deduced from plant records. Results of pilot tests enabled the pseudo-noise to be correctly selected for the main test. All tests and their results are briefly described.

Finally, the analytic and empiric models of the plant are derived and the validity of the model obtained from the correlation method is tested by comparing theoretical predictions with experimental observations.

LIST OF CONTENTS

INTRODUCTION

The recent development of an economic on-line uranium analyser by the National Institute for Metallurgy provides the necessary instrumentation for implementing continuous automatic control of the extraction section of an uranium extraction plant. For any control system to be successful the effects of variations in the system inputs on the output have to be known [16] and the problem considered in this thesis is the derivation of a dynamic model of the multi-stage liquid-liquid extraction process in an uranium plant using on-line correlation techniques.

Review of Mixer-Settler Models

Although liquid-liquid extraction is one of the oldest industrial processes, few mathematical models, based on fundamental conservation laws, have been derived which successfully describe its dynamic behaviour. Publications on the subject suggest that the problem has mainly been of academic interest in the past which is probably due to the physical complexity of industrial systems and the lack of available instrumentation.

In 1967 Burns and Hanson [12] investigated a five stage mixer-settler system similar to those found in industry and observed the experimental transient responses to step changes in the feed concentrations. They concluded that theoretical analyses of mixer-settler dynamics under practical conditions was extremely difficult. More recently (1973) [14] a similar study was made of a ten stage mixer-settler extractor to determine plant sensitivity to variations in flow rates and concentrations of feed streams. It was found that the feed flow rate was the most important variable to control followed by the organic phase flow rate and the settler interface levels, but no attempt was made to explain the observations by analysis. Cadman and Hsu [13] (1970) derived a mathematical model for mixer-settler systems from mass balance equations in order to simulate the effects of different control policies on plant operation, but did not check the validity of their model experimentally. The model was later (1972) shown to be satisfactory for estimating steady state plant conditions but not for predicting the dynamics.[10] Slight modification allowed the effects of flow rates to be predicted and the model obtained was shown to give results which agreed with experimentation.[9] Since the flow rates in the plant considered are readily controlled, this model was of particular interest. However attempts to determine its parameter values for the uranium extraction section using step response analyses were thwarted by noise in the measurements and by secondary effects which resulted in inconsistent step responses.[26]

The Correlation Technique

The correlation technique for system identification is not sensitive to external noise (including secondary effects) and was used in the present work to determine the experimental impulse response of a mixer-settler extraction section. The mathematical basis for the technique was first derived by Lee [5] in the early 1950 s but due to practical difficulties was not extensively applied. However the advent of specialized test signals with pseudo-random statistical properties requiring shorter records for correlation and the increased availability of digital computers re-generated interest in the technique after 1960. Due to the inherent noise rejection of the method [3, 5] it is well suited to testing non-linear or production-line systems in which the perturbation test signal should not disturb the system operation unduly. Application of the method to identifying the transfer function of a hydraulic servo-motor is an example of the successful on-line identification of a system non-linearity which enabled the system to be linearized and hence controlled.[8]

Basically the technique regards the unknown system as a black box whose variables are classed as *inputs*, *outputs* or *disturbances* depending on whether they are controllable, measureable or un-measureable.[17] The impulse response is obtained by perturbing the input with a suitable test signal and correlating this with the resulting output. Once the impulse response is known as a set of data points, the problem reduces to one of selecting a suitable basic form of transfer function and fitting it to the existing data by a curve fitting technique such as a least squares method.

Mathematical Modelling

Choice of the form of transfer function will determine whether a model is analytic or empiric. The analytic transfer function is usually derived from equations based on some fundamental law - conservation of mass in the process considered - and it is possible to interpret the co-efficients of the model in terms of plant observables such as *flow rates*, *hold-up volumes*, *transport lags* and *equilibria*. For the empiric model the co-efficients are usually those of a differential polynomial and are pure constants with no indication of their dependence on plant observables. The disadvantage of not being able to relate the model constants to plant conditions by some function are illustrated by considering the simple mixer-settler model. The residence time is a model parameter which is obtained by experiment for both the analytic and the empiric model. From the former the residence time is known to be an inverse function of the flow rate but in the empiric model each flow rate would require an experiment to determine the model parameter at the new plant conditions. This type of disadvantage is inherent in all empiric models and so an analytic model is always preferred if it can be derived.[15]

Experimental determination of the plant impulse response from correlation techniques will yield the plant weighting function as a set of data points since the correlation is done digitally. An analytic model is usually in the form of a function and can be fitted to the data by a standard curve fitting method. In general the analytic model is not very flexible in its form and will not pass through all the data points. Other model forms without this defect are known; for example the spline model has recently been applied to modelling industrial processes [11] with great success since it is well suited to describing sampled impulse responses. But no control theory employing spline models could be found and so their main use at present seems to be in interpolation of process weighting functions for use in time domain analyses of process dynamics. Since the interpolation is not suited to frequency analyses of the impulse response, the spline model is not used here.[22]

Assumptions

The definitions of the correlation functions and hence the validity of all formulae used in this thesis are subject to certain assumptions regarding the statistical properties of the signals measured. It is assumed [23] that

(i) The signals are stationary - i.e. their statistical properties are independent of the choice of time origin.

(ii) The signals are members of an ensemble - i.e. part of a group of functions for which the probability of occurrence is defined.

(iii) The ensemble is ergodic - i.e. all members of the ensemble have the same statistical properties.

CHAPTER 1 SYSTEM WEIGHTING FUNCTION FROM CORRELATION FUNCTIONS

1.1 CORRELATION FORMULAE FOR LINEAR SYSTEMS

As an introduction to the theoretical aspects of correlation methods applied to the identification of systems' transfer functions, a resume of the mathematical arguments [5] leading to the derivation of the pertinent formula is given. The results obtained are used later in the development of computer programs which are based on discrete approximations of the equations derived here.

1.1.1 MATHEMATICAL FUNDAMENTALS

Correlation and convolution integrals form the basis from which the input-output correlation theorem for linear system identification is derived and are explicitly stated here for ease of reference. A few properties required for derivation of the correlation theorem and evaluation of the integrals in practice are also listed.

The time and Laplace domain control terminology used in the following sections is defined in figure (1.1).

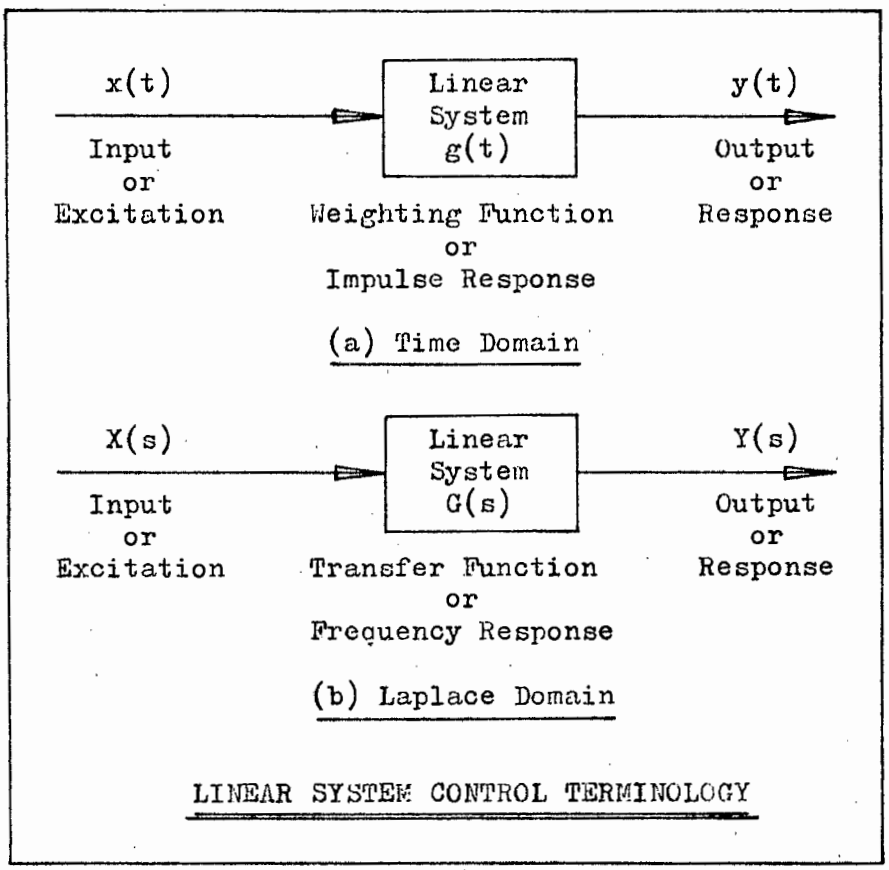

Figure 1.1

The Cross-correlation Function

Definition

The cross-correlation function, $\phi_{xy}(\tau)$, of the functions, x(t) and y(t), is defined by the integral

$$\phi_{xy}(\tau) = \lim_{T \to \infty} \frac{1}{2T} \int_{-T}^{T} x(t)\, y(t+\tau)\, dt \qquad (1.1)$$

Note: If y(t) = x(t), the correlation function, $\phi_{xy}(\tau)$, is called the auto-correlation function of x(t).

Properties

(a) For practical applications of equation (1.1) finite data records are used and the correlation function obtained is an approximation to the true function. It is recommended that the correlation function be considered valid only for delays less than five to ten percent of the record length.[24] But for functions that are periodic in an interval T_1, the use of data records of length $2T_1$ will give exact results provided the limit is removed, T is replaced by T_1 and the functions are considered to be cyclic in T_1. Proof is established simply by considering the cross-correlation function, $\phi_{xy}(\tau)$, as the mean of the product $x(t)y(t+\tau)$ for all time, which for periodic functions is equal to the mean over one period.

(b) In the frequency domain a relationship of extreme practical importance in calculating correlation functions can be established between the Fourier Transforms of the functions $\phi_{xy}(\tau)$, x(t) and y(t), namely,

$$\Phi_{xy}(j\omega) = X^{*}(j\omega)\, Y(j\omega) \qquad (1.2)$$

where $X^{*}(j\omega)$ is the complex conjugate of $X(j\omega)$.

One consequence of equation (1.2) is that any harmonic component present in a function will appear in amplitude in the auto-correlation function (ACF) although all phase information about the component is lost. Thus the ACF can be used as a test for the randomness of a function.

The Convolution Integral

Definition

For a linear system characterised by the weighting function, g(t), the system response, y(t), to the excitation, x(t), is given by the convolution integral

$$\begin{aligned} y(t) &= \int_{0}^{t} x(s)\, g(t-s)\, ds \\ &= \int_{0}^{t} g(s)\, x(t-s)\, ds \end{aligned} \qquad (1.3)$$

The Integration Limits

The limits of the integrals in equation (1.3) can be extended to plus and minus infinity (as required for deriving the following theorem) by defining g(s) and x(s) to be zero for s < 0. The former condition is imposed by causality in a real system.

1.1.2 INPUT OUTPUT CROSS-CORRELATION THEOREM

Theorem

For a linear system the cross-correlation function of the input and corresponding output, $\phi_{xy}(\tau)$, is the response of the system to excitation by the auto-correlation function of the input, $\phi_{xx}(\tau)$. Expressed mathematically in terms of the convolution integral this is simply

$$\phi_{xy}(\tau) = \int_{-\infty}^{\infty} g(s)\ \phi_{xx}(\tau-s)\ ds \qquad (1.4)$$

Proof

Cross-correlation of the system input, x(t), and output, y(t), is given by definition as

$$\phi_{xy}(\tau) = \lim_{T \to \infty} \frac{1}{2T} \int_{-T}^{T} x(t)\ y(t+\tau)\ dt$$

Substituting for $y(t+\tau)$ in terms of the input, x(t), as given by equation (1.3) and changing the order of integration this becomes

$$\phi_{xy}(\tau) = \int_{-\infty}^{\infty} g(s) \lim_{T \to \infty} \frac{1}{2T} \int_{-T}^{T} x(t)\ y(t+\tau-s)\ dt\ ds \qquad (1.5)$$

Comparison with equations (1.1) and (1.3) completes the proof.

Advantages Inherent in Equation (1.4)

In system identification from analysis of its inputs and outputs, the definitions of its weighting function is implicit in equation (1.3) and also in equation (1.4) which, in addition to the convolution integral, requires the lengthy calculation of two correlation functions. Since the mathematical derivations above do not bring out the benefits of the correlation method, two arguments, one in the frequency domain and the other in the time domain, which show the superiority of equation (1.4) over (1.3) in obtaining weighting functions are put forward below.

(a) Consider the Laplace Transforms of the system weighting function, input and output which leads to the familiar expression for the system transfer function

$$G(s) = \frac{Y(s)}{X(s)}$$

Substituting 'jω' for 's', the transfer function frequency response is obtained in terms of the frequency analysis of the input and output:

$$G(j\omega) = \frac{Y(j\omega)}{X(j\omega)} \qquad (1.6)$$

Application of equation (1.6) to evaluate the system transfer functinn is equivalent to using equation (1.3). Obviously at frequencies where $X(j\omega)$ is zero the noise present in the measurements of $y(t)$ and hence in $Y(j\omega)$ might make $Y(j\omega)$ non-zero and result in a singularity in $G(j\omega)$ entirely due to noise. Multiplication and division of equation (1.6) by the complex conjugate of the input Fourier Transform, $X(j\omega)$, will reduce this effect by forcing the numerator to zero at frequencies where the denominator is zero. This operation can be regarded as a form of filtering in which the filter transfer function is $X^*(j\omega)$. Thus using

$$G(j\omega) = \frac{Y(j\omega)}{X(j\omega)} \frac{X^*(j\omega)}{X^*(j\omega)} \qquad (1.7)$$

in system weighting function analysis is preferable to using equation (1.6). Comparison of equations (1.2) and (1.7) yields

$$G(j\omega) = \frac{\Phi_{xy}(j\omega)}{\Phi_{xx}(\omega)} \qquad (1.8)$$

Equation (1.8) is the frequency domain equivalent of equation (1.4) and since equations (1.6) and (1.3) are similarly related, it is obvious that, in identification of systems, the correlation technique has inherent advantages over the direct approach in that it suppresses noise effects.

(b) In the time domain the system weighting function, $g(t)$, can be evaluated by considering the mean squared error, ε^2, between the actual and the predicted system outputs which is defined by

$$\varepsilon^2 = \lim_{T \to \infty} \frac{1}{2T} \int_{-T}^{T} \{ \int_{-\infty}^{\infty} g(u)\, x(v-u)\, du - y(v) \}^2\, dv \qquad (1.9)$$

where $x(t)$ and $y(t)$ are the system input and output as measured experimentally. Expansion, reversal of integration order and substitution for the correlation functions make equation (1.9)

$$\varepsilon^2 = \int_{-\infty}^{\infty} g(u) \int_{-\infty}^{\infty} g(v)\, \phi_{xx}(u-v)\, dv\, du - 2 \int_{-\infty}^{\infty} g(u)\, \phi_{xy}(u)\, du + \phi_{yy}(0) \qquad (1.10)$$

Since the correlation functions, $\phi_{xx}(\tau)$ and $\phi_{xy}(\tau)$, are known from measurements of the system input and output, equation (1.10) can be regarded as a defining equation for the system weighting function, $g(t)$. Using the calculus of variations it can be proved [5] that the error, ε^2, is a minimum if

$$\int_{-\infty}^{\infty} g(u)\ \phi_{xx}(v-u)\ du\ -\ \phi_{xy}(v)\ =\ 0 \quad \text{for } v > 0 \qquad (1.11)$$

Thus using equation (1.4) will automatically result in a system weighting function that minimizes the mean squared error between the predicted and the actual system output.

Excitation Signal Selection

Theoretically any test signal could be applied to the unknown system to obtain its weighting function from either equation (1.3) or (1.4) provided the spectrum of the input covers the system bandwidth. However since the weighting functions are factors of the integrands in both equations, it is preferable to choose the input so that it will simplify this integral. Ideally use of an impulse input eliminates the integration but for equation (1.3) an impulse would not in practice excite the system sufficiently and a step input is usually used. However the test signal for equation (1.4) could be selected to have an ACF which approximates an impulse and still not require impractical inputs.

$$\phi_{xx}(\tau) \simeq A\ \delta(\tau)$$

where $\delta(\tau)$ is the unit impulse function
and A is a proportionality constant.

The cross-correlation function (CCF) then becomes

$$\phi_{xy}(\tau) \simeq A\ g(\tau) \qquad (1.12)$$

Thus a simplifying requirement for the correlation method is the use of a test perturbation signal with an impulse type ACF. One such time signal is the pseudo-random ternary sequence noise (PRTS noise) generated from ternary maximal length sequences.

1.2 TERNARY MAXIMAL LENGTH SEQUENCES

No unique time function is associated with any particular ACF and so numerous time signals have ACFs which approximate an impulse function. One of the earliest known is the bandlimited Gaussian noise signal which is readily generated from noisy diodes, radio-activated photo-mulipliers etc.[3] But, being aperiodic it requires very long - theoretically infinite - correlation time and yields poor results when applied to system identification.[20]

Pseudo-random periodic noises generated from Hall, twin prime, octic, quadratic, binary or q-level maximal length sequences are periodic [1] and so the correlation time is reduced to one period. The important properties of white noise [3] listed below are still retained:

(a) The energy in the noise excitation is theoretically evenly

distributed over all frequencies so that normal operation of the system is undisturbed by introduction of the noise into the input.

(b) Unwanted signal components in the measurements of the output do not affect the results of the correlation provided the signals are stochastically independent.

(c) Stored energy in the system does not affect the test results.

Of the pseudo-noises mentioned, the q-level m-sequence - including binary as a special case - are easily generated from recursion formulae by using q-state shift registers or a digital computer. In addition their correlation functions can be tailored to approximate the unit impulse function to any degree of accuracy simply by altering the number of registers and the frequency of clocking them which is readily accomplished on a digital computer. Different sequences with the same correlation functions can be obtained by altering the co-efficients of the recursion relation which are related to the feedback loops of the q-state registers.

1.2.1 TERNARY M-SEQUENCE GENERATION

Ease of generation recommended the binary and ternary m-sequences as suitable noise sources. The ternary was selected in preference to the binary since it is as easy to generate on a computer as the binary and its ACF has zero mean value while that of the binary has an off-set inversely proportional to the sequence length. This off-set complicates interpretation of the resulting weighting function and its effects might have to be estimated by applying the inverted binary pseudo-random noise to the system. (Called the 'inverse repeat test').

The shift register configuration or software logic that will produce a ternary m-sequence is derived from a primitive polynomial which specifies the co-efficients of the recursion relation. A list of primitive polynomials has been compiled by Church.[2] The theoretical aspects of the procedure are rather specialized and are best studied with the aid of an example by using a polynomial to illustrate the derivation of a recursion relation.

Consider the ternary polynomial

$$x^3 +_3 2x +_3 1 \qquad (= 1021 \text{ in shorthand}) \qquad (1.13)$$

where $+_3$ is modulo 3 addition.[3]

Letting the sequence generated be $x_1, x_2, \ldots, x_{k-1}, x_k, x_{k+1}, \ldots$ the delay operator, D, can be defined so that

$$D^n x_k = x_{k-n} \quad \text{for } n = 0,1,2,3,\ldots \qquad (1.14)$$

Substituting 'D' for 'x' in equation (1.13) the resulting operator equation is allowed to act on 'x' and set to zero

$$D^3 x +_3 2 D x +_3 x = 0 \qquad (1.15)$$

Re-arranging, using modulo 3 algebra and arithmetic ^{3} and applying equation (1.14), the recursion relation is formed:

$$x_k = 2 x_{k-3} +_3 x_{k-1} \qquad (1.16)$$

This equation is readily implemented using shift registers with feedback or

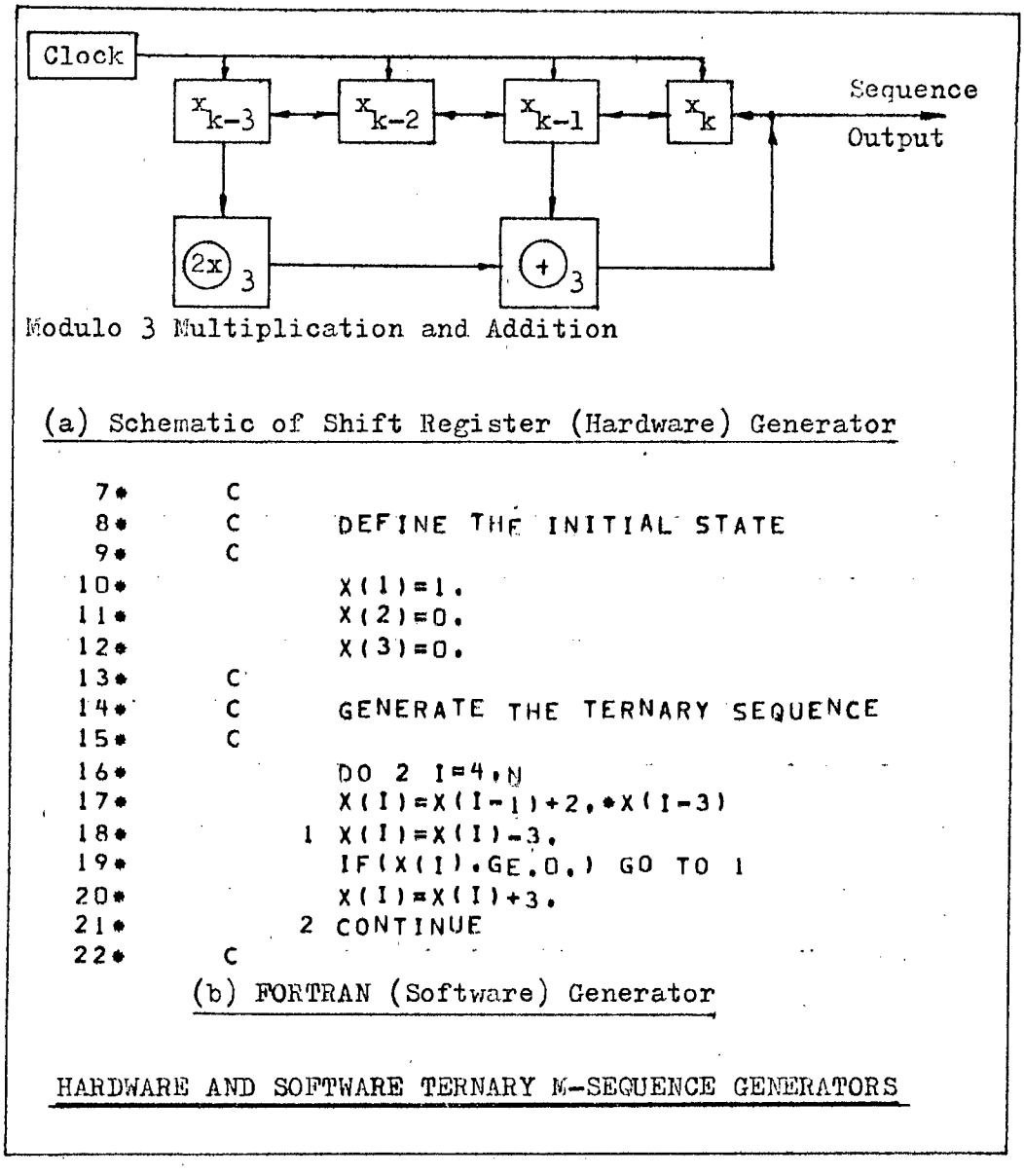

Figure 1.2 (a)

digital computers as shown in figure (1.2a) and generates a sequence, x, with states '2', '0' and '1' as in figure (1.2b). The sequence is periodic and for a polynomial of order 'n', the sequence will repeat after $(3^n - 1)$ digits.

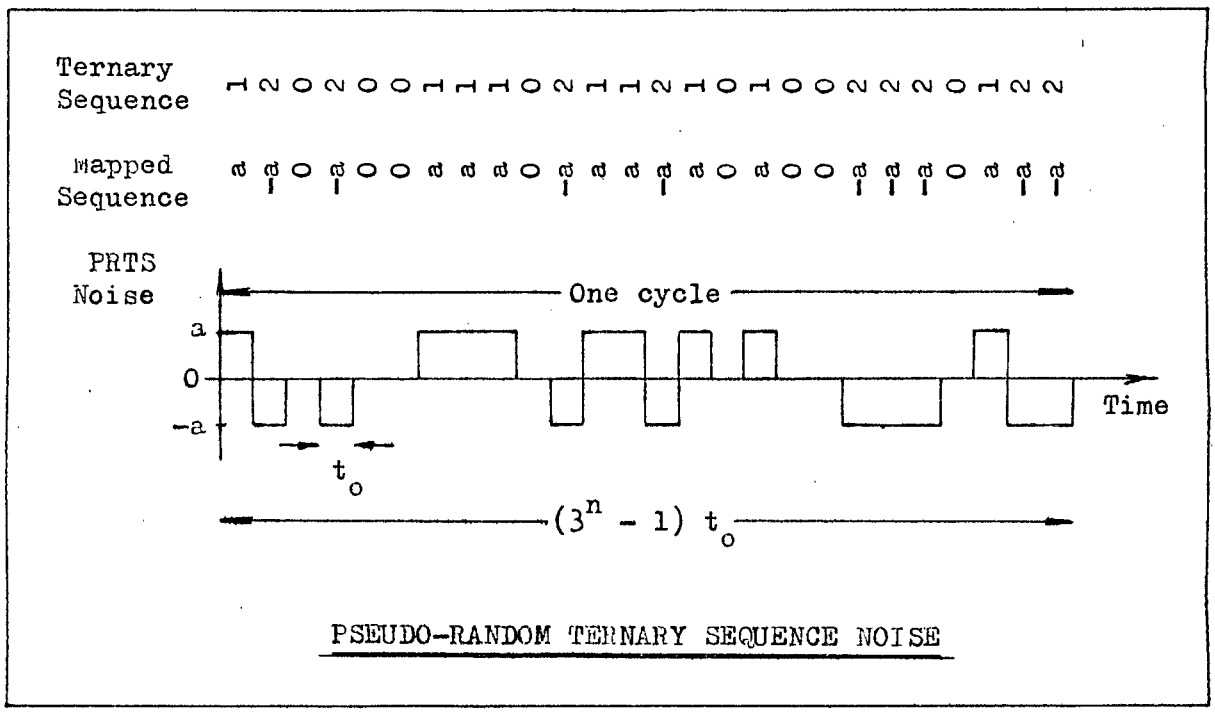

Figure 1.2 (b)

1.2.2 CORRELATION FUNCTION OF THE TERNARY SEQUENCE

By mapping the sequence states '2', '0' and '1' to the amplitudes '-a', '0', and 'a' of a time signal, the resulting signal is PRTS noise with a periodic ACF that approximates a series of impulses - figure (1.3)

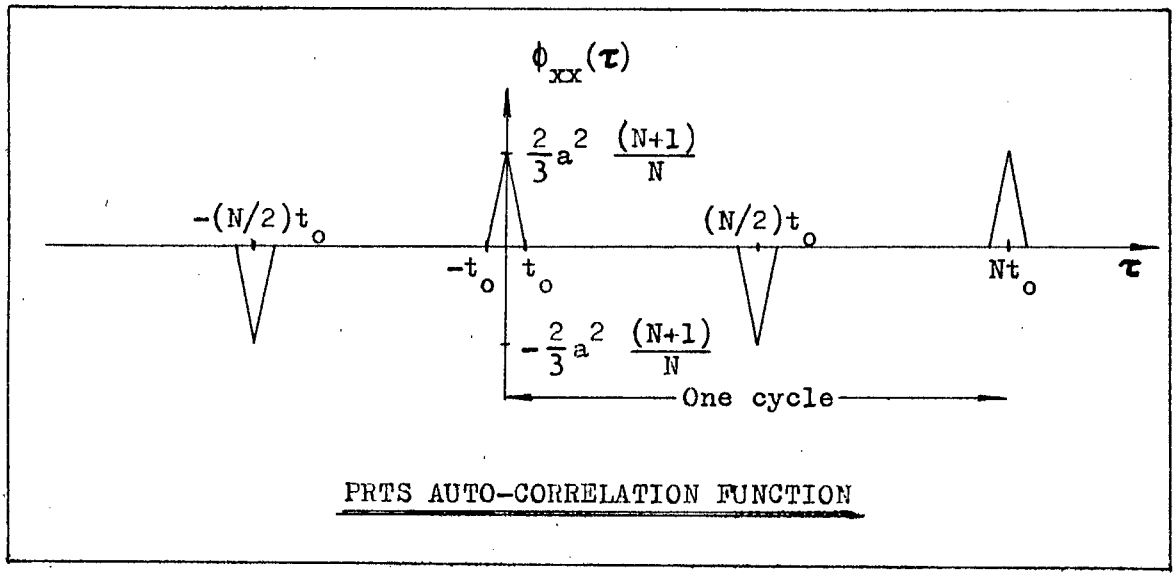

Figure 1.3

For a sequence, periodic in N digits, each of which exists for time t_o, the ACF is given by [3, 7]

$$\phi_{xx}(\tau) = \frac{2}{3}\ a^2\ \left(\frac{N+1}{N}\right) \qquad \text{for } \tau = 0, \pm Nt_o, \pm 2Nt_o, \ldots$$

$$= -\frac{2}{3}a^2\left(\frac{N+1}{N}\right) \qquad \text{for } \tau = \pm\frac{1}{2}Nt_o,\ \pm\frac{3}{2}Nt_o,\ldots \qquad (1.17)$$

$$= 0 \qquad \text{for other integral values of } \tau$$

At non-integral τ values, $\phi_{xx}(\tau)$ is found by linear interpolation. The 'impulse'area is the value for 'A' in equation (1.12) and has the value $\frac{2}{3}a^2\left(\frac{N+1}{N}\right)t_o$

Correlation Function Power Spectrum

The range of frequencies for which the pseudo-noise power spectrum is approximately constant as for white noise is of importance in estimating to what degree the ACF will approximate the impulse function. The noise power spectrum is given by the Fourier Transform of the correlation function and has units of PRTS amplitude-time squared per radian in the expression

$$\Phi_{xx}(\omega) = \frac{2}{3}a^2\left(\frac{N+1}{N}\right)t_o\left\{\frac{\sin\frac{\omega t_o}{2}}{\frac{\omega t_o}{2}}\right\}^2 \qquad (1.18)$$

From a graph of this function which is shown below it can be seen that

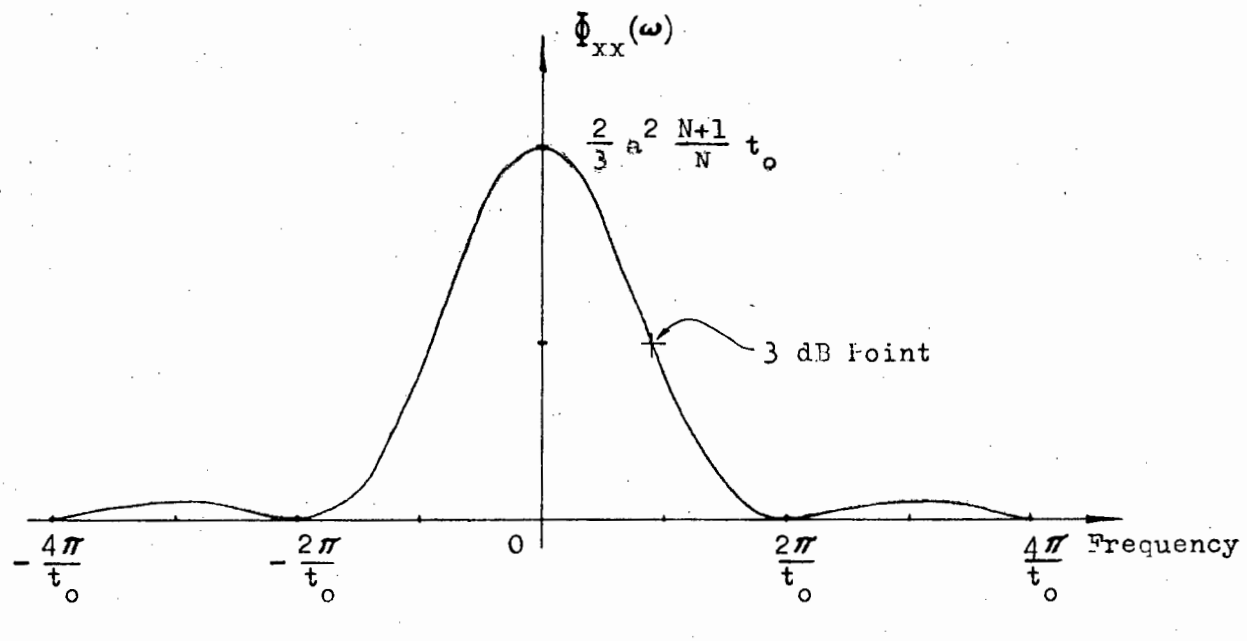

AUTO-CORRELATION FUNCTION POWER SPECTRUM

the 3 dB point occurs at a frequency of roughly π/t_o and so by selection of a suitable digit interval, the ACF can approximate the impulse function to any degree of accuracy.

The foregoing has covered the purely theoretical tools necessary for identifying a process from correlation functions and it now remains to consider the effects introduced by applying the test in practice.

1.3 SYSTEM IDENTIFICATION FROM THE CROSS-CORRELATION FUNCTION

Correlation techniques for system identification utilize the input output cross-correlation theorem and the properties of the PRTS noise to produce an impulse response for the system. But various aspects of the method required detailed investigation before it could be applied in practice to the uranium plant.

The PRTS noise has three parameters - digit length, period and amplitude - which determine its characteristics and suitability for 'optimal' identification of any particular system. In addition, application of the PRTS noise to the plant input variable required experimental apparatus and introduced effects which, together with noise components in the measurements caused by disturbances in the plant, are not explicitly accounted for in the equations derived so far.

1.3.1 TERNARY M-SEQUENCE SELECTION

Unlike step and frequency response tests the PRTS noise perturbation input for cross-correlation identification has to be selected with reference to the characteristics of the system being tested. Information is needed concerning system bandwidth, settling time and sensitivity to variations in the input. Such data was not available for the uranium plant although plant records provided rough estimates and a pilot test was run to obtain estimates of the above characteristics. The PRTS noise parameters for the pilot test and the main test were selected on the basis of the following criteria.

Digit Duration

The digit length, t_o, determines the bandwidth of the PRTS noise and is selected to ensure that the pseudo-noise approximates white noise for all frequencies of interest. The 3 dB point of the PRTS noise occurs at a frequency of π/t_o radian s^{-1} and so the ideal value for t_o is half the smallest time constant of interest in the system.

Period

Once the digit duration is set, the period of the PRTS noise is altered by the order of its generating polynomial. The period must exceed twice the system settling time to avoid interference of the CCF impulse responses resulting from the periodic ACF impulses of the PRTS noise. Thus the polynomial order is chosen to give the PRTS noise a period of 8 to 10 times

the longest time constant in the system. It is preferable to increase the digit length, t_o, to avoid interference than to increase the polynomial order.[6]

Amplitude

This is selected on the qualitative criteria that it should produce measurable variations in the system output but not disturb the normal operation unduly. Plant personnel experience supplied an estimate for the amplitude needed.

Plant Characteristics

Rough estimates of the plant time constants - smallest and largest - required to select the PRTS noise parameters for the pilot test were obtained by studying the normal operating signals. Time analyses yielded the settling time - figure (1.4) shows a change in state for the uranium concentration of the loaded solvent - and frequency analyses the bandwidth - figure (1.5) shows graphs of the loaded uranium concentration and its Fourier Transform.

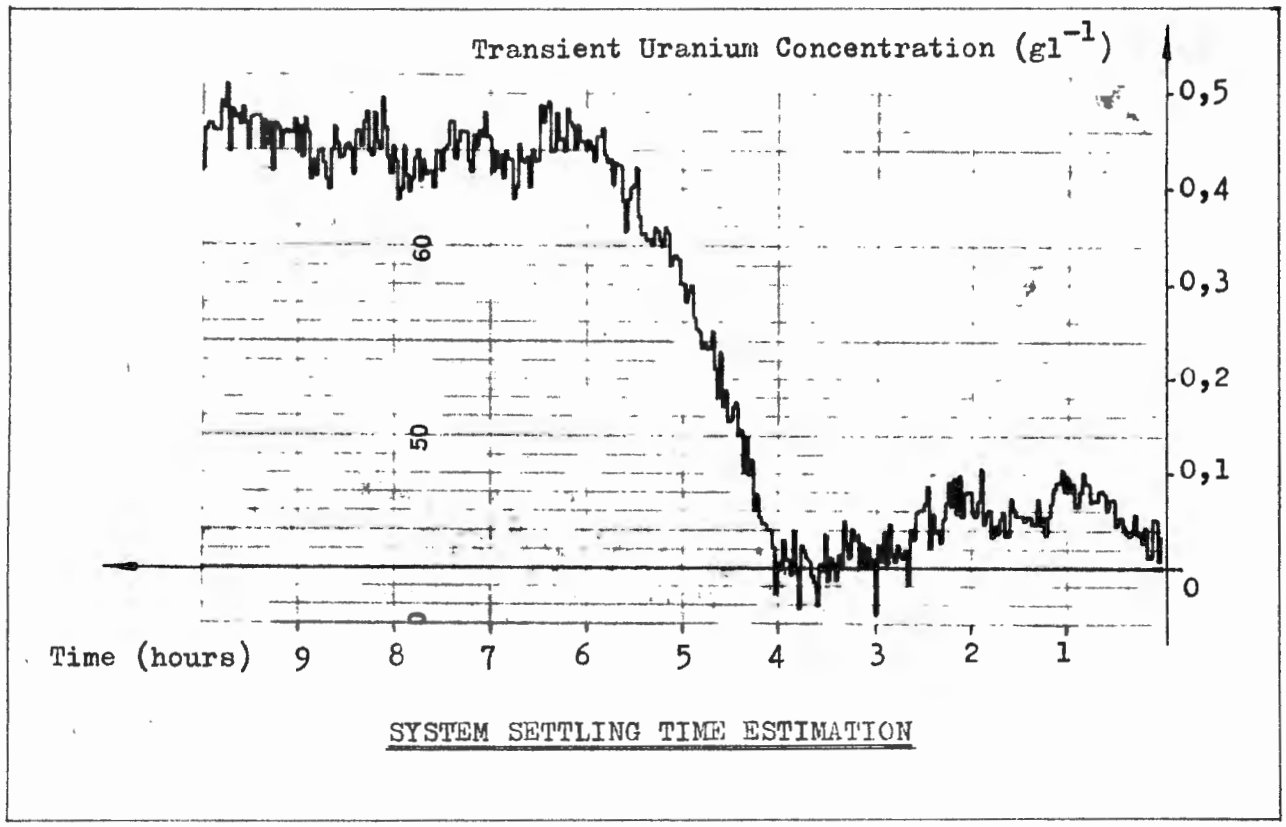

Figure 1.4

It can be seen from these graphs that the system appears to have a settling time of approximately 2 hours and that the major frequency component is below 1 mrad s^{-1}.

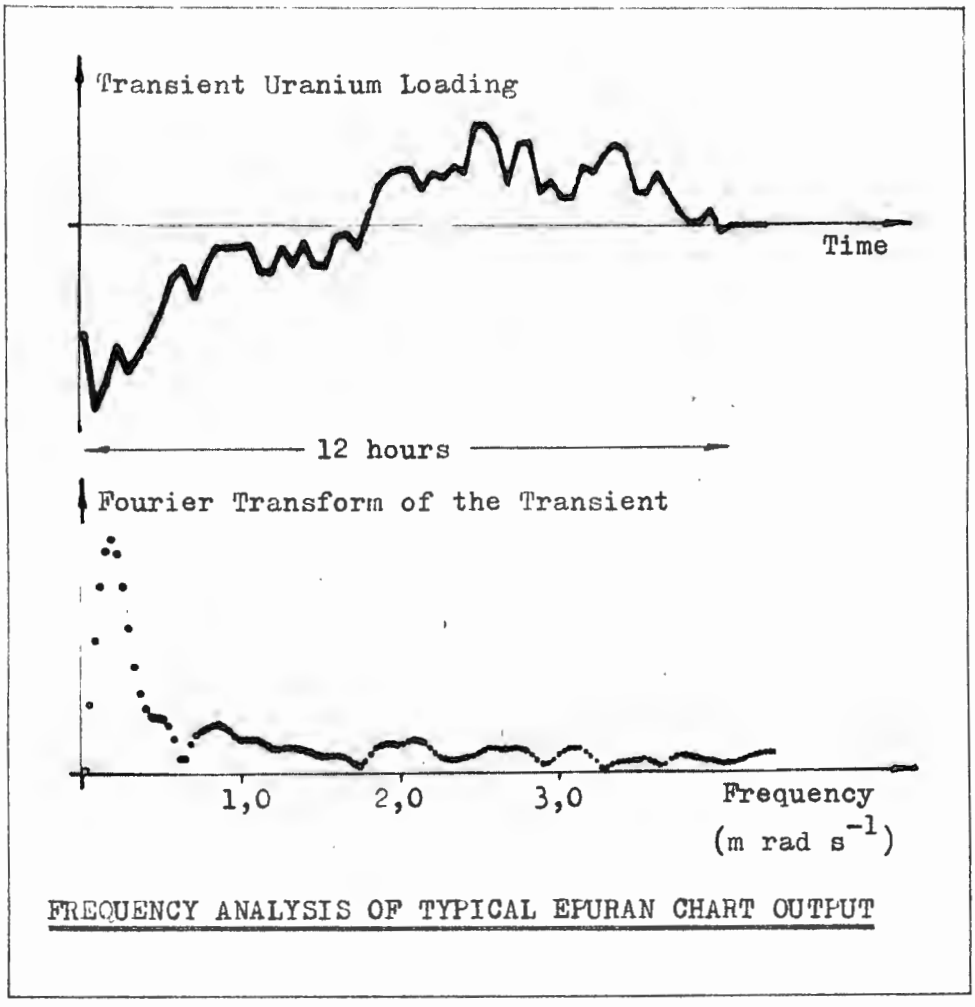

FREQUENCY ANALYSIS OF TYPICAL EPURAN CHART OUTPUT

Figure 1.5

Variations in the PRTS Parameters

A second order system was simulated on an analog computer and tested by correlation techniques to determine the effects of incorrect PRTS noise parameter selection on the calculated weighting function. The system used is detailed in appendix A but for the present discussion its relevant characteristics are:

Settling Time	800 ms
Smallest Time Constant	200 ms

Thus ideal parameters can be selected for the PRTS noise using the criteria discussed above and the system can be identified from the CCF. In addition to the ideal PRTS noise, three others were chosen to show the effect of (i) Too short a digit length, t_o, (ii) Too long a digit length and (iii) Too short a period, Nt_o. The parameters are tabulated below.

	Ideal	(i)	(ii)	(iii)
Polynomial	1021	1021	1021	112
Digit Length t_o	80 ms	32 ms	512 ms	128 ms
Period Nt_o	2,08 s	830 ms	13,3 s	1,02 s

The PRTS noise was generated on the Varian computer and recorded on one track of a 7 track instrument tape recorder. The pre-recorded track provided the system input test signal while the system response was simultaneously recorded on another track thus synchronizing the records of the input and output. The analog data on the tape was converted to digital data and analysed on the Varian using the software developed for correlating and the results were displayed on the graphic terminal. The CCFs are given in

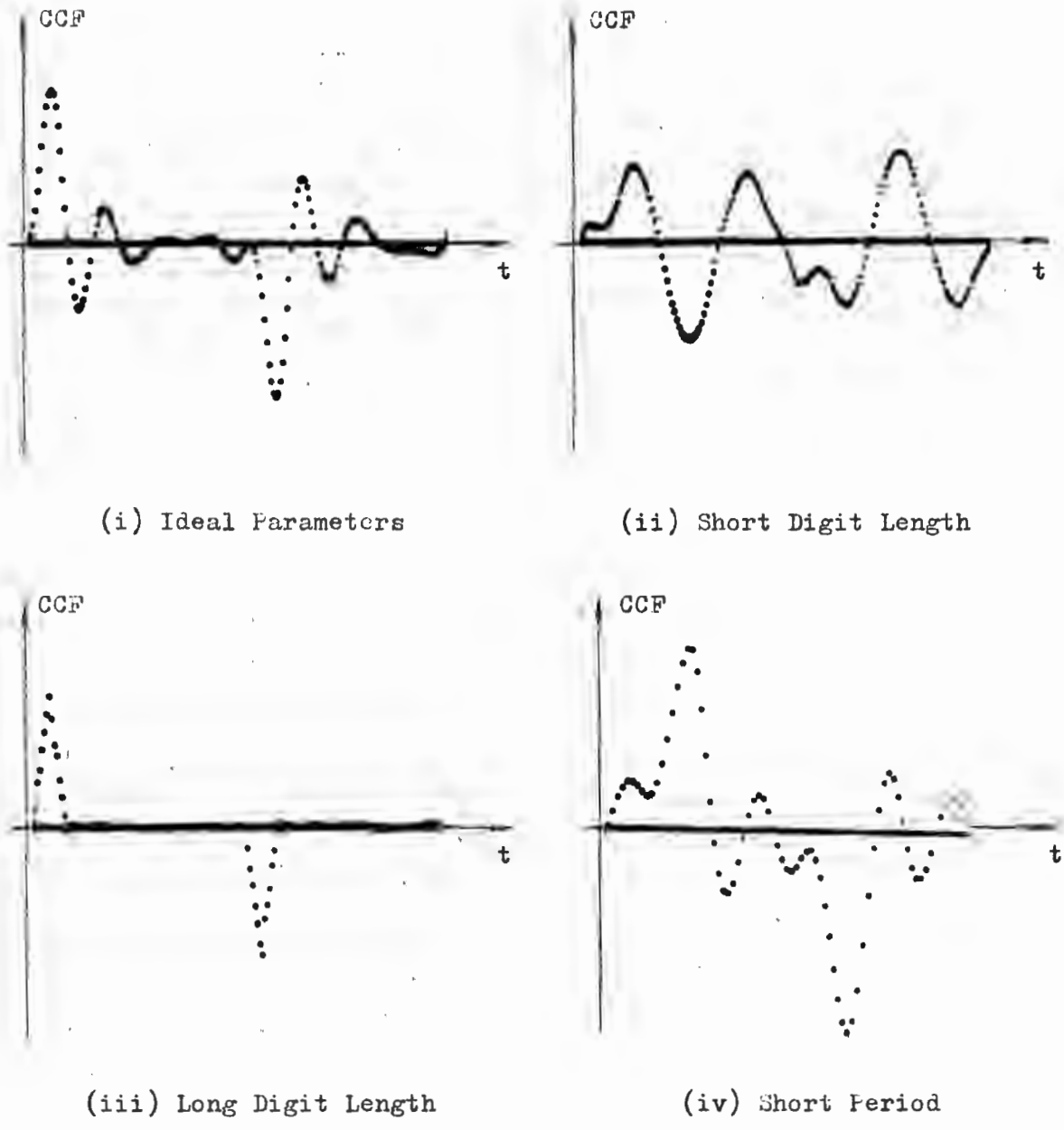

CROSS-CORRELATION FUNCTIONS OF SIMULATED SYSTEM USING DIFFERENT PRTS NOISE SIGNALS

Figure 1.6

figure (1.6). It is seen that incorrect parameter selection manifests itself in the resulting correlation functions calculated.

1.3.2 PERTURBATION TEST OF THE URANIUM PLANT.

Execution of a perturbation experiment required control elements and transducers to apply the PRTS noise to the plant and to measure the response. Although plant hardware is discussed in detail in sections (3.3) and (3.4), the modifications of equation (1.4) needed to cover the practical aspects of the correlation experiment is given here. The analysis served to identify, and hence minimize where possible, the potential error sources introduced and allowed calculation of their relative importance.

In the perturbation experiment the PRTS noise, x(t), is added to the normal steady state operating plant input, r(t), as shown in the diagram below to form the plant test control signal, v(t), which is converted to the plant input, f(t). Noise generated in the plant and the instrumentation is

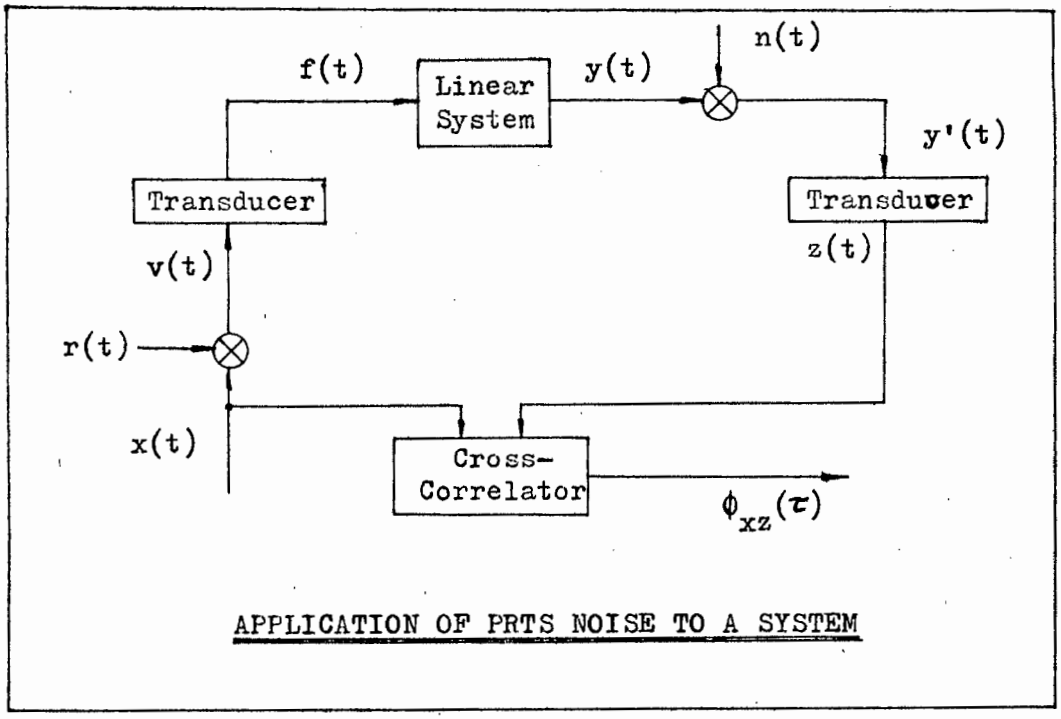

APPLICATION OF PRTS NOISE TO A SYSTEM

accounted for by the signal n(t) which is added to the system response, y(t) due to f(t), to give y'(t). This is finally transduced by the instrumentation to form the measured system output, z(t). Since correlation is done with the signals x(t) and z(t), the weighting function calculated will be distorted by the characteristics of the transducers and by noise caused by plant disturbances. Assuming that the errors introduced by the input and output transducers can be expressed as additive components, $e_i(t)$ and $e_o(t)$, in f(t) and z(t) respectively, the CCF, $\phi_{xz}(\tau)$, that is calculated from the experimental data is

$$\phi_{xz}(\tau) = \int_{-\infty}^{\infty} g(s)\ \phi_{xx}(\tau-s)\ ds + \int_{-\infty}^{\infty} g(s)\ \phi_{xr}(\tau-s)\ ds + \int_{-\infty}^{\infty} g(s)\ \phi_{xe_i}(\tau-s)\ ds + \phi_{xn}(\tau) + \phi_{xe_o}(\tau) \qquad (1.19)$$

The first term is the desired convolution integral as given by equation (1.4) and the others are error terms introduced by the hardware required to perform the experiment and the noise present in the plant. A term by term analysis is now made of equation (1.19) to determine the relative magnitudes of the various terms with reference to the uranium plant.

(a) The Auto-correlation Function Term $\int_{-\infty}^{\infty} g(s)\ \phi_{xx}(\tau-s)\ ds$

From section (1.2.2) it is known that the power spectrum of the ACF of PRTS noise only approximates the flat spectrum of a true impulse function and in system identification the first term of the CCF, $\phi_{xz}(\tau)$, has to be modified to give the true system impulse response. The correction factors are found by expanding g(s) about s=t as a Taylor series:

$$g(s) = g(t) + (s-t)\ g'(t) + (s-t)^2\ g''(t) / 2! + \ldots$$

and substituting this into equation (1.4) gives

$$\phi_{xy}(\tau) = A_o(\tau)\ g(\tau) + A_1(\tau)\ g'(\tau) + A_2(\tau)\ g''(\tau) + \ldots \qquad (1.20)$$

where the correction factors, $A_n(\tau)$ are given by

$$A_n(\tau) = \frac{1}{n!} \int_o^{T_1} (s-\tau)^n\ \phi_{xx}(\tau-s)\ ds$$

The factors $A_n(\tau)$ are only valid for CCFs which become zero between successive ACF impulses since, in deriving $A_n(\tau)$, the integration limits of equation (1.4) have been replaced by 0 and T_1. In equation (1.20) g(t) is unknown and it is usual to assume that the high order terms of the equation can be neglected. Although no quantitative comment can be made about this assumption until g(t) is known, the relative magnitudes of the $A_n(\tau)$ for PRTS noise - shown in figure (1.7) - do not contradict it. For 'n' greater than '2' the factors rapidly become smaller and for the interval $t_o < t < T_1$ $A_n(t)$ are equal to $A_n(t_o)$. So the only correction factor applied to $\phi_{xz}(\tau)$ is $A_o(\tau)$ which has the following form

$$A_o(\tau) = \frac{1}{3} a^2 \left(\frac{N+1}{N}\right) \left(t_o + 2\tau - \frac{\tau^2}{t_o}\right) \qquad \text{for } 0 < \tau < t_o$$

$$= \frac{2}{3} a^2 \left(\frac{N+1}{N}\right) t_o \qquad \text{for } t_o < \tau < T_1$$

Figure (1.8) shows a graph of this correction factor and the effect of

applying it to a hypothetical CCF. In passing it should be noted that the existence of an appreciable transport lag, t_1, will require the application of a correction factor $A_o(t-t_1)$ where t_1 is estimated from the CCF.

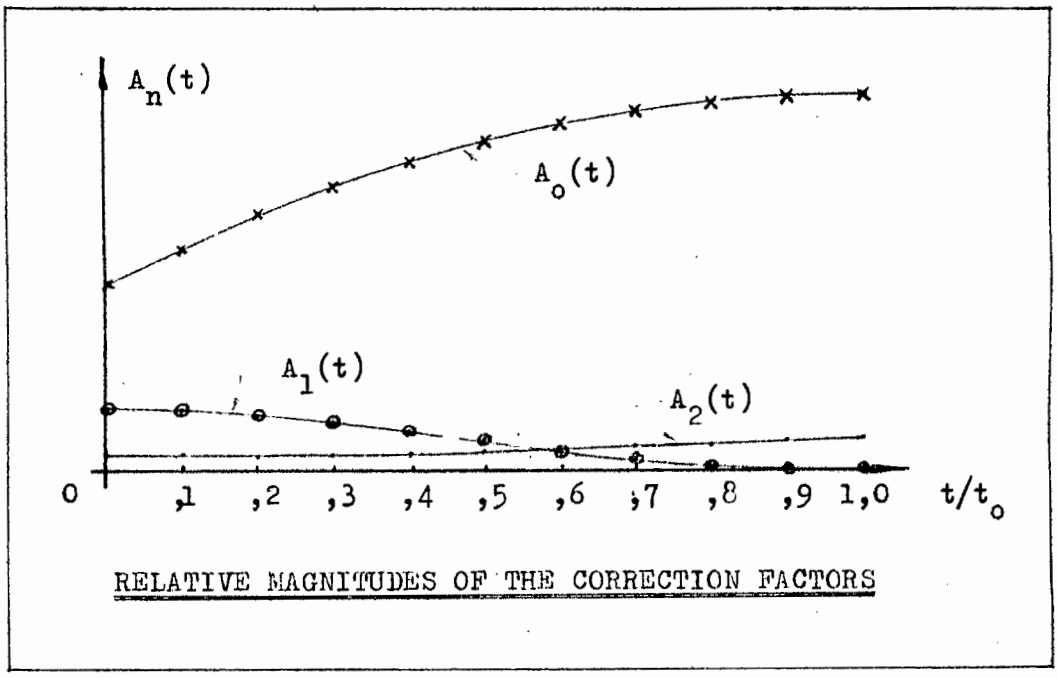

Figure 1.7

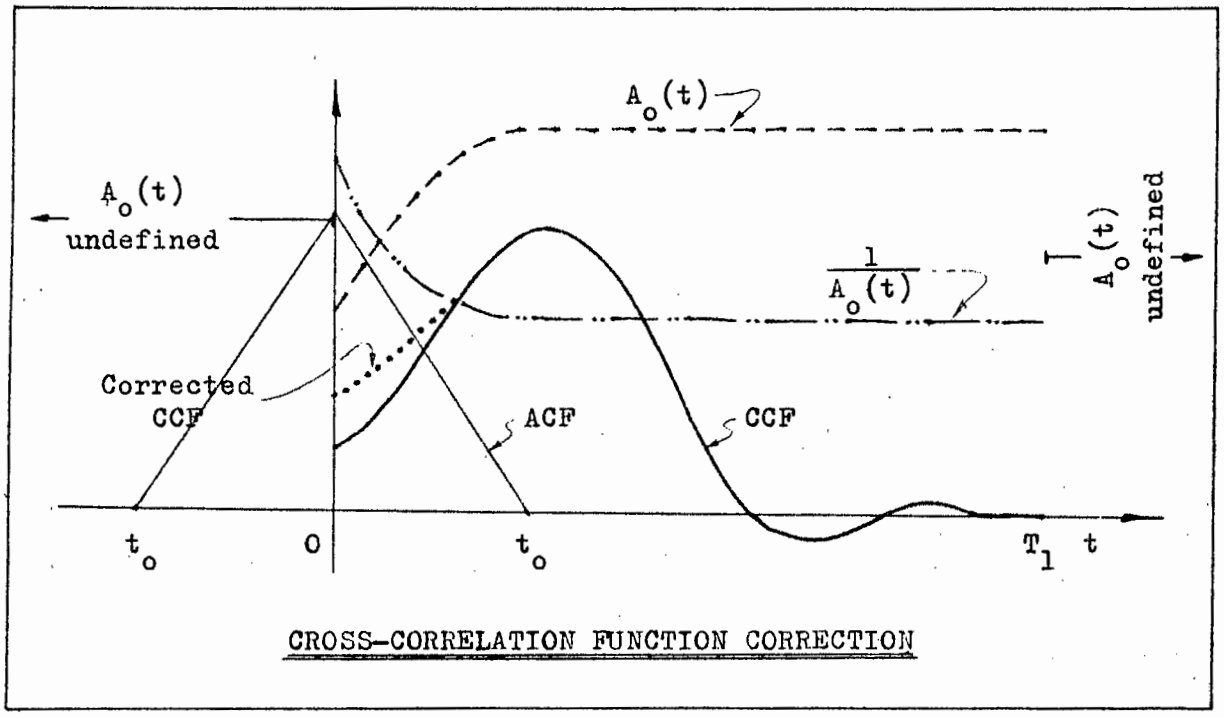

Figure 1.8

(b) The Error Terms

(i) The Normal Operating Term, $\int_{-\infty}^{\infty} g(s)\ \phi_{xr}(\tau-s)\ ds$

In the uranium plant variations in the storage tank levels - despite the pneumatic level control system - affected the efficiency of the centrifuge pumps and imposed transients on the steady state input flow rate. Manual control of the flow rate set point minimized these deviations from the steady state flow rate, so the CCF of the PRTS noise and these transients was sufficiently small - less than 1% - relative to the PRTS ACF to be neglected.

(ii) The Input Transducer Error Term, $\int_{-\infty}^{\infty} g(s)\ \phi_{xe_i}(\tau-s)\ ds$

The PRTS noise was provided as a voltage signal on one track of an instrument tape-recorder which was added to the DC voltage from a power supply which represents the steady state operating signal to form the voltage signal for controlling the feed flow rate to the plant. Voltage to current, current to pressure transducers and the final control element, the butterfly valve, constitute the input transducer. Main sources of error in the transducer are linearization of the square law valve characteristics and imperfections of the current to pressure transducer linearity. Hysteresis in the valve is eliminated by a valve positioner which ensures that the valve opening corresponds to the pressure signal applied to the pneumatic actuator. The combined effects of these factors produced a 1,5% maximum deviation of the amplitude of the flow from that specified by the PRTS noise voltage signal and was neglected. It was not possible to calibrate the valve on-line but any error introduced by this would be systematic and was ignored.

(iii) Plant and Instrumentation Noise, $\phi_{xn}(\tau)$

For the uranium plant this was the most significant error term in equation (1.9). Analytically it is convenient to consider the noise as consisting of three components, random noise, $n_r(t)$, periodic noise, $n_p(t)$, and noise due to equipment drift, $n_d(t)$. The CCF $\phi_{xn}(\tau)$ then becomes

$$\phi_{xn}(\tau) = \phi_{xn_r}(\tau) + \phi_{xn_p}(\tau) + \phi_{xn_d}(\tau) \qquad (1.22)$$

The random noise of spectral density n^2 correlates with the PRTS noise to give [3]

$$\phi_{xn_r}(\tau) \rightarrow \frac{a\ n}{\sqrt{T_c}} \qquad (1.23)$$

where a is the PRTS noise amplitude and T_c is the data lengths used in calculating the CCF. Thus the effects due to random noise can be eliminated to any degree simply by increasing the length of the data record used for correlating.

Theoretically a periodic component of a frequency that is not an integral multiple of the PRTS fundamental frequency is uncorrelated with the PRTS, and, one of a multiple frequency is attenuated and re-appears as the correlation function. In practice, the use of finite data samples introduces spectral leakage effects [19] and the rejection is not as effective.

First and higher order moments of a PRTS noise are non-zero, and low-frequency drift in the measured output will consequently correlate with the PRTS noise. Since drift in the equipment used was most likely to be linear with time, the effect of drift on the CCF, $\phi_{xn_d}(\tau)$, was minimized by removal of the DC component and the linear trends in the output data before processing.

The effect of noise in the system output on the weighting function extracted from the CCF is difficult to analyse so the correlation technique was applied to a 'noisy' second order system simulated on an analog computer. Various 'noise' signals were added to the system output to determine (i) the extent of the noise rejection inherent in the correlation properties of PRTS noise and (ii) the superiority of the method over the normal step response analyses for obtaining the system weighting function. Details of the system and the experimental results are given in appendix A. From the results it can be concluded that the rejection of 'noise' (i.e. any signal component in the output not due to the PRTS noise input) is effective provided the PRTS noise is stochastically independent of the 'noise'.

(iv) The Output Transducer Error Term, $\phi_{xe_o}(\tau)$

Strictly speaking, the instrumentation noise considered above is 'transducer error', but it is indistinguishable from the plant noise in practice. The error introduced by the transducer has components due to random isotope decay rates and linear calibration of the uranium analyser but these factors produce less than 1% error and were neglected.

Summary

Correlation techniques have been shown to have distinct advantages over step response analyses in obtaining plant transfer functions, especially in the presence of noisy measurements. But the noise rejection is paid for by requiring complex data analysis necessitating digital computer facilities. An added difficulty is the selection of an 'ideal' PRTS noise test signal whose choice paradoxically requires some apriori knowledge of the plant characteristics.

Practical realization of the method for identifying the uranium plant introduces numerous error factors which were minimized by the existence of such elements as valve positioners and also by the use of high quality experi-

mental equipment. So the main source of error in the calculated impulse response was due to noise generated in the plant. This was uncontrollable and the statistical properties of the PRTS noise were relied upon to eliminate its effect.

CHAPTER 2 THE URANIUM EXTRACTION SECTION

The solvent extraction section in the solvent extraction plant of an uranium plant constituted the ' system' to be identified by on-line correlation techniques. Prior to the design and execution of perturbation tests on the plant, a preliminary study of the extraction section was made to determine (i) its relation to the uranium plant, (ii) the operation and geometry of the mixer-settlers and the feed storages, (iii) the characteristics and limitations of the instrumentation and control elements, (iv) the steady state model of the mixer-settler operation and the present manual control philosophy and (v) the dynamic characteristics of the plant as deduced from harmonic analysis of the normal operating signals.

2.1 THE URANIUM PLANT

An outline of the uranium plant illustrates the relationship of the extraction section to the extraction plant and the uranium plant which is shown schematically in figure (2.1) below.

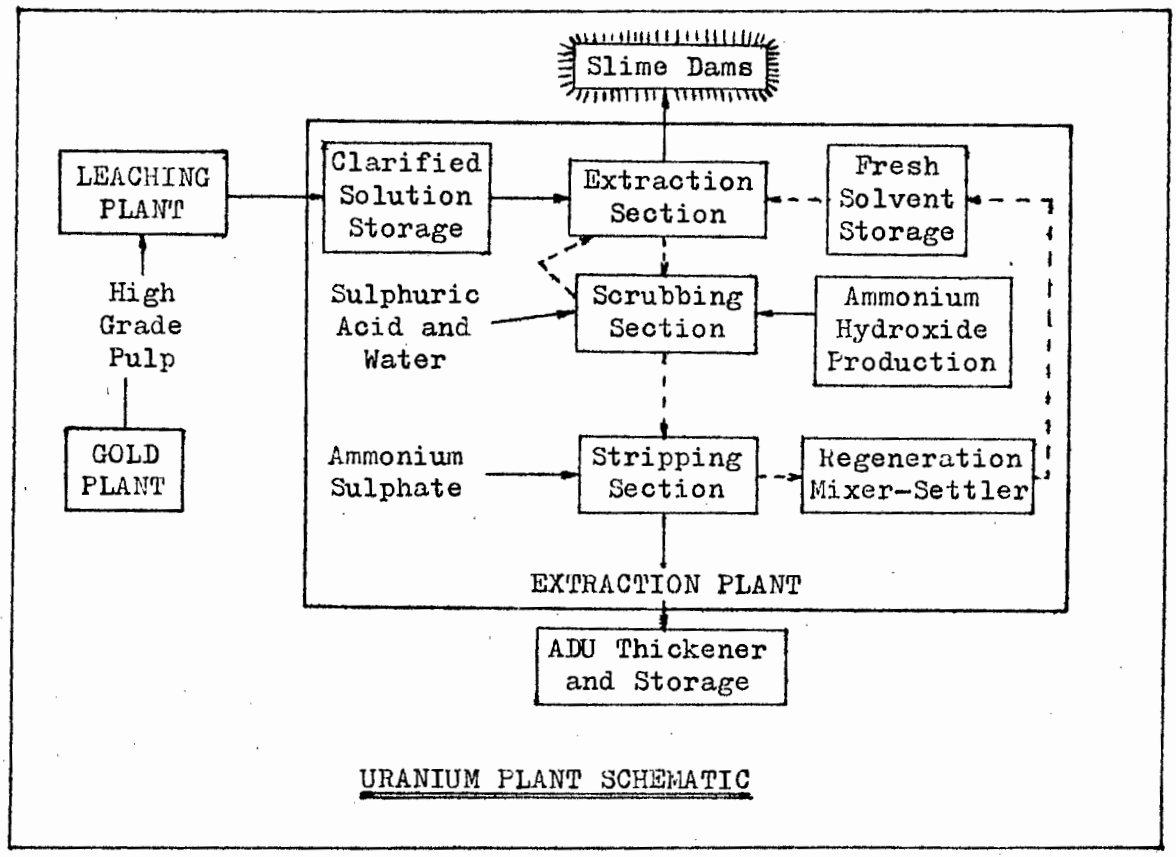

Figure 2.1

The uranium plant consists of two separate plants: (1) the leaching plant and (2) the uranium extraction plant which is further divided into the

extraction, the scrubbing and the stripping sections.

Uranium enters the leaching plant as a high grade pulp and is treated with sulphuric acid and manganese dioxide to form an aqueous solution of uranium oxide which, after filtering, is called 'clarified pregnant solution'. This solution is the input to the extraction plant. In the extraction section the uranium is transferred to an organic phase by successively mixing and settling the aqueous solution with the organic solvent. The loaded solvent impurities are removed in the scrubbing section and the uranium is returned to an aqueous phase in the stripping section and then percipitated with ammonia. After thickening and filtering the uranium slurry is stored for later processing in a central plant.

2.2 THE EXTRACTION SECTION

2.2.1 THE SECTION LAY-OUT

The extraction section consists of three mixer-settlers connected in series as shown in figure (2.2). Two immiscible fluids, water or aqueous phase

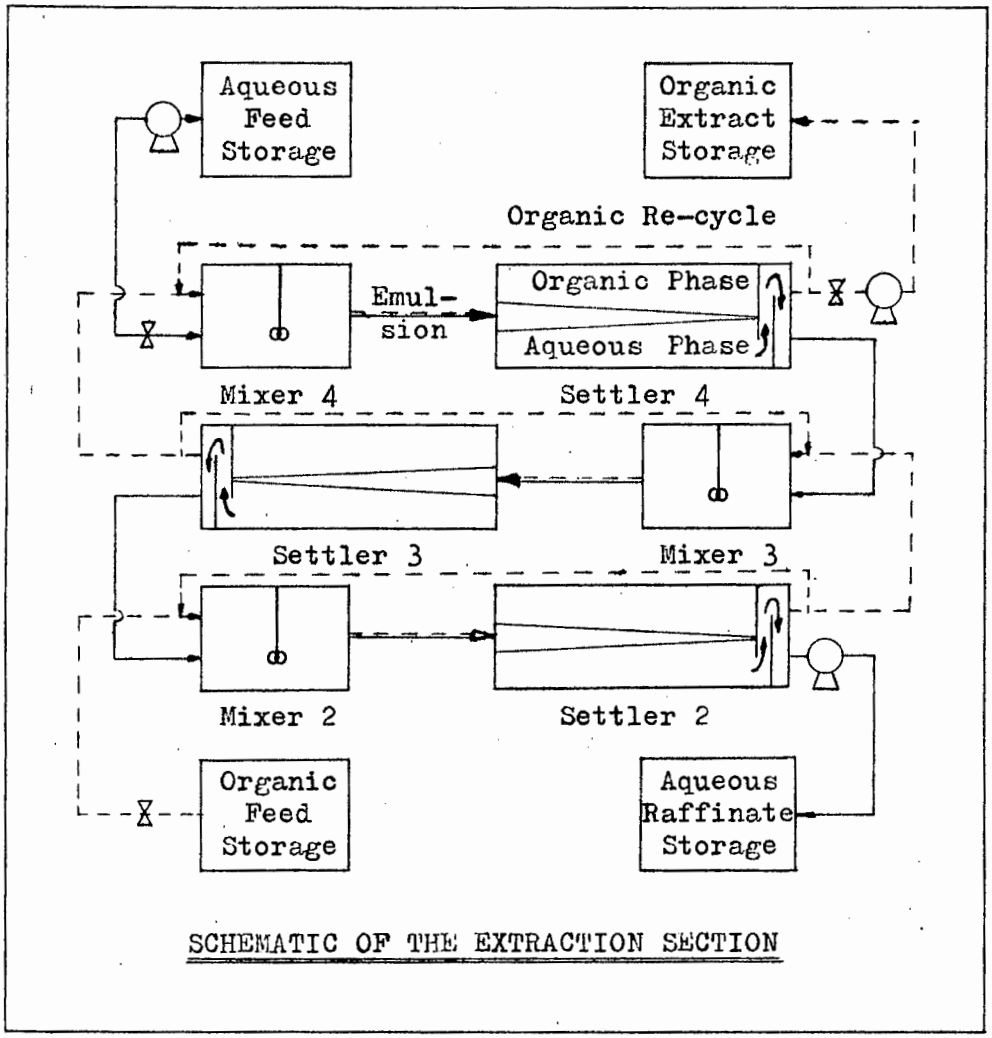

SCHEMATIC OF THE EXTRACTION SECTION

Figure 2.2

and paraffin or organic phase, flow counter-current through the section and co-current through each stage. The two phases flow between stages under the pull of gravity and are 'pumped' only by the action of the mixer impeller at each stage. Storage tanks on the feed, product and waste streams buffer the section from the rest of the plant.

Uranium rich aqueous solution is pumped from the aqueous feed storage tank by a centrifuge pump to mixer-settler 4. Its flow rate is regulated by a butterfly valve which uses a differential pressure flow meter (D.P.Cell) and a pneumatic controller in its control loop. In the section uranium is taken up by the organic phase and after mixer-settler 2 the aqueous 'raffinate' phase overflows from settler 2 and is pumped to the raffinate storage without flow control. Stripped solvent flow from the organic feed storage is controlled by a control valve and control loop which, except for capacity, is identical to the pregnant solution system. After mixer-settler 4 the loaded - uranium rich - solvent is pumped to the organic extract storage tank. The flow rate here is also controlled. In the section itself interstage flow can be controlled by manual adjustment of the weirs for the aqueous phase and butterfly valves for the organic phase on individual mixer-settler units.

2.2.2 THE MIXER-SETTLER UNIT.

Each stage consists of a mixer and a settler of 1,6 and 45 m^3 capacities respectively. The mixers have a screw type pump-mix impeller that mixes the two phases entering the mixer to form an emulsion which is lifted by the action of the impeller to overflow along a duct to the settler where it is dispersed by a circular distributor plate. The mass transfer of uranium from the aqueous to the organic phase occurs mainly in the mixer since the transfer time is less than the mixer residence time. In the settler the emulsion separates out with further mass transfer and the two phases are channelled into separate outgoing streams by a system of weirs and baffles. All the settlers were tested for settling efficiency and found to be better than 99% efficient - no organic phase was present in the aqueous phase samples taken and the maximum aqueous present in the organic phase was 4,5 ml in 950 ml for stage 4.

All the aqueous phase flows directly to the next stage from the settler but a large fraction of the organic is re-cycled back to the mixer. Re-cycling increases the effective residence time for the organic phase in each stage and more uranium is taken up by the solvent. So a small volume of organic phase can process a considerably larger volume of aqueous phase - a ratio of the order 1:10 in the plant considered.

2.2.3 MANUAL CONTROL AND OPERATION OF THE EXTRACTION SECTION

Control of the extraction section aims at maintaining the maximum loading

by a relatively small, abrupt change of pregnant flow rate - 5 to 10%. This meant that the plant is ideally suited to identification by PRTS noise excitation and correlation techniques since it required small amplitude test perturbations and hence greater rejection of noise. Corrective action requires the manual adjustment of the weirs and butterfly valves to change the interstage flow rates and so restore stage equilibrium. Since the mixer volume is negligible in comparison with the settler, the interface level of the settler is used to give an indication of the stage ratio of aqueous to organic phase. Due to the free flow nature of the mixer-settlers any change in one stage will affect the others and the skill of the operator plays a large part in the adjustment of the interstage flows to restore equilibrium.

2.3 PLANT INSTRUMENTATION AND CONTROL ELEMENTS

The accuracy of the calculated CCF is dependent on the equipment used to perturbate the plant and to measure the response. The existing plant elements, the pregnant solution control valve and the EPURAN uranium analyser system, were used for applying the PRTS noise to the plant and to measure the response. The characteristics of these elements will now be considered.

2.3.1 EPURAN URANIUM ANALYSER

Operation

The analyser operation is based on the exponential X-ray absorption law. The detector uses 60 KeV X-rays to give the maximum differential in the mass absorption co-efficient of the uranium and the elements hydrogen, carbon, oxygen and sulphur which constitute the organic solvent.

The solvent is pumped from settlers 3 and 4 through the sample chambers of two EPURAN detectors. The detector contains the radio-isotope, the photo-multiplier and the pre-amplifier. The transport lag between the settler and the detector is less than 100 s and can be neglected in so far as it affects the uranium concentration reading. The decay signal from the detector is amplified and passed through a single channel analyser (SCA) which produces a 5V 0,5 µs pulse for every input from the detector with energies in the range 29 to 64 KeV. These pulses are accummulated in the scaler for 1000 s periods. Clock pulses - every 1000 s during the experiments - applied to the scaler, decoder and digital printer initiate printing and decoding of the count which has accummulated in the scaler. After printing the scaler is reset and starts another 1000 s count interval. Figure (2.3) shows the schematic of an EPURAN uranium analyser.

On settler 4 the pulses from the SCA are also fed to a digital subtractor and a ratemeter which produces an analog signal proportional to the counts

registered in 100 s. The 0 to 100 mV signal corresponds approximately to 2 to 4 gl^{-1} uranium loading and drives a chart recorder. During the experiments this signal was also recorded on the instrument tape recorder.

Versatility

The uranium concentration of the pregnant solution is sufficiently high to fall within the theoretical range of operation of the EPURAN analyser and

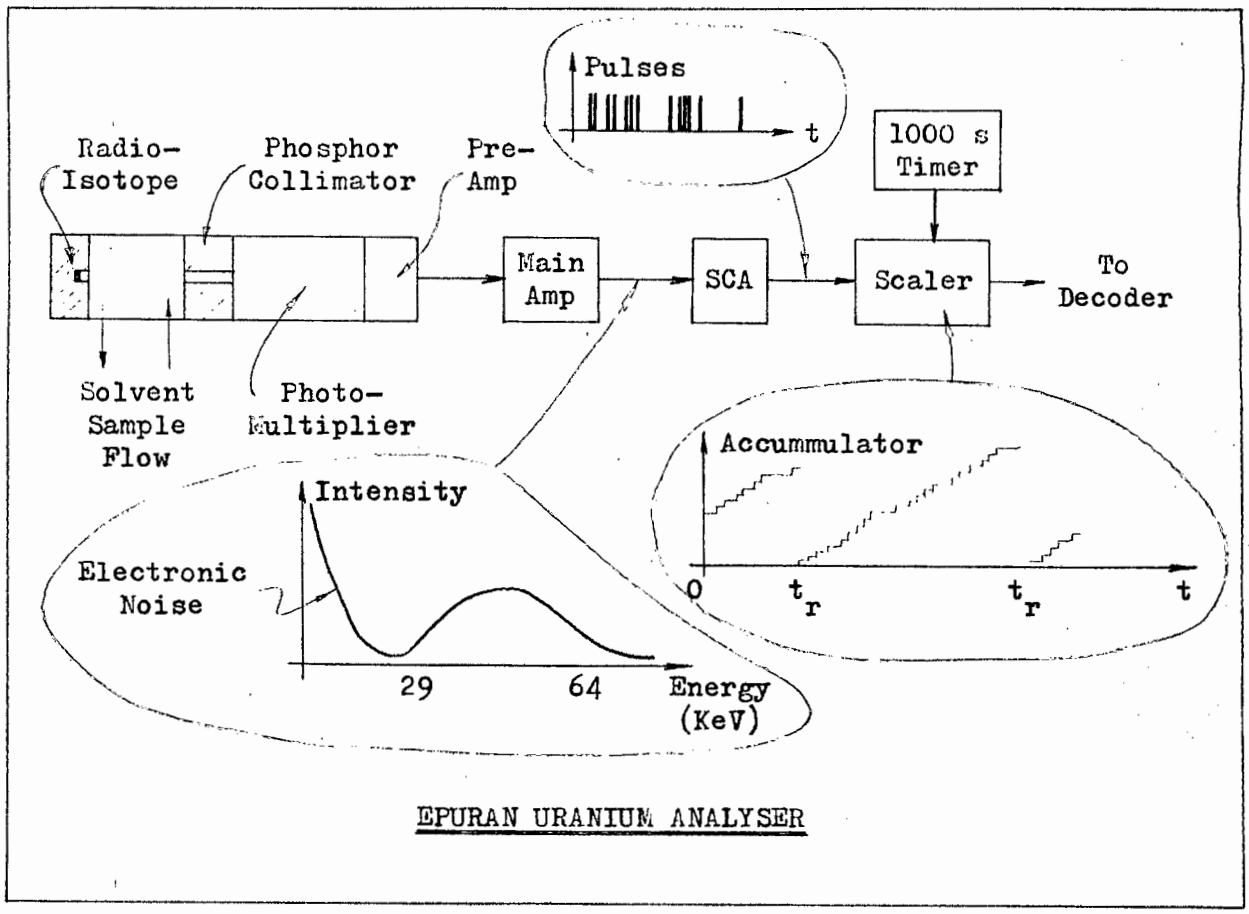

Figure 2.3

as this measurement is of interest in control of the section the EPURAN was used to analyse the pregnant solution on-line for a trial period. However due to the differences between the organic and aqueous phase absorption characteristics it did not yield any useful results.

The EPURAN System

The complete EPURAN system of on-line uranium analysers used in the experiments is shown in figure (2.4). In addition to the counts from the solvents from stages 3 and 4, the temperature of the settlers solvent, the photo-multiplier tube (PMT) head and the room temperature are also printed on the printer output. So temperature correction was readily implemented.

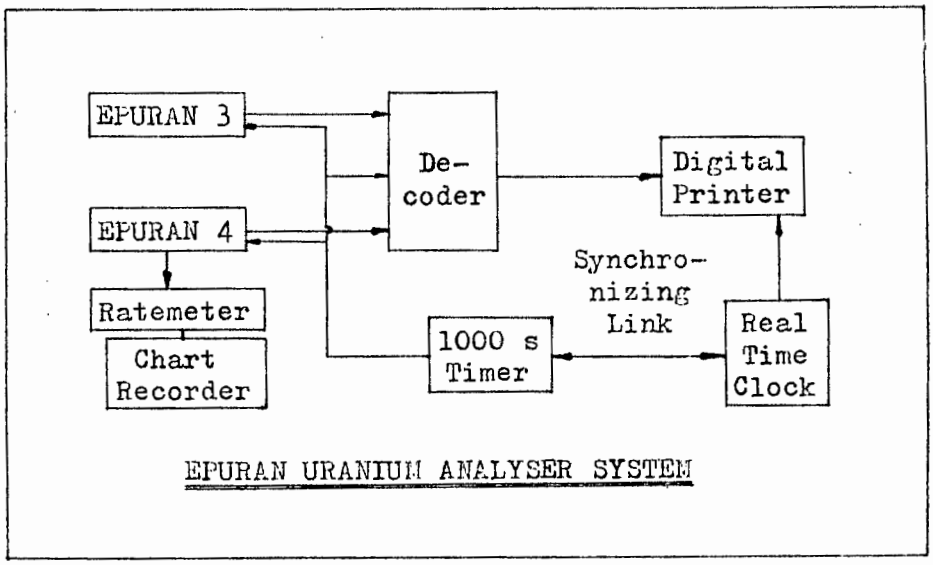

Figure 2.4

Calibration

The EPURAN analysers were calibrated by taking samples synchronously with the print-out during the perturbation tests. These samples were analysed by the mine assay office using X-ray spectroscopy techniques and the assay is regarded as accurate. Previous work [27] showed that a linear calibration curve for all the EPURAN analysers was adequate, so using 35 samples from stage 3 and 38 from 4, the following calibration lines were obtained by a least squares line fit to the data. The range of the readings was from 0,18 to 2,48 gl^{-1} for stage 3 and 2,30 to 3,60 gl^{-1} for stage 4 which covers the normal operating ranges of the instruments.

$$y_3 = -4{,}325 \times 10^{-6}\, c_3 + 11{,}610 \quad gl^{-1}$$
$$y_4 = -3{,}903 \times 10^{-6}\, c_4 + 13{,}286 \quad gl^{-1} \qquad (2.2)$$

where c_3 and c_4 are the counts registered in 1000 s for stages 3 and 4 resp. and y_3 and y_4 are the equivalent uranium concentrations

Standard deviations of the uranium concentrations calculated using the calibration lines from the measured uranium concentrations were 0,023 for stage 3 and 0,010 gl^{-1} for 4 which is more optimistic than those found for the EPURAN on its eight day calibration run [27], namely, 0,083 gl^{-1} for stage 3 and 0,095 for 4. This might be due to a number of factors such as temperature etc.

Discussion

EPURAN is a highly complex instrument and the question of stability and reliability of the readings is extremely important. The system has been extensively tested and the main points are given here.

Tested over a one month period on a static sample of solvent the maximum

spread in readings was 2,6% of the mean value [25] showing that the electronic and detector drift is effectively zero. Hence the EPURAN was considered to be stable for the duration of the experiments.

An all-inclusive indication of the EPURAN accuracy is given by the spread in readings used to derive equation (2.2), but it was thought necessary to identify potential sources of error so that these could be checked during the execution of the experiments to avoid unnecessary instrumentation errors. The main sources of error are [25]

(i) The random decay of the radio-isotope which introduces 0,01 gl^{-1} random error in the EPURAN output due to statistical decay rates. No control could be exercised over this high frequency error but filtering and input-output correlation in determining the plant weighting function would eliminate it to a large extent.

(ii) Changes in the heterogenous matrix of the solvent caused by air bubbles originating at the solvent sampling points or in the pumps, or by aqueous phase whenever the stage is running 'continuous aqueous'. Both these effects were noticeable in the ratemeter output. Normal and abnormal outputs are shown in figure (2.5). The air bubbles produce long

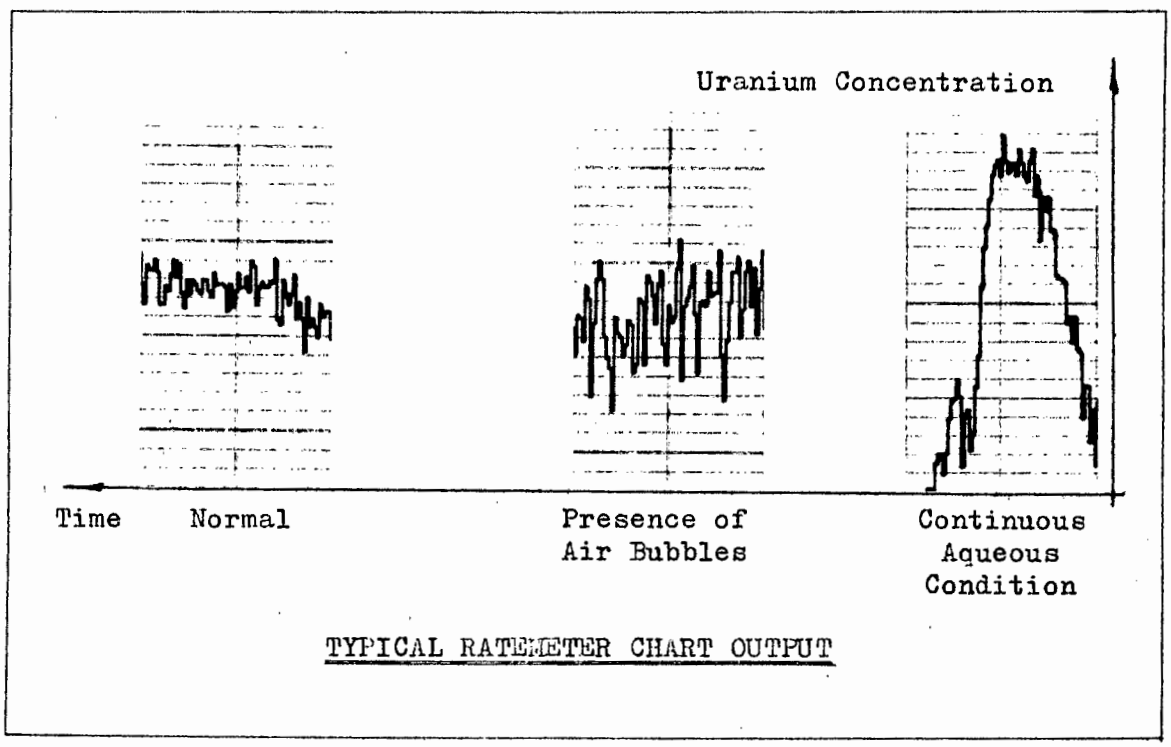

Figure 2.5

'spikes' in the ratemeter output - a high frequency effect - and the 'continuous aqueous condition' produces large rates of change in the readings - i.e. a low frequency effect. Confirmation of these effects could be obtained by stopping the EPURAN feed pump; the air bubbles or aqueous phase bubbles could, if present, then be observed in the static solvent in the PMT head feeder tube.

(iii) Changes in the homogenous organic solvent matrix caused by addition of fresh paraffin to the plant. This alters the density of the solvent and so affects the absorption relation. None was added during the experiments.

(iv) Solvent temperature changes produce 0,009 gl^{-1} change in the uranium concentration readings for every degree centigrade temperature change. The temperature is monitored and recorded so all readings were corrected to eliminate this effect.

2.3.2 THE PNEUMATIC CONTROL VALVE

The PRTS noise, as a pressure signal, was applied to the valve on the pregnant solution feed stream to alter the flow according to the noise. Although the valve is a non-linear element, the fluctuations about the mean flow were intended to be small so that it could be linearized with minimum error.

Pressure to Flow Characteristics

It was not possible to check the valve characteristics by measuring the flow with a calibrated instrument so the valve specifications given by the manufacturers were used. The D.P.Cell flow readings were in agreement with these specifications in which the steady state pressure to flow characteristics are given by

$$Q = 13,1 \sqrt{P - 3,0} \qquad (2.3)$$

where Q is the flow rate in ls^{-1}
and P is the actuating pressure in p.s.i.

Transient Operation

For the experiments equation (2.3) was linearized about its mean operating point using a Taylor series expansion and the transient pressure to flow characteristics are given by

$$\Delta Q = 2,82\ \Delta P \qquad (2.4)$$

where ΔQ and ΔP are the changes in Q and P about their mean values.

Over the range of operation this linearization introduced a maximum theoretical error of 1,6% in the transient flow which is negligible for the purposes of the experiments.

2.4 EXPERIMENTAL EQUIPMENT

Based, initially, on the practical considerations of the instrumentation and the present system of control, and later, supported by the observations of Castro et Al. [14], it was decided to evaluate the impulse response between the pregnant solution feed flow and the uranium loading of the loaded solvent. The PRTS noise was generated on the Varian computer, converted to an analog signal and recorded on one track of the instrument tape recorder. Thus for controlling the pregnant solution flow rate during the experiment, the PRTS noise signal was mixed with a DC voltage from a power supply which represented the plant

steady state operating flow signal to form a flow control voltage which was converted to a pressure signal and applied to the valve actuator.

Pressure to voltage converters were used in conjunction with the D.P. Cells to produce voltage signals proportional to the pregnant solution and solvent flow rates. These signals were recorded on other tracks of the tape recorder together with the ratemeter output so that all plant operating conditions were synchronized with the perturbing PRTS noise signal.

2.4.1 FLOW CONTROL

Voltage Control Signal

The PRTS noise from the recorder had a 1 volt amplitude which was mixed with the DC voltage from a variable voltage source using an operational amplifier mixer shown below to give a flow perturbation signal for the experiment.

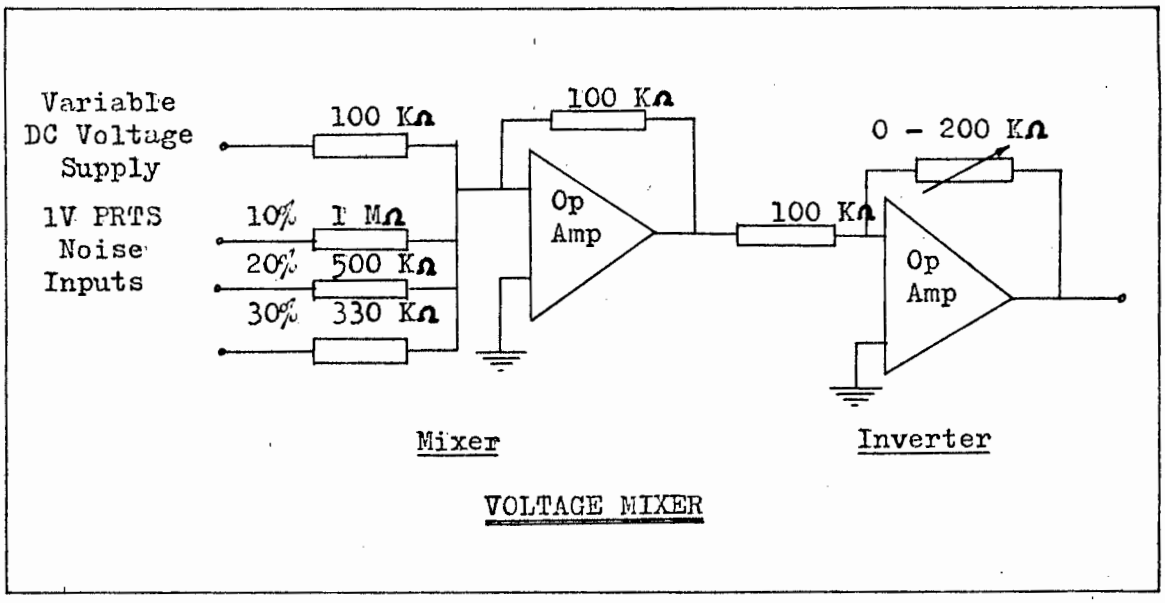

VOLTAGE MIXER

Facilities for varying the degree of modulation of the flow by the PRTS noise and also the steady state flow signal was provided by the three inputs for the PRTS, the variable DC supply and the mixer gain. For design convenience, the output voltage had to fall within the range 0 to 1 V to suite the following transducer stages.

The mixer transfer function is given by

$$V_c = K\ (V_{DC} + a\ V_{PRTS})$$

where V_c is the control voltage fed to the transducer

K is the mixer gain

V_{DC} is the voltage from the DC voltage supply

V_{PRTS} is the voltage from the tape recorded PRTS noise

a is the percentage modulation.

Voltage to Pressure Conversion

The voltage from the mixer (0 to 1 V) was converted to a current (4 to 20 mA) and used to drive a current to pressure transducer (3 to 15 p.s.i.). Calibration of the transducer system was done on the plant after the equipment had been installed. The calibration line of voltage to pressure is given in appendix D and the least squares line for the data is

$$P = 11,97\ V + 2,88 \qquad (2.5)$$

where P is the actuating pressure in p.s.i.
and V is the input voltage in volts.

Thus the overall voltage to flow transduction from voltage to pressure to flow is given by

$$\Delta Q = 33,76\ \Delta V \qquad (2.6)$$

where ΔQ and ΔV are the changes in Q and V.

This expression is valid only for small perturbations about the mean steady state operating point.

For large step changes in the voltage - as imposed when starting - the transducer (current to pressure) went into oscillation, probably due to limit cycling, which had to be stopped by switching off the equipment and re-starting by applying a gradual voltage increase to the system. The PRTS noise voltage changes were sufficiently small not to induce this transducer instability.

The Pneumatic System

The valve flow control signal from the voltage to pressure transducer

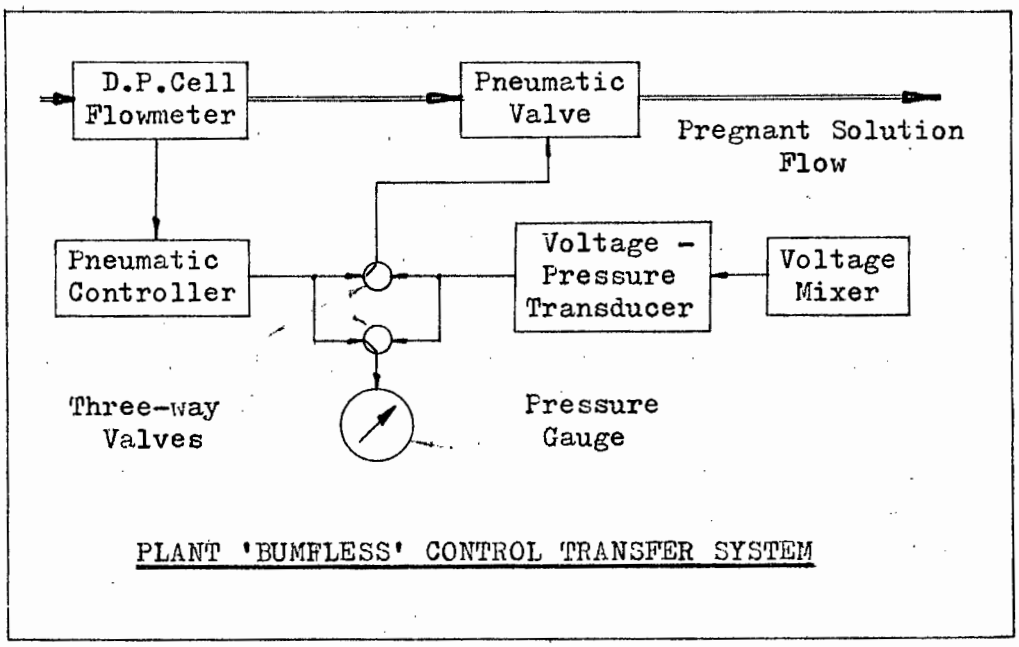

Figure 2.6

replaced the signal from the pneumatic controller during the experiment. To avoid disturbing the plant 'bumpless' transfer of control was achieved by monitoring the controller output pressure and adjusting the voltage mixer gain until the output pressure from the transducer equalled the existing valve actuating pressure. The system used for control transfer is shown in figure (2.6).

No attempt was made to achieve 'bumpless' transfer from the experimental flow control back to normal flow control since the pneumatic control system settled in less than 15 s thus creating little disturbance to the plant.

2.4.2 FLOW AND URANIUM CONCENTRATION MONITORING

Pregnant Solution Flow

The D.P.Cell had the same transfer characteristics as the control valve and so, at the operating point, the cell output pressure signal is given by

$$\Delta P = 0{,}354\ \Delta Q \qquad (2.7)$$

where ΔQ is the transient pregnant solution flow rate in ls^{-1}
and ΔP is the transient output pressure in p.s.i. from the D.P.Cell.

Loaded Solvent Flow

On the solvent streams, the D.P.Cell is smaller than that on the aqueous feed and its characteristics are

$$P = 1{,}75 \times 10^{-2}\ Q^2 + 3{,}0 \qquad (2.8)$$

where Q is the flow rate in ls^{-1}
and P is the output pressure from the D.P.Cell

When linearized about the operating point this becomes

$$\Delta P = 4{,}77\ \Delta Q \qquad (2.9)$$

where ΔP is the transient pressure change in p.s.i.
and ΔQ is the transient flow rate change in ls^{-1}

Pressure to Voltage Transducer

Both flow signals were applied to pressure gauges and angle-to-current transducers produced current signals which were applied to the resistors to give voltage signals proportional to the flow rates. On-line calibration points and a least squares fit gave the following pressure to voltage characteristics.

$$\begin{aligned} V &= 0{,}0794\ P - 0{,}198 \quad \text{(aqueous phase)} \\ V &= 0{,}0816\ P - 0{,}236 \quad \text{(organic phase)} \end{aligned} \qquad (2.10)$$

where V is the transducer output in volts
and P is the D.P.Cell output in p.s.i.

Thus the complete transduction of flow to voltage is given by

$$\begin{aligned} &\text{Pregnant solution flow rate} && \Delta V = 0{,}0281\ \Delta Q \\ &\text{Loaded Solvent Flow Rate} && \Delta V = 0{,}0143\ \Delta Q \end{aligned} \qquad (2.11)$$

for small perturbations about the steady state operation in the main experiments.

Loaded Solvent Uranium Concentration

The 0 to 100 mV signal from the EPURAN 4 ratemeter corresponds roughly to a 2 to 4 gl^{-1} uranium loading. The actual calibration was done using the assayed uranium concentrations and the corresponding ratemeter output. The least squares line is

$$y_4 = 0{,}0149\ r_4 + 2{,}305 \qquad (2.12)$$

where y_4 is the uranium concentration in the loaded solvent in gl^{-1}
and r_4 is the ratemeter reading on the chart in percentage.

DISCUSSION

The plant hardware has only been considered from the point of view of the steady state errors which might be introduced by linearization and calibration of the equipment. But transient responses of the equipment is of extreme importance in studies of dynamic behaviour and the equipment was checked on the plant to ensure that it did not interfere with the results of the experiments. The slowest element in the experimental arrangment was the pneumatic valve on the pregnant solution stream and its response time of less than 10 s to a step change of 10 ls^{-1} in the flow was far faster than the expected plant response time.

2.5 MASS BALANCE MODELS

In order to glean some information concerning plant behaviour prior to the execution of the perturbation tests, a suitable theoretical model proposed in literature [9] was simulated on the digital computer and tested. The model will be discussed in two sections: (i) the lumped parameter mixer-settler model which forms the basic plant unit and (ii) the plant as composed of three mixer-settler units in series.

2.5.1 THE MIXER-SETTLER MODEL

Although the most popular mass balance model described the stage output

concentrations in terms of the input concentrations and not in terms of the flow rates, it does show that re-cycling of the organic phase is equivalent to increasing its stage residence time. It can also be shown that the residence time is very sensitive to changes in the re-cycle ratio, r, when it exceeds 0,5.

The model of one mixer-settler unit is derived here and used to illustrate this effect. The basic equations obtained are used in the next section in deriving a suitable model for the plant.

Consider stage n

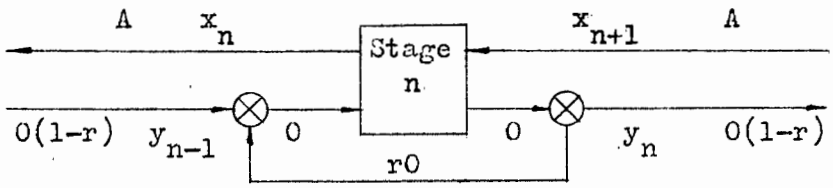

where A and O are aqueous and organic phase flow rates respectively

x_n and x_{n+1} are the uranium loadings of the output and input aqueous phase streams respectively.

y_n and y_{n-1} are the uranium loadings of the output and input organic phase streams respectively.

V_a and V_o are the aqueous and organic phase hold-up volumes respectively.

Then from a simple mass balance across the stage for each individual phase the following equations were obtained:

$$T_a \dot{x}_n = x_{n+1} - x_n$$

$$\frac{T_o}{(1-r)} \dot{y}_n = y_{n-1} - y_n \qquad (2.13)$$

where $T_a = V_a/A$ is the aqueous phase residence time

$T_o = V_o/O$ is the organic phase residence time

Equations (2.13) were simulated on the digital computer using Runga-Kutte integration. The stage parameters used were obtained from plant records and previous work done on the plant [28] and are given in the table below.

Phase	Residence Time (s)	Flow Rate (ls^{-1})
Aqueous	2160	30,3
Organic	756	1,75

The program was written in BASIC for execution on the Varian computer; the listing for the program is given in appendix E. Two options were provided in the program: (i) The simple lumped parameter model described by equation (2.13) could be changed to that of a distributed parameter model due to Van de Vusse [18]

which, for reasons given below, is not used here and (ii) A time lag could be imposed on the streams flowing through the settler to simulate transport and separation lags.

Observation

(i) The Van de Vusse model was not found to be useful since it sacrificed simplicity for little gain in versatility. This was attributed to the existence of a dominant pole in the distributed parameter model transfer function which produced predominantly lumped parameter model behaviour.

(ii) Of all the parameters the model of equation (2.13) is most sensitive to changes in the re-cycle ratio, the sensitivity increasing with 'r' for r greater than 0,5. This is shown in figure (2.7). The sensitivity is explained by considering the solution of equation (2.13) when an impulse is applied to the model. The percentage change in output at any time is proportional to the ratio r/(1-r) times the percentage change in r which is greater than 1 for r greater than 0,5.

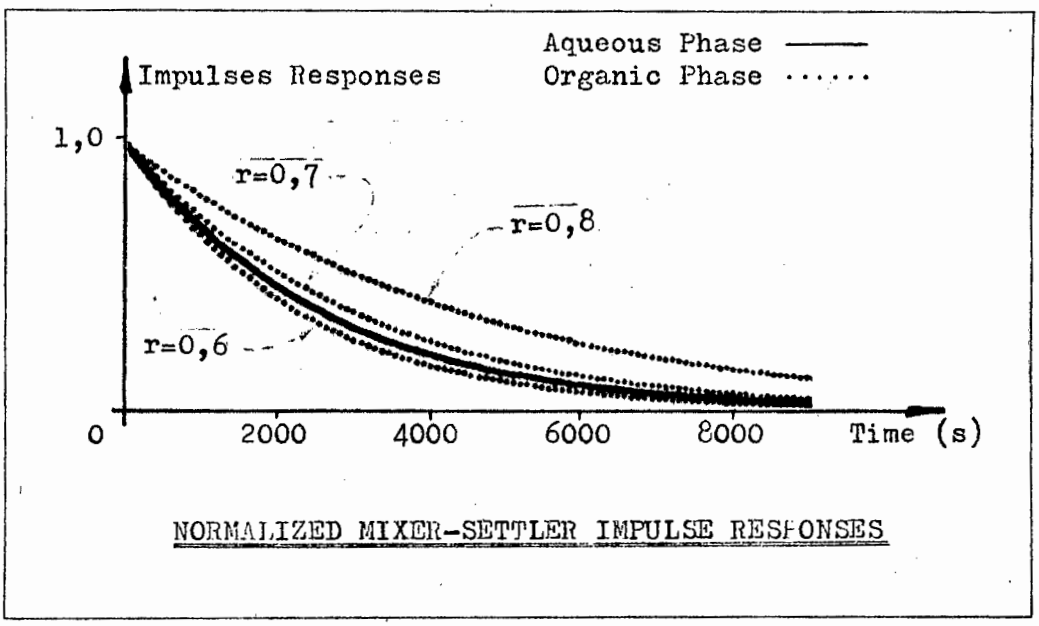

Figure 2.7

2.5.2 PLANT MODEL

A theoretical model of plant behaviour was required to satisfy two specific needs: (i) To estimate the effect that changes in the uranium concentrations of the feed streams had on the uranium loading of the solvent extract since the input concentrations could not be controlled during the PRTS noise tests.
(ii) To provide a 'form' of transfer function which could be fitted to the experimental CCF impulse response.

Combining the two equations (2.13) and linearizing to produce the concentrations in terms of the flow rates and input stream uranium concentrations,

the uranium loading of the organic phases in the plant can be expressed by the matrix differential equation

$$\dot{\underline{y}}(t) = \underline{A}\,\underline{y}(t) + \underline{B}\,\underline{u}(t) \qquad (2.14)$$

where the vectors are $\underline{y}^T = \{y_2, y_3, y_4\}$

$$\underline{u}^T = \{0, A, x_5, y_1\}$$

and the matrices are

$$\underline{A} = \begin{bmatrix} -(a_2O^o + b_2A^o) & c_2A^o & \emptyset \\ a_3O^o & -(a_3O^o + b_3A^o) & c_3A^o \\ \emptyset & a_4O^o & -(a_4O^o + b_4A^o) \end{bmatrix}$$

$$\underline{B} = \begin{bmatrix} a_2(y_1^o - y_2^o) & c_2(y_3^o - y_2^o) & \emptyset & a_2O^o \\ a_3(y_2^o - y_3^o) & c_3(y_4^o - y_3^o) & \emptyset & \emptyset \\ a_4(y_3^o - y_4^o) & a_4x_5 - c_4y_4 & a_4A^o & \emptyset \end{bmatrix}$$

The constants a_i, b_i and c_i are defined below, $\emptyset$ is zero, and the superscript 'o' denotes the steady state value.

Derivation

The model is based on the previous mixer-settler model and its derivation follows the lines of Ottertun's model with regard to linearization of the basic equations obtained from a mass balance.[9] The matrices are derived by considering stage 'n' of a three stage plant - the stages are n = 2, 3 and 4 in keeping with the numbering adopted on the uranium plant.

In addition to the assumptions made in section (2.5.1) , it is assumed that the parameters are independent of stage number and that the cross-phase relationships are given by

$$\begin{aligned} y_n^o / x_n^o &= K_n \text{ for steady state values} \\ y_n / x_n &= k_n \text{ for transient values} \end{aligned} \qquad (2.15)$$

The two equations (2.13) can then be combined by the relationships of equation (2.15) and the solvent uranium loading of each stage is then given by

$$\dot{y}_n = a_nOy_{n-1} + (a_nO + b_nA)\,y_n + c_ny_{n+1} \qquad (2.16)$$

where y_i, A and O are functions of time and the constants are

$$a_n = \frac{1 - r}{V_o + V_a/K_n}$$

$$b_n = a_n/\{(1-r)K_n\}$$

$$c_n = a_n/\{(1-r)K_{n+1}\}$$

Defining the vector $\underline{r}$ as

$$\underline{r}^T = \{y_{n-1},\ y_n,\ y_{n+1},\ 0,\ A\}$$

and changing to functional notation, equation (2.16) can be expressed as

$$\dot{\underline{y}} = f(\underline{r}) \qquad (2.17)$$

which at steady state is $\dot{\underline{y}} = \emptyset = f(\underline{r}^o)$

Using Taylor series expansion of equation (2.17) about the steady state operating point

$$f(\underline{r}) = f(\underline{r}^o) + \sum_{n=1}^{5} \left(\frac{\delta f}{\delta \underline{r}}\right)^o (\underline{r} - \underline{r}^o) + \text{higher derivatives}$$

Substituting for the derivatives from equation (2.16), re-defining the variables r_i of the vector $\underline{r}$ to be the transient values (i.e. $\underline{r}_i = \underline{r}_i - \underline{r}_i^o$) and changing K_n to k_n in the constants a_i, b_i, and c_i, equation (2.16) becomes

$$\dot{y}_n = a_n 0^o y_{n-1} - (a_n 0^o + b_n A^o) y_n + c_n A^o y_{n+1} + a_n(y^o_{n-1} - y^o_n)0 + c_n(y^o_{n+1} - y^o_n)A \qquad (2.18)$$

which yields the matrix equation (2.14) when generalized to three stages in series and written in matrix form.

Digital Simulation of Equation (2.14)

The solution to equation (2.14) is given by [21]

$$\underline{y}(t) = \exp\{\underline{A}(t-t_o)\}\ \underline{y}(t_o) + \int_{t_o}^{t} \exp\{\underline{A}(t-s)\}\ \underline{B}\ \underline{u}(s)\ ds \qquad (2.19)$$

Assuming that (i) the output vector, $\underline{y}$, is observable at time intervals T i.e. at times t_o, t_o+T, $t_o+2T,\ldots,t_o+kT,\ldots$ and (ii) the input vector, $\underline{u}$, is constant over each interval, T, equation (2.19) can be used to express the value of $\underline{y}(t+T)$ in terms of the value at time t - i.e. $\underline{y}(t)$ - as required for digital simulation of equation (2.19)[9]:

$$\underline{y}(t+T) = \exp\{\underline{A}t\}\ \underline{y}(t) + \int_{0}^{T} \exp\{\underline{A}s\}\ ds\ \ \underline{B}\ \underline{u}(t) \qquad (2.20)$$

This equation is evaluated by calculating the following matrices and using equation (2.21) which is equivalent to equation (2.20):-

$$\exp\{\underline{A}t\} = \sum_{n=0}^{\infty} \frac{\underline{A}^n T^n}{(n+1)!} \qquad \text{(The transition matrix)}$$

$$\underline{S} = \int_0^T \exp\{\underline{A}s\}\, ds = \sum_{n=0}^{\infty} \frac{\underline{A}^n T^{n+1}}{(n+1)!}$$

$$\underline{C} = \underline{I} + \underline{A}\,\underline{S}$$

$$\underline{D} = \underline{S}\,\underline{B}$$

$$\underline{y}(t+T) = \underline{C}\,\underline{y}(t) + \underline{D}\,\underline{u}(t) \qquad (2.21)$$

The program to evaluate this equation was written in BASIC and executed on the Varian computer. A full listing of the program is given in appendix E.

Convergence

After k intervals the plant output is given by

$$\underline{y}(t_o + kT) = \underline{C}^k\,\underline{y}(t_o) + \sum_{n=0}^{k} \underline{C}^{k-n-1}\,\underline{D}\,\underline{u}(t_o + nT)$$

and it is obvious from this that for reasonable input functions the convergence of the simulation is determined by matrix $\underline{C}$.

In all simulations the results, $\underline{y}$, obtained from equation (2.21) were used to show convergence. However a more formal check was provided by the row norm of $\underline{C}$ and the following relationship which ensures convergence if satisfied

$$\|\underline{C}\|_\infty < 1 \Rightarrow \lim_{k\to\infty} \underline{C}^k \to \underline{0}$$

where $\|\underline{C}\|_\infty$ is the row norm of matrix $\underline{C}$.

Simulation Parameters

The parameters used in simulating the plant behaviour from equation (2.21) were obtained from previous plant tests [28] and plant records as listed below:

	Aqueous Phase	Organic Phase	Plant
Mixer-settler Volume	23 m^3	23 m^3	47 m^3
Hold-up Volume	23 m^3	2,3 m^3	-
k_n	-	-	324
Re-cycle Ratio	-	0,65	-

The steady state vector about which the plant behaviour is modelled is

$$\{\underline{y}^o\}^T = \{y_2^o, y_3^o, y_4^o\} = \{0{,}12 \quad 1{,}30 \quad 3{,}10\} \quad \text{in } gl^{-1}$$

$$\{\underline{u}^o\}^T = \{O^o, A^o, x_5^o, y_1^o\} = \{2{,}03 \quad 23{,}3 \quad 0{,}23 \quad 0{,}00\} \quad \text{in } gl^{-1} \text{ and } ls^{-1}$$

Simulation Results

The characteristic matrix for the system, $sI - A$, has real negative eigenvalues so the step and impulse responses are exponential with no oscillatory mode superimposed. The print-out from a typical simulation program run is shown below. Graphic output of the results was not possible because of the limited core size of the Varian.

```
SIM TIME: 8000    NO OF PNTS: 100  DELTIME: 80

SYSTEM MATRIX A

-9.07601E-04     3.03308E-05     0
 4.21767E-04    -9.07601E-04     3.03308E-05
 0               8.77270E-04    -9.07601E-04

SYSTEM MATRIX B

-5.06140E-05     1.53605E-06     0               8.77270E-04
-4.97680E-04     2.34314E-06     0               0
-7.59206E-04     9.66028E-04     9.82715E-03     0

MATRIX C = I + A*S

 .930003         2.25668E-03     2.73453E-06
 3.13805E-02      .930082        2.25668E-03
 1.09981E-03     6.52711E-02      .930044

MATRIX D = S*B

-3.95174E-03     1.18821E-04     7.47519E-07     6.76956E-02
-3.85403E-02     2.72083E-04     9.08354E-04     1.12758E-03
-5.99179E-02     7.45520E-02      .758334        2.68390E-05

    TIME              ORGANIC PHASE URANIUM LOADING

                    STAGE 2         STAGE 3         STAGE 4

 0                  0               0               0
 400                5.27136E-04     2.67531E-03      .324384
 800                9.33374E-04     7.34427E-03      .551156
 1200               1.26727E-03     1.25654E-02      .710374
 1600               1.55202E-03     1.75928E-02      .822637
 2000               1.79850E-03     2.20824E-02      .902123
 2400               2.01212E-03     2.59155E-02      .958629
 2800               2.19612E-03     2.90925E-02      .998958
 3200               2.35314E-03     3.16715E-02     1.02784
 3600               2.48574E-03     3.37336E-02     1.04861
 4000               2.59654E-03     3.53633E-02     1.0636
 4400               2.68823E-03     3.66401E-02     1.07444
 4800               2.76341E-03     3.76334E-02     1.08232
 5200               2.82454E-03     3.84018E-02     1.08805
 5600               2.87390E-03     3.89935E-02     1.09223
 6000               2.91347E-03     3.94475E-02     1.09529
 6400               2.94502E-03     3.97949E-02     1.09754
 6800               2.97004E-03     4.00599E-02     1.09919
 7200               2.98978E-03     4.02617E-02     1.10041
 7600               3.00529E-03     4.04151E-02     1.1013
READY
```

Since the equations have been set up assuming that plant operation is linear, the magnitude of the plant responses are linearly related to the perturbation amplitude. Hence all the simulations were run for 10% step changes in the input variables - i.e. the components of vector $\underline{u}$ - and the responses to other changes were deduced from the results.

The row norm of matrix $\underline{C}$ is seen to be less than unity for the plant and the simulations are thus convergent for bounded inputs. The speed of convergence can be estimated from the norm which is of the order of 0,9.

Useful information regarding the plant behaviour which was obtained from the simulations are

(a) The response of the model to changes in the inputs is insensitive to variations in the transient cross-phase relationship. (A 300% change in k_n produced a 2% change in the final uranium concentration of the loaded solvent following a step change in the pregnant solution flow rate.)

(b) Step responses to 10% changes in the steady state variables resulted in the following final values

Input Variable	y_2	y_3	y_4
(i) Preg Soln Flow	0,009	0,121	3,670
(ii) Fresh Solv Flow	-0,026	-0,210	-0,479
(iii) Preg Soln U Conc	0,001	0,008	0,269
(iv) Fresh Solv U Conc	0,010	0,005	0,004

Conclusions

The Uranium concentration of the loaded solvent is apparently most sensitive to changes in the pregnant solution flow rate. This is in agreement with the observations of Castro et Al.[14] Thus variations in the uranium concentrations of the aqueous and organic phase feed streams during the perturbation tests are unlikely to produce appreciable changes in the extract solvent loading which might swamp the response to the pregnant solution flow rate changes. Any variations will be low frequency because both streams are drawn from large buffer storage tanks and the statistical properties of the PRTS noise will eliminate them to a large extent.

Model settling times which were observed are of the order of 8000 s which supports the conclusions drawn from figure (1.4) showing a record of normal plant operation.

Changes of less than 10% in the pregnant solution flow rate will produce variations in the uranium concentration of the loaded solvent which could be measured using the EPURAN system provided the digit length of the PRTS noise is of the order of a few 1000 s to avoid aliasing in the samples taken.

CHAPTER 3 DATA HANDLING

All data handling - capture, processing and display - was done using a Varian 620/i mini-computer which has magnetic and paper tape facilities, analog to digital (A/D) and D/A converters, a graphic display with a hard-copy unit and a teleprinter. Software was developed to input and output data via the desired peripherals, to generate and output PRTS noise and to calculate the necessary functions of which the most important are the correlation functions, the Fourier Transforms and the Bode Diagrams. Programs were written in DAS, the Varian assembler language, and use the mathematical routines from CALC, the plotting routines of TPLO and a translation of the IBM FORTRAN IV Fast Fourier Transform algorithm, FOUR1.

3.1 SOFTWARE EXECUTIVE PROGRAM

For convenience, the software operations were completely controlled by commands entered via the teleprinter by the operator. The software executive program interfaces between the operator and the available data handling software allowing easy data input and output from peripherals as well as data processing by the available routines. After entering the program parameters, the program specified is executed and on completion of the task, or when an operator interrupt is sensed, control is transferred back to the executive program for the next instruction. The routines avalable in IDKIT - the name given to the data handling programs developed - and their calling characters appear in table (3.1)

TABLE 3.1

Calling Character	Routine Name	Function / Operation
A	AID	Transfers control to AID III M
B	BODE	Calculates the $\log_{10}$ and angle of the specified data
C	CRLTN	Correlates the data specified.
D	DATA	Lists the data storage allocations
E	EXPN	Allows the exponent, natural logarithm or square root to be calculated
F	FFT	Fourier Transforms the specified data
G		
H		
I	INPT	Inputs data from the specified peripheral to the specified data arrays
J		

K		
L		
M	MATHS	Allows addition, subtraction, multiplication and division of the specified data by a constant
N	NYQST	Graphs complex data on a Nyquist plot
O	OTPT	Outputs specified data to the specified data array
P	PRCG	Generates PRTS noise in the specified data array
Q		
R	RRNG	Transfers data from one array to another
S	STRT	Allows operator specification of data storage
T	TRIG	Allows 'sin', 'cos' or 'arctan' of the specified data to be calculated
U	UNIT	Selects the magnetic tape unit
V	VARI	Removes the DC component from the specified data
W	WNDW	Applies a data window to the specified data
X		
Y		
Z	ZERO	Zeros specified data array

3.1.1 DATA ADMINISTRATION

To initialize IDKIT, the available data storage area has to be divided into data arrays of sizes allocated by the operator using the routine 'STRT'. Each array is given a name so that, once specified, the array can easily be referenced. Individual samples in an array are referred to by their position in the array and since the different data types - integer, real and complex - occupy different numbers of computer words per sample, the array type must also be supplied. The notation adopted for referencing data is thus similar to that employed by FORTRAN: The first sample is in position '1' and the n th in position 'n'. Whenever a section of an array is required, it is referenced by setting the array limits when it is specified. E.g. For an N point array, DATAR, the limits can be set by '..DATAR,(i,j,k),..' which means '..the points in DATAR from the i th to the j th, inclusively, considering every k th sample..' Default values of '1', 'N' and '1' are assigned to 'i', 'j' and 'k' if ommitted.

The programs have been designed to allow repetative or redundant specifications to be omitted whenever possible. For example, such default action occurs when successive calls are made on a routine to act on the data array/s. The routine calling character will be sufficient to initiate the routine which will use the parameters supplied in the previous call.

3.2 OUTLINES OF THE PROGRAMS

No detailed flow charts are given for the programs since the routines do not have any major decision loops and loops were only employed to access all

samples in an array. However the function of each routine together with a brief description of its operation whenever this is important is given.

(a) AID

Transfers control from IDKIT to AID III M which is a Varian general purpose system-control program. Control is returned to IDKIT by executing location 010200.

(b) BODE

Converts complex data that is stored in 'real', 'imaginary' form to 'log-modulus', 'angle' form.

Operation

For an N sample array, X, stored in successive 32-bit locations as Re{X(I)} and Im{X(I)} the following operations are performed for $1 < I < N$

$$\mathrm{Re}\{X(I)\} = 0{,}43295\ \mathrm{LOG}_e\{\sqrt{(\mathrm{Re}\{X(I)\})^2 + (\mathrm{Im}\{X(I)\})^2}$$

$$\mathrm{Im}\{X(I)\} = \mathrm{ARCTAN}\ \frac{\mathrm{Im}\{X(I)\}}{\mathrm{Re}\{X(I)\}}$$

where LOG_e and ARCTAN are CALC routines.

(c) CRLTN

Correlates one or two complex data arrays storing the ACF or CCF in the first array specified.

Operation

The correlation is executed using the relationship of equation (1.2) and the Fast Fourier Transform - FFT. So to correlate arrays X and Y the following operations are performed on the arrays:

First	X = FFT of X	
	Y = FFT of Y	(omitted for the ACF)
then for $1 < I < N$	$X(I) = X^*(I)\ Y(I)$	for the CCF
	$X(I) = X^*(I)\ X(I)$	for the ACF
and finally	X = Inverse FFT of X	

Note: (i) The FFT, FOUR1, operates on 2^m samples where 'm' is an integer, so for arrays of length M and N ($M < N$) samples, the program computes the maximum 'm' satisfying $2^m < M$ and correlates only 2^m points of each array. Data outside this 2^m point record is ignored.

(ii) For cyclic correlation it is often more convenient to use arrays with different data lengths, say, N and M, and to form augmented records of 2^m samples by the addition of zeros than it is to sample the data to contain exactly 2^m samples per cycle. The resulting correlation function is then valid for N-M+1 samples which corresponds to lags for which the shorter data record

remains opposite the longer. For example consider the arrays X of N samples and Y of M with M < N

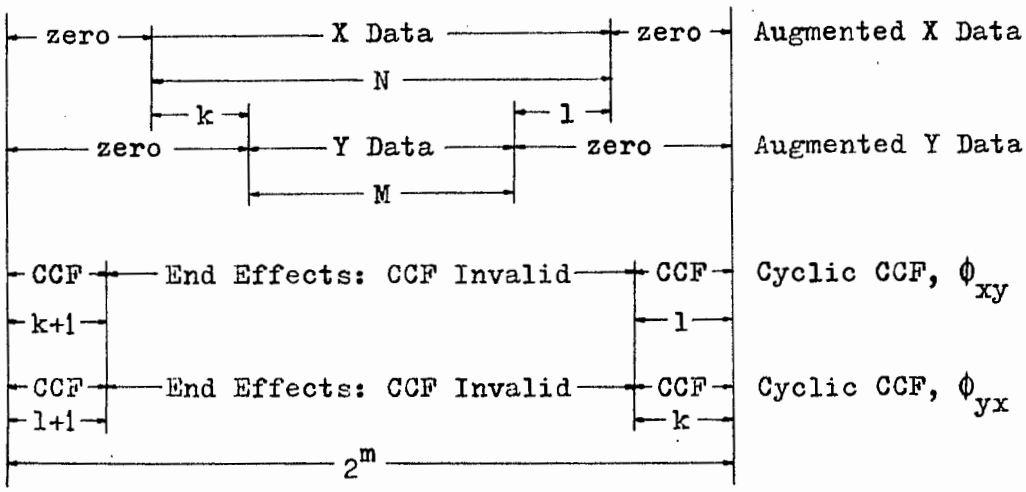

A correction factor '$2^m/M$' must be applied to the resulting aperiodic CCF to obtain the true value of the cyclic correlation function. This factor was expected theoretically - see appendix B - and it should be noted that it is independent of N which is greater than M.

(iii) For system identification using N samples for the PRTS, M for the response and 2^m for the correlation, an additional factor of '$2^m/N$' has to be applied to the CCF to correct for the ACF of the N sample PRTS which is $N/2^m$ too small.

(d) DATA

Lists the data storage allocations made in initializing IDKIT. The data array names, types, sizes and absolute memory locations are given.

(e) EXPN

Permits calculation of the exponential, natural logarithm and square root of the data array specified.

(f) FFT

Calculates the Fast Fourier Transform or inverse transform of the data specified.

Operation

FOUR1, the IBM FFT algorithm, is used to evaluate the summation - see also appendix B.

$$X(k\Omega) = \sum_{n=0}^{N-1} X(nT) \exp\{jk\Omega nT\}$$

where $NT\Omega = 2\pi$ and N is a power of 2.

For the forward transform, the array $X(k\Omega)$ formed from X(kT) by FOUR1 is divided by N to give the FFT of X(nT). In the inverse transformation the division is omitted.

(i) INPT

Allows data input to the specified data array from the peripherals listed below. The input of data is initiated on receipt of the last parameter required by the peripheral driver routine called.

Peripherals

(i) Teleprinter/Graphic Display: Operator input of numeric data.

(ii) A/D Converter: Conversion of analog signals to digital data samples and storage of the data.

(iii) Magnetic Tape: Data input from mass data storage.

(iv) Paper Tape: Input of paper tape binary data.

(m) MATHS

Permits addition, subtraction, multiplication , division or exponentiation of the data by a constant entered.

(n) NYQST

Graphs complex data on an orthogonal set of 'real' and 'imaginary' axes.

(o) OTPT

Outputs data to the Varian peripherals listed below. Initiation of the routine is similar to that of 'INPT'.

Peripherals

(i) Teleprinter/Graphic Display: Listing of arrays as numeric data.

(ii) Graphic Display: Graphic representation of the data.

(iii) Magnetic Tape: Data mass storage

(iv) Paper Tape: Storage of data as binary data on paper tape.

(v) D/A Converter: Output of digital data as analog signals.

(p) PRCG

Generates a PRTS noise according to the parameters entered.

Operation

Calculates the feedback loops for the shift registers from the polynomial co-efficients supplied and generates the PRTS noise using the results of equation (1.16). The initial state of the registers can be explicitly specified if desired.

(s) STRT

Initially the data storage is divided into named sections each having its type - integer, real or complex - and size in number of data samples. STRT converts this information into absolute memory addresses which are stored in an administrative register for later use.

(t) TRIG

Permits calculation of the 'cos', 'sin' or 'arctan' of the data array specified. Units of the angles are radians and the routines used are the tri-

gonometric programs from CALC.

(u) UNIT

Selects the unit to be used when addressing the magnetic tape units.

Operation

The master or slave unit are selected by typing 'U0' or 'U1' respectively.

(v) VARI

Calculates the transients of the specified data array as required before correlating or Fourier transforming.

Operation

The transients are obtained by first calculating the mean of the data and then subtracting this from each data sample to give the transient data sample. The original data is destroyed by the routine.

(w) WNDW

Applies one of three windows to the data array specified. The types available are (i) First Order (ii) Hanning and (iii) Hamming which are dealt with in detail in appendix B.

Note: (i) The use of data windows prior to calculation of the FFT improves the accuracy of the resulting transform but will not improve the correlation function calculated using the FFT.

(ii) The window cannot be applied cyclicly - i.e. To use it the data cannot lie symmetrically about the 't=0' axis but must occupy a section 'i' to 'j' where i < j.

(z) ZERO

Inserts zeros into the array section specified. It is used to initialize an array or to form the added samples of an augmented array.

3.2.1 PROGRAM LISTINGS

A full listing of the above programs and their supporting sub-routines are given in the program file for the thesis - appendix E. The appendix contains listings of all the other programs used with explanations where required.

3.3 SUMMARY OF IDKIT

The complete data processing facility dedicated to calculating system weighting functions using correlation techniques can be summarized by the diagram given in figure (3.1).

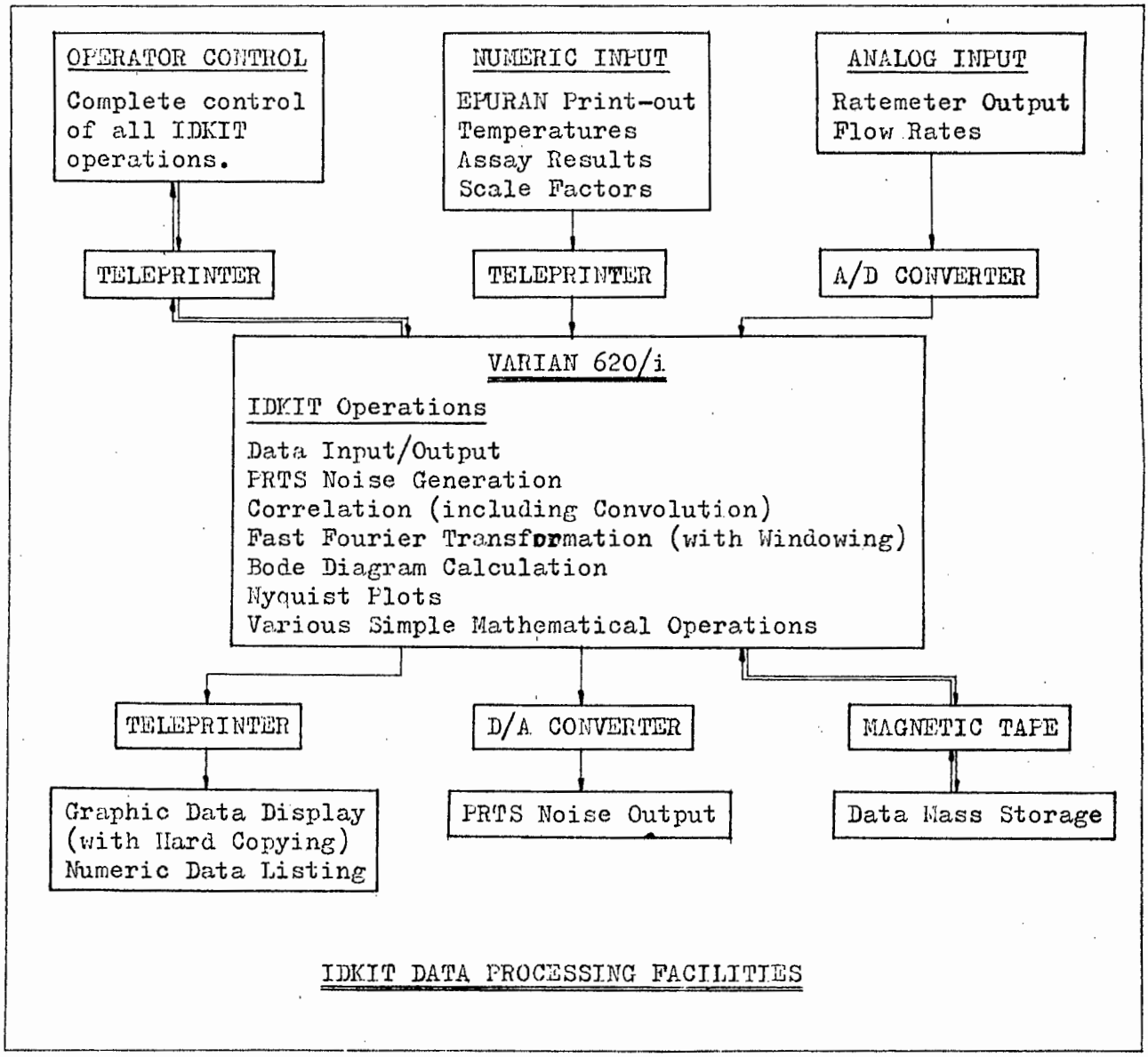
OPERATOR CONTROL
Complete control of all IDKIT operations.
NUMERIC INPUT
EPURAN Print-out
Temperatures
Assay Results
Scale Factors
ANALOG INPUT
Ratemeter Output
Flow Rates
TELEPRINTER
TELEPRINTER
A/D CONVERTER
VARIAN 620/i
IDKIT Operations
Data Input/Output
PRTS Noise Generation
Correlation (including Convolution)
Fast Fourier Transformation (with Windowing)
Bode Diagram Calculation
Nyquist Plots
Various Simple Mathematical Operations
TELEPRINTER
D/A CONVERTER
MAGNETIC TAPE
Graphic Data Display (with Hard Copying)
Numeric Data Listing
PRTS Noise Output
Data Mass Storage
IDKIT DATA PROCESSING FACILITIES

Figure 3.1

CHAPTER 4 PLANT PERTURBATION EXPERIMENT AND CORRELATION RESULTS

Once the software was completed and the correlation technique had been thoroughly tested by identifying systems simulated on an analog computer, attention was focused on the plant.

Briefly the procedure adopted for perturbing the plant is as follows. Two PRTS noise signals of different periods were generated at the computing centre using PRTS parameters which were selected on the strength of observations made of normal plant operating behaviour. The PRTS noise was recorded on an analog tape recorder so that the tape could be used to convey information between the plant and the computer. During the experiment the plant was controlled by the PRTS noise while all relevant data was recorded on the magnetic tape. After the experiment the completed tape was taken back to the computing centre and the data collected on it was processed to yield the plant weighting function.

4.1 PRTS NOISE SELECTION

Applying the criteria discussed in section (1.3.1) the digit length of the PRTS noise was chosen to be 3520 s which represents a compromise between the requirements of the plant bandwidth as determined from plant records - section 1.3.1 - and the number of samples per digit that the EPURAN analyser had to provide to avoid aliasing. Thus an 8 digit PRTS would have a period of 7,7 hours and would, judging from plant records, allow the resulting cross-correlation function to settle between the pulses of the auto-correlation function of the PRTS noise. However experience gained in the laboratory had shown that the system settling time of an unknown system is usually underestimated when selecting a PRTS period and a 26 digit PRTS noise with a period of 25,1 hours was also recorded. Details of the two PRTS noise signals are given in the table below.

PRTS Noise	8 Digit PRTS	26 Digit PRTS
Polynomial	112	1021
Digit Length	3520 s	3520 s
Period	7,72 h	25,1 h
Amplitude	3,79 and 0,76 $1s^{-1}$	0,76 $1s^{-1}$
ACF Impulse Area	$3,80x10^{4}$ and $7,63x10^{2}$	$7,04x10^{2}$ $1^{2}s^{-1}$

Both sequences were generated using the Varian computer, converted to an analog signal by the D/A converters and recorded on the instrument tape recorder at its fast speed. The use of magnetic tape required to convey the data between the plant and the computing facilities also ensured that the main

experimental measurements made would be synchronized with each other and the PRTS noise. This is important in correlation techniques since a lag between the input and output measurements will manifest itself in the input-output CCF as an equal lag. The tape recorder also provided a means of decreasing the time required for data handling during processing because its speed range allows a gain of 32 in time between the fastest and the slowest speeds.

An important practical point not considered in the simulations was the availability of feed liquor for the perturbations. The existence of feed storage tanks of finite capacity favoured a nett increase in pregnant solution consumption during the tests rather than a decrease since the buffer tank is kept full by an automatic level control system. The consumption curves for the two test signals are the time integrals of the transient pregnant solution flow rates and were designed to be predominantly positive. The curves are shown in figure (4.1) and it is obvious that in order to satisfy the storage tank

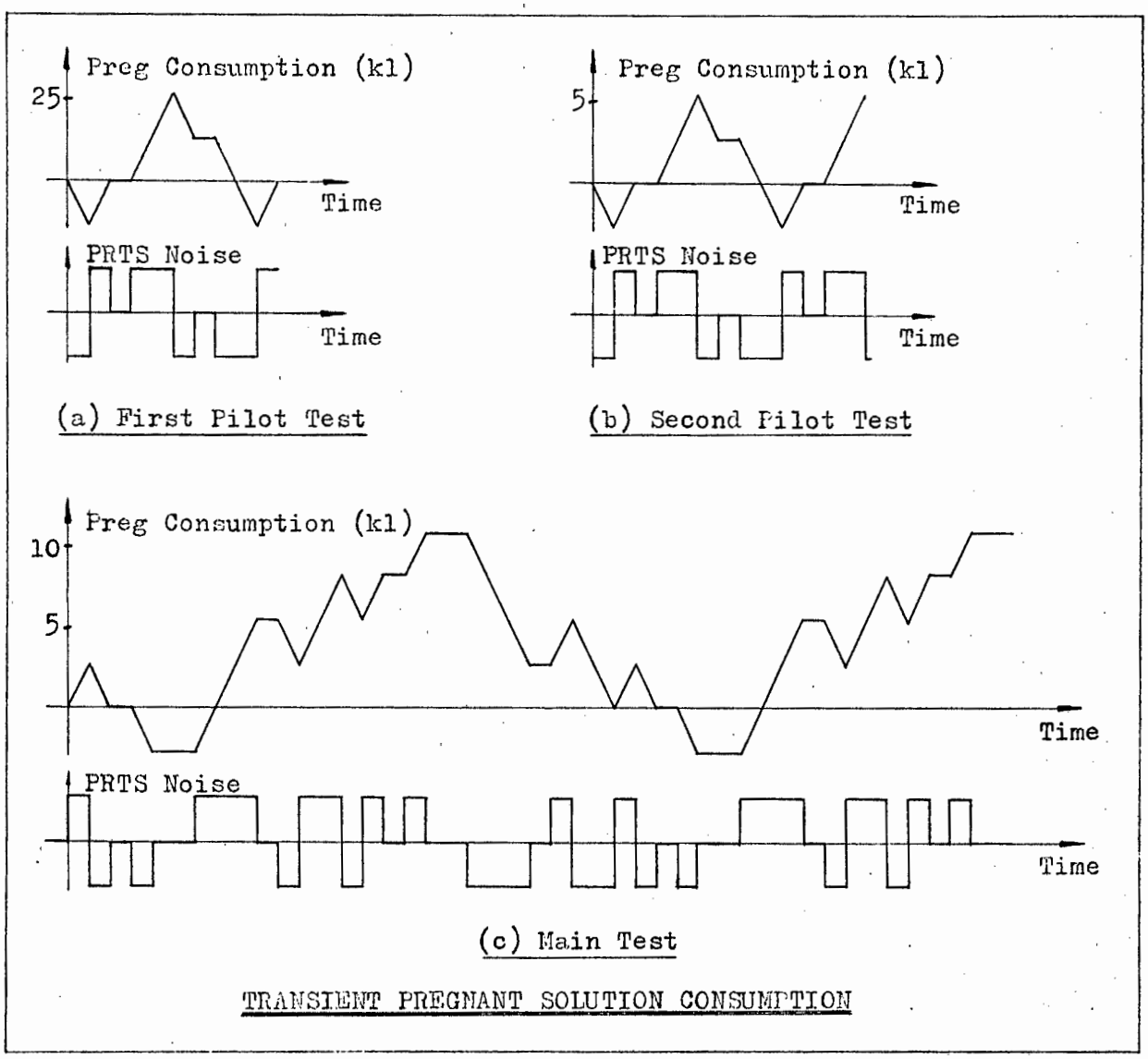

Figure 4.1

requirements, the starting points of the PRTS noise signals have been chosen to give large first order time moments. The disadvantages of this are well known [4] but since it mainly aggravates the drift inherent in the experimental instrumentation, its effects can be eliminated by de-trending the data prior to correlation - appendix B.

4.2 EXPERIMENTS

On the plant the recorder was connected to the experimental equipment which had previously been installed and calibrated, and the complete experimental set-up was checked for linearity and calibrated. The electronic voltage mixer and the DC supply were adjusted to give the desired flow perturbation amplitudes - first 3,79 ls^{-1} (=50 gpm) and then later 0,76 ls^{-1} (=10 gpm) - on steady state flow rates of 26,51 ls^{-1} (=350 gpm) and 30,31 ls^{-1} (=400 gpm) for the pregnant solution.

Prior to initialization of each test, steady state conditions were attained on the plant and the production of the leaching plant checked to ensure that the supply of pregnant solution required for the duration of the experiment could be maintained. The leaching plant was always operating normally so the latter condition was readily satisfied for all the experiments but the former presented some problem. The plant was down on the first day scheduled for the tests and although this shut-down was useful for breaking the pneumatic lines to the pregnant solution control valve and installing the control transfer system of figure (2.6), it meant a delay of 12 to 24 hours from the time of starting the plant until steady state conditions were obtained. Occurrence of the continuous aqueous condition was the most problematic single factor which prevented steady state operation since the stages are highly inter-active due to the free-flow inter-stage connections. Hence each stage was affected by the aqueous condition before the plant settled.

During the experiments thunder storms due to the geographical position of the plant, and mining operations were uncontrollable factors external to the plant which were likely to disturb the plant at any time. Shortly after the start of one experiment it had to be postponed when an unusually powerful under-ground explosion tripped the plant's electrical system and the plant had to be re-started and allowed to settle before the test could be re-run.

4.2.1 THE PILOT TESTS

The 8 digit PRTS noise test was run first since it required a short experimental time - approximately 12 hours - and few difficulties are experienced in maintaining plant stability over such a period. In addition rough estimates for the CCF had to be calculated using a desk calculator to check whether the CCF interfered between pulses of the PRTS noise ACF. For an 8 digit PRTS test the records used for correlation could be limited to 50 samples each without

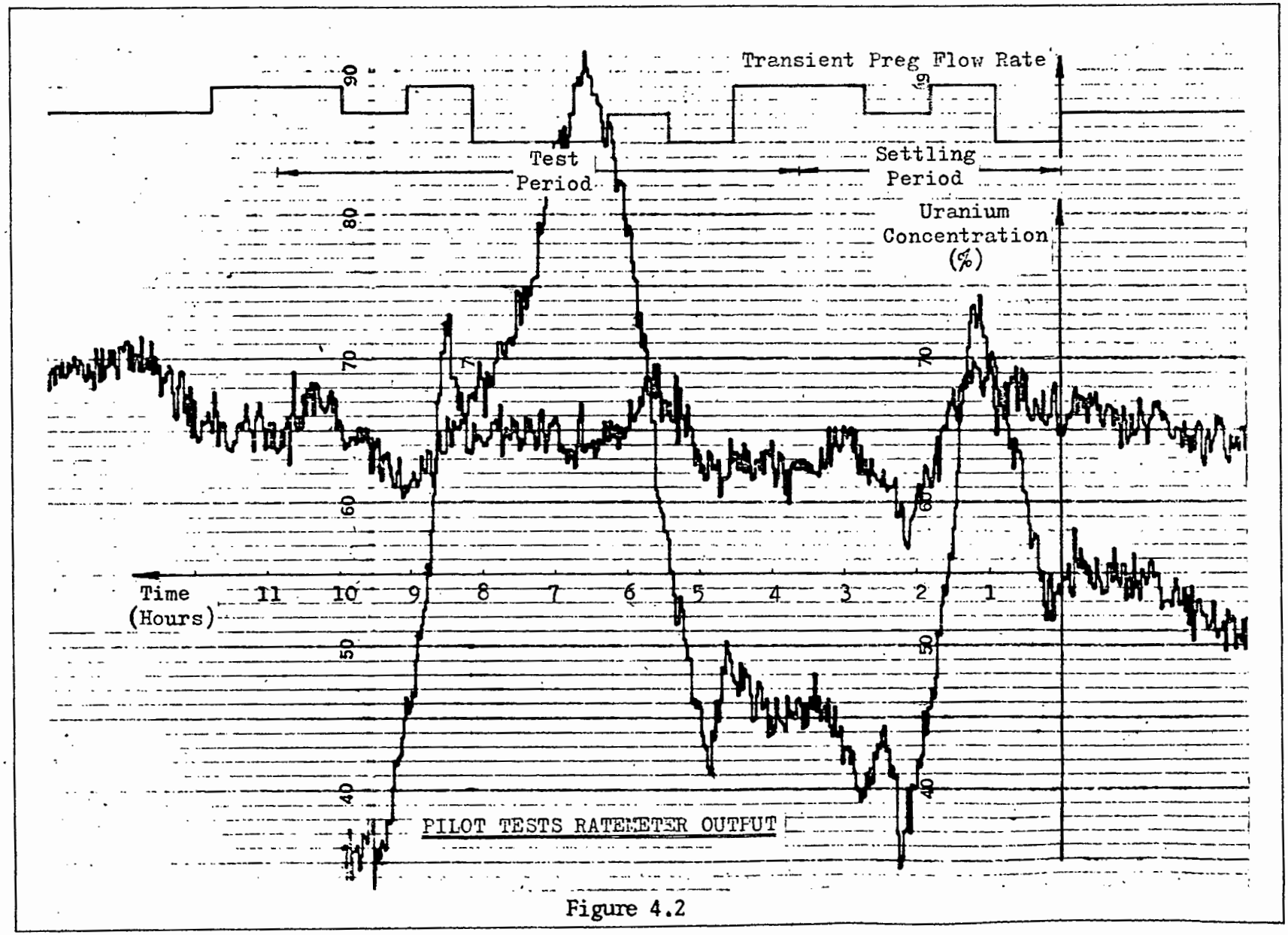
Transient Preg Flow Rate
Test Period
Settling Period
Uranium Concentration (%)
90
80
70
60
50
40
Time (Hours)
11
10
9
8
7
6
5
4
3
2
1
PILOT TESTS RATEMETER OUTPUT

Figure 4.2

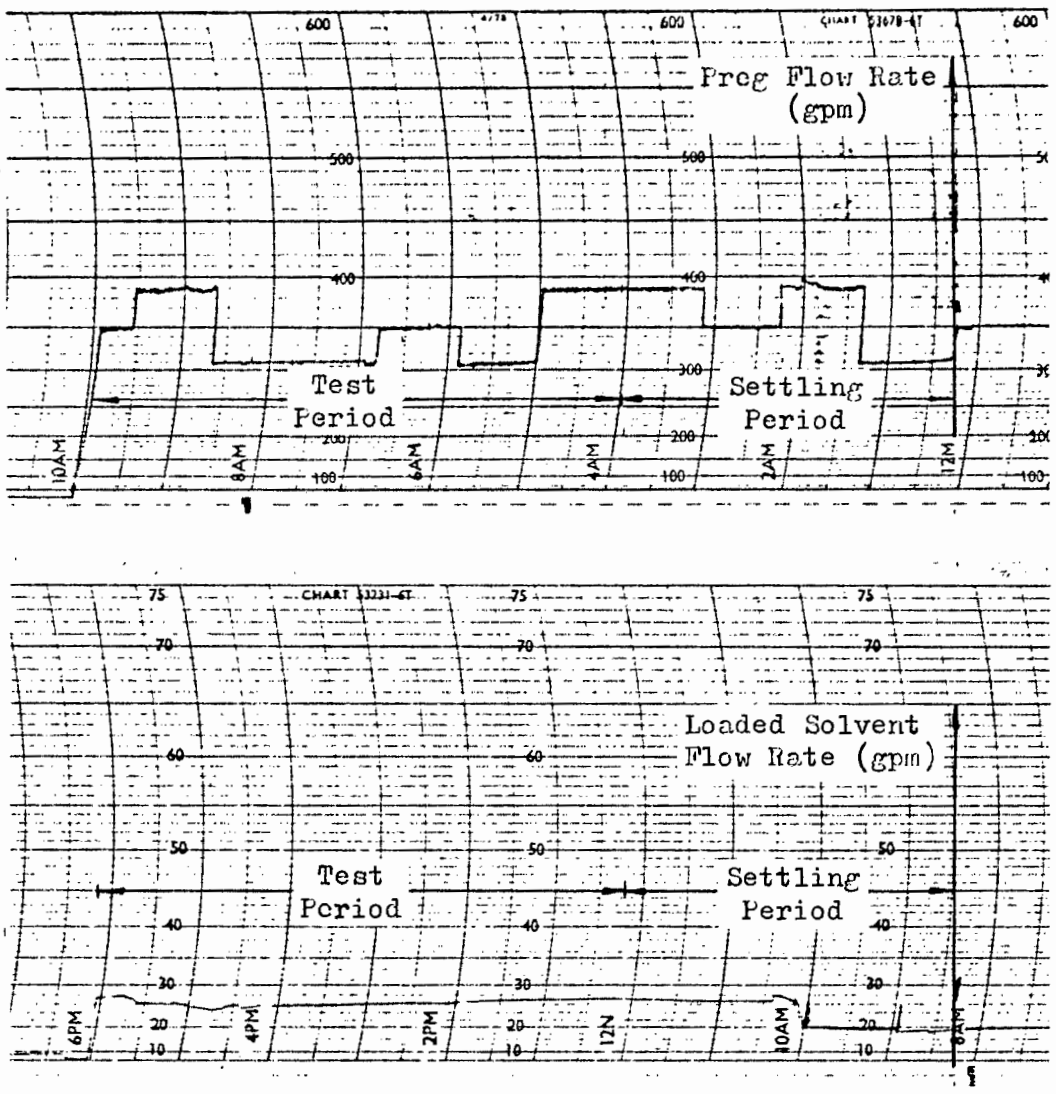

PILOT TEST FLOW RATES

Figure 4.3

having aliasing problems.

Plant simulations - section (2.5.2) - had shown that a perturbation amplitude of 0,76 ls^{-1} would cause sufficient variations in the uranium loading on the loaded solvent to be detected by the EPURAN analyser on settler 4. However it was decided to attempt a more violent initial perturbation of 3,79 ls^{-1} which would ensure large variations in the uranium loadings and also give an indication of plant reaction to large pregnant solution flow rate changes thus revealing possible non-linearities. The results showed that the plant is readily forced into the 'continuous aqueous condition' so correlation of the measurements taken were unreliable as the inter-stage flow rates required continuous adjustment in attempts to eliminate the aqueous condition. The chart record of the uranium concentration of the loaded solvent is given in figure (4.2) which also shows the results of the next experiment for comparison. The plant flow charts for the test are given in figure (4.3). The large low frequency variations in the solvent loading closely resemble those of the continuous aqueous condition shown in figure (2.5) and the graph was held to be unreliable. So although the CCF interfered it was considered to be invalid for two reasons. Firstly because of the continuous aqueous condition and secondly because no settling half cycle was applied to the plant as it tripped before completion of the test run. The CCF calculated from the results is shown in figure (4.4) and the interference is clearly seen.

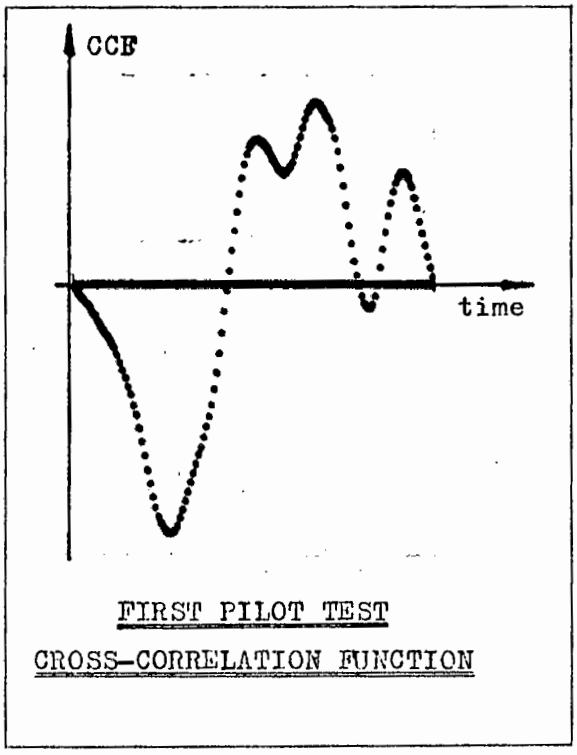

Figure 4.4

Since the first test had required continual adjustment on inter-stage

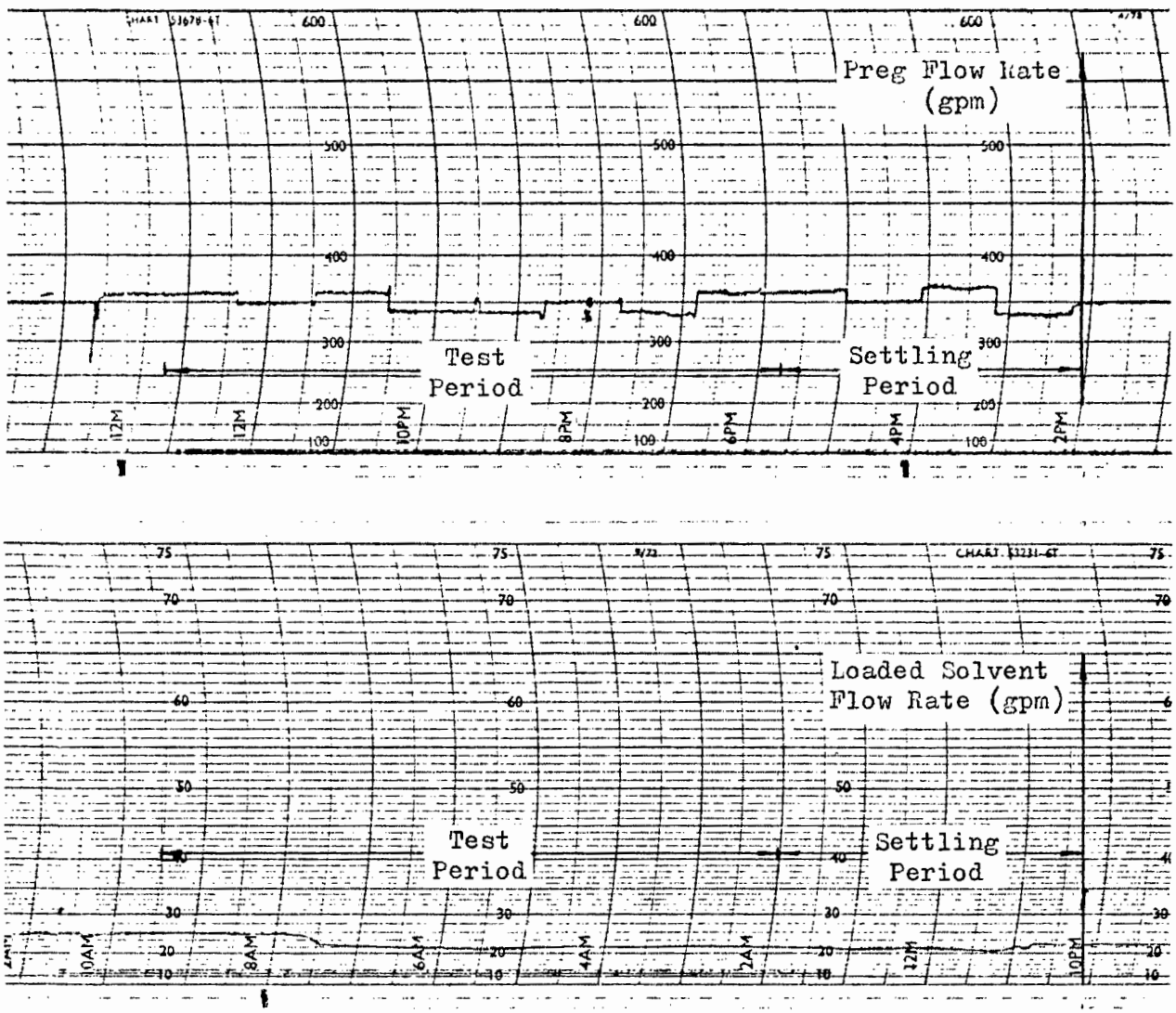

PILOT TEST PLANT FLOW RATES

Figure 4.5

flows during its execution the plant could not be regarded as operating about a single steady state operating point. In fact each alteration of the weirs and valves made to eliminate the aqueous condition shifted the steady state operating point of the plant. So as to avoid the necessity for adjusting the plant during the experimental cycle, the pregnant solution flow rate for the second 8 digit test was perturbed by 0,76 ls^{-1} and the resulting uranium concentration variation , which is the small amplitude trace on the chart in figure (4.2) appears more normal by comparison with figure (2.5). The corresponding record of plant flow rates is shown in figure (4.5). The ratemeter output was sampled for the whole of the test period and then correlated with the PRTS noise which perturbed the pregnant solution flow rate to give the CCF shown in figure (4.6). Again there was interference, indicating that the PRTS noise

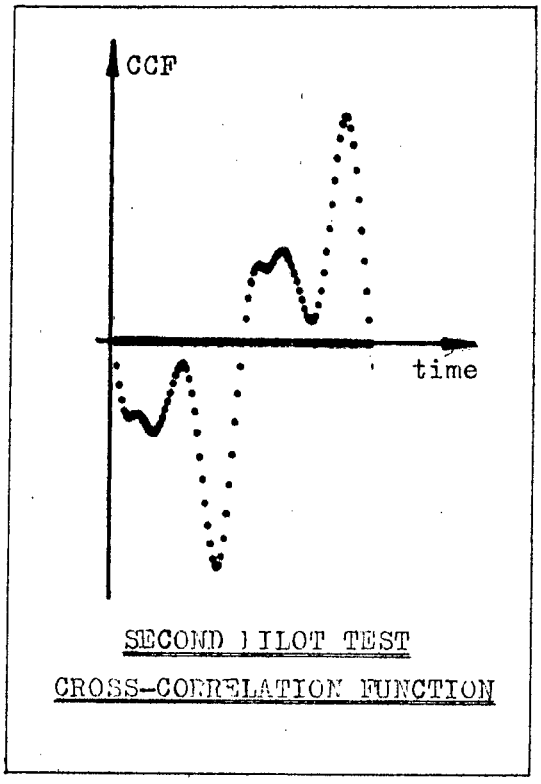

Figure 4.6

period was too short. Thus the first test might not have been as invalid as at first suspected.

4.2.2 THE MAIN TEST

Results obtained from the pilot tests showed that the digit length of 3520 s and the flow perturbation of 0,76 ls^{-1} were suitable for perturbation of the plant in obtaining its weighting function. However the period of the test signal was too short and so the 26 digit PRTS noise signal was applied to the plant next. This test would require approximately 36 hours of stable plant

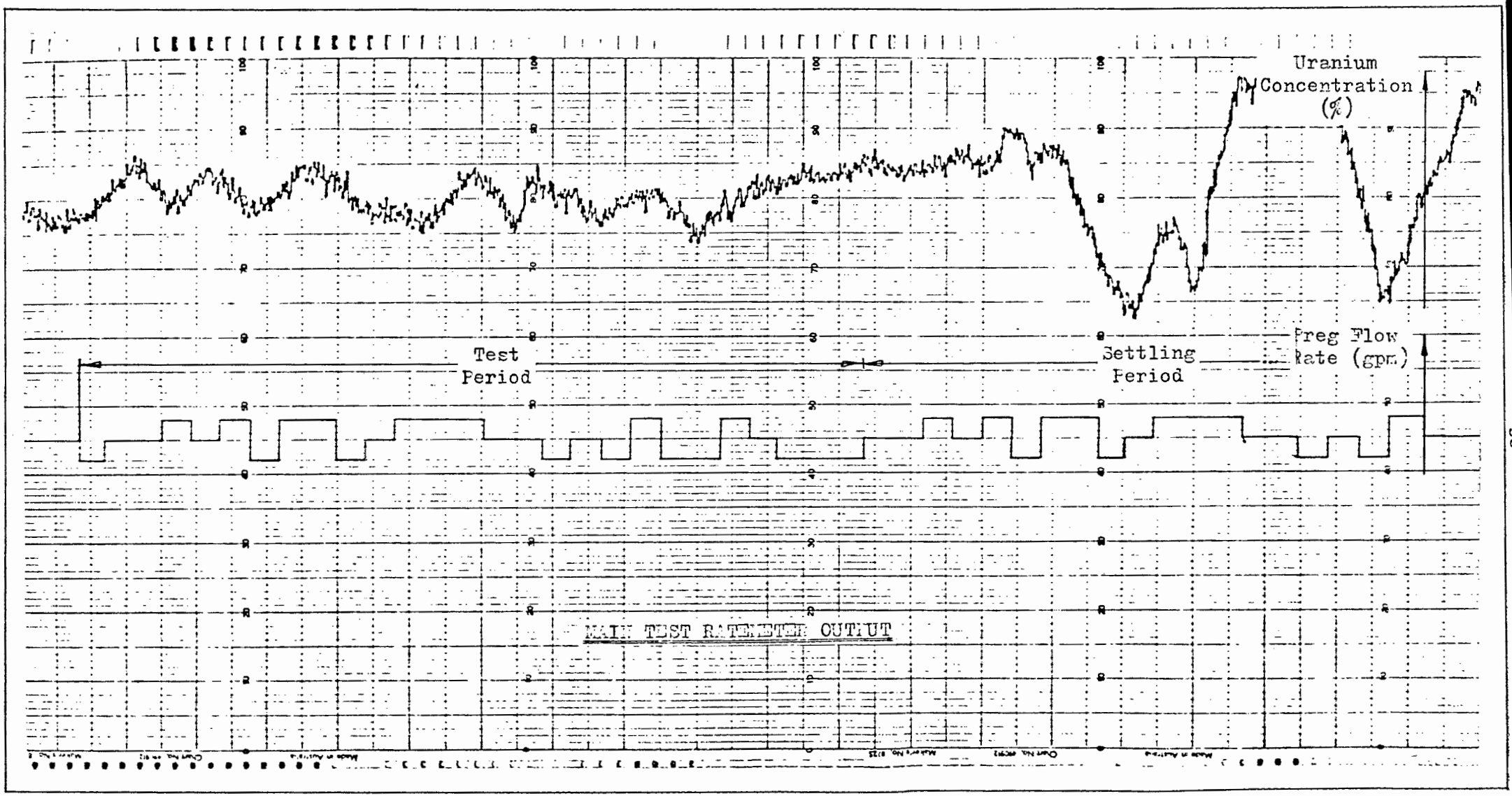
Uranium
Concentration
(%)
Test
Period
Settling
Period
Preg Flow
Rate (gpm)
MAIN TEST RATEMETER OUTPUT

Figure 4.7

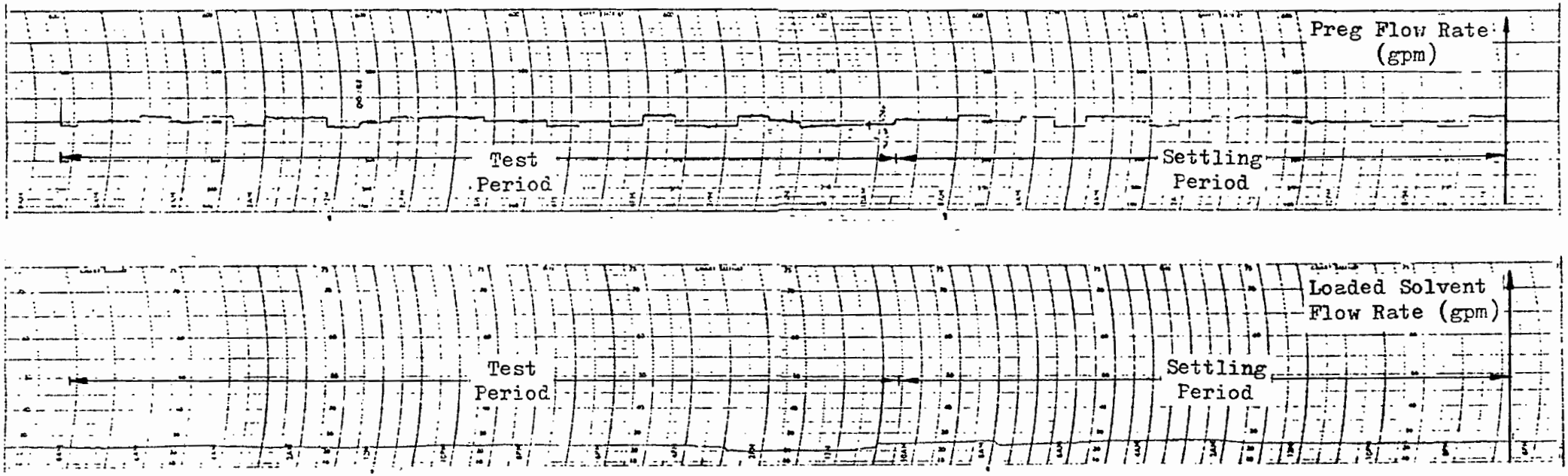

MAIN TEST PLANT FLOW RATES

Figure 4.8

operation. From experience gained during the execution of the pilot tests it was felt that such an extended period of steady state operation would be difficult to obtain even though plant records showed that periods of stable operation in excess of 72 hours were not uncommon.

Perturbations of the pregnant solution flow rate were started following a period of steady state operation of the plant but during the first shift an in-experienced plant operator managed to aggravate the continuous aqueous condition present in mixer-settler 4. However shortly after the start of the second shift and before the test period, the plant returned to normal. For the duration of the test cycle no weirs or valves were adjusted to alter inter-stage flows so that the plant was effectively being perturbed about a single steady state operating point. The ratemeter output and plant flow charts are given in figures (4.7) and (4.8).

The uranium concentration of the loaded solvent during the main test was calculated from the digital print-out rather than the ratemeter output since the 1000 s count interval of the former effectively filtered out the noise due to the random decay rate of the radio-isotope which only manifests itself over the 100 s interval as used for the ratemeter. However using a 1000 s sampling interval for the pregnant solution flow rate - i.e. the PRTS noise - resulted in severe aliasing so the 1000 s interval for the uranium record was effectively reduced to 250 s by digital interpolation of the EPURAN output record and aliasing in the flow rate samples was avoided by using a 250 s sampling interval. The actual record of the EPURAN digital output and the interpolated version of the uranium loading are shown in figure (4.9). The oscillations in the latter (called 'ringing') are due to slight aliasing in the actual record samples and were eliminated before the record was used for correlation.

Random noise in measurements taken for identifying a system using correlation is more readily rejected than harmonic noise - appendix A - so it is advantageous to check the system output record for randomness before correlating it with the input. The ACF is the most convenient test for randomness in this case: A random function will have an ACF which rapidly falls off from its zero lag value. The ACF of the transient uranium concentration of the loaded solvent recorded during the main test is given in figure (4.10) and clearly shows that the loading variations are predominantly random.

4.3 INPUT OUTPUT CROSS-CORRELATION

The plant input, the transient pregnant solution flow rate, and its corresponding output, the uranium concentration of the loaded solvent, measured during the main test period were converted to digital data and stored in two 512 sample data records for correlation. The data is graphed in figure (4.11). Thus the correction factors applied by multiplication to the CCF calculated

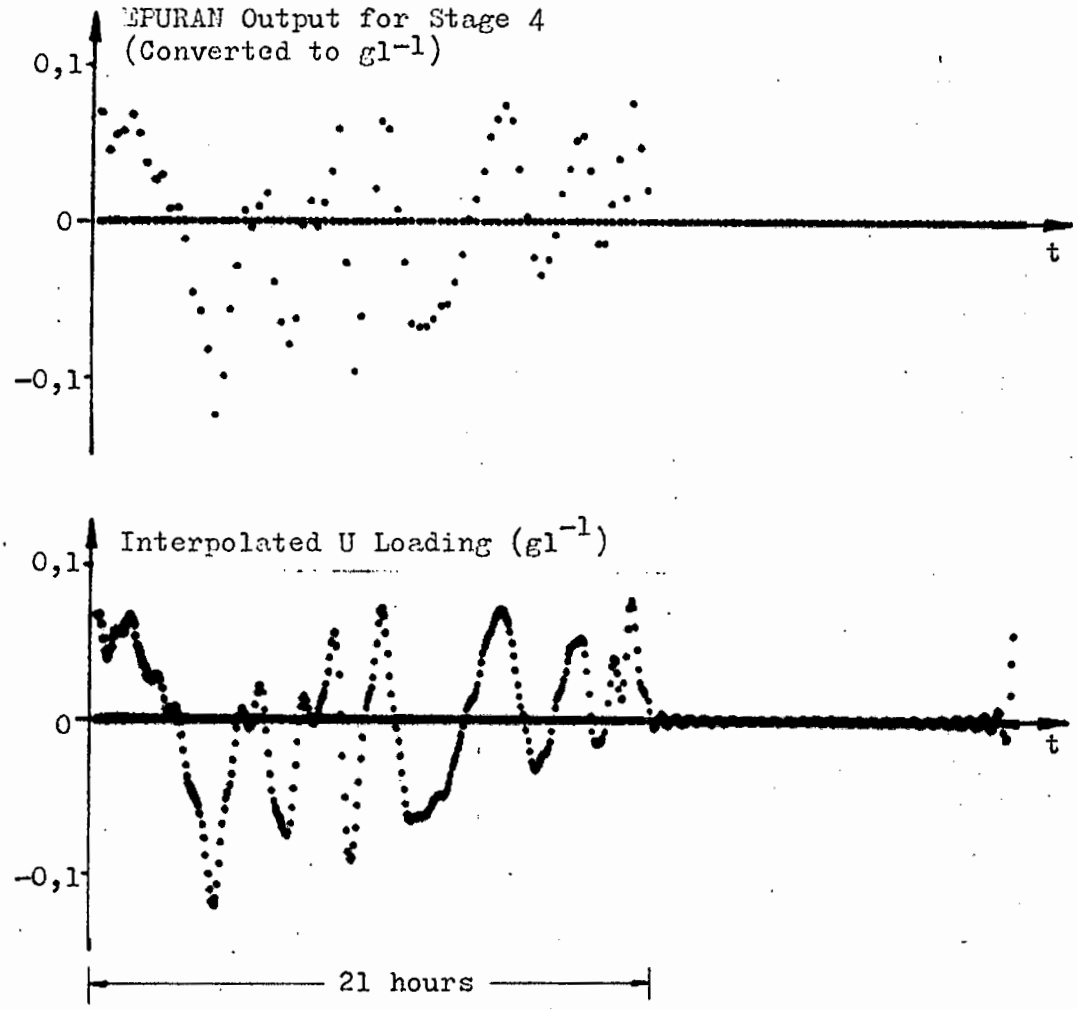

MAIN TEST LOADED SOLVENT URANIUM CONCENTRATION

Figure 4.9

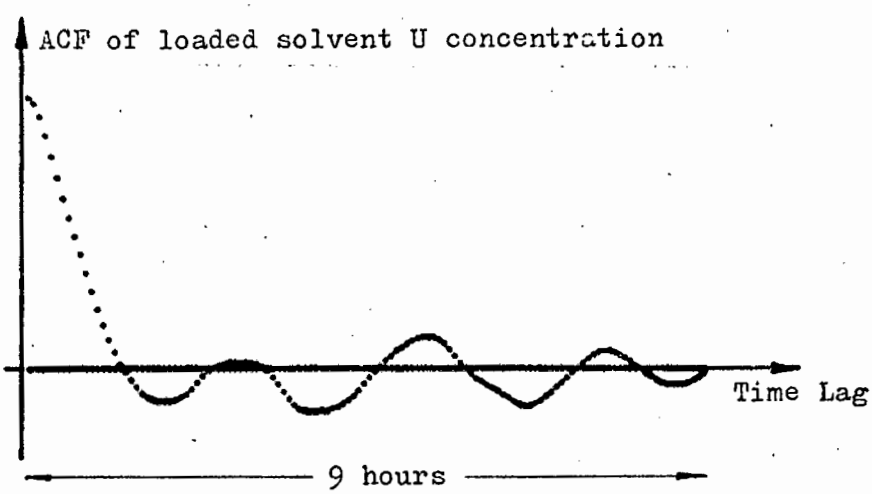

ACF OF TRANSIENT PLANT OUTPUT DURING THE MAIN TEST

Figure 4.10

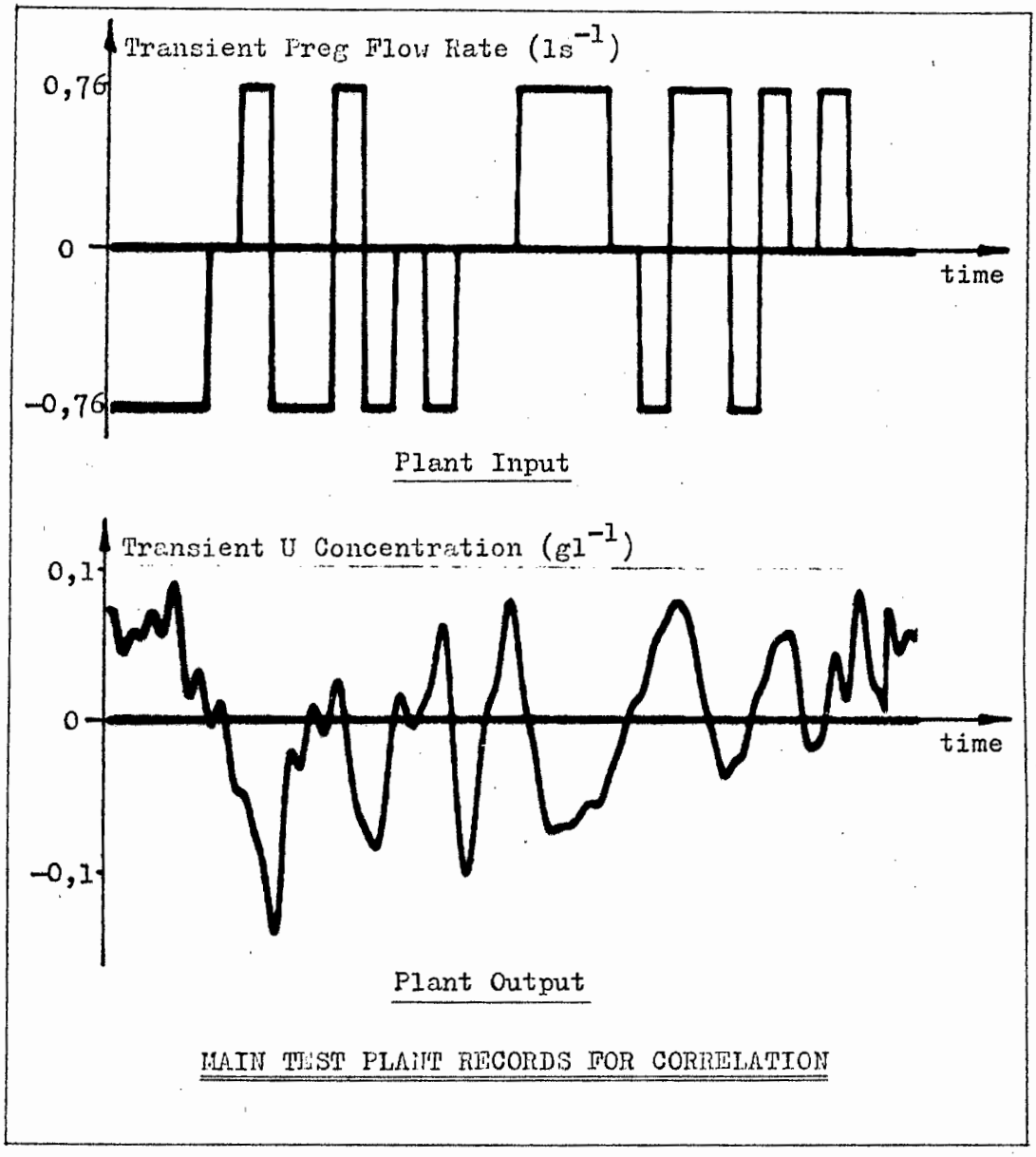

Figure 4.11

to give the impulse response between the pregnant solution flow rate and the extract uranium loading are:

$1 / 7{,}04 \times 10^{2}$	to correct for the ACF impulse area.
512/312	since a 312 sample pregnant solution flow rate record was augmented with zeros to form a 512 sample record.

The plant weighting function obtained from the main test is given in figure (4.12). The shape of the impulse response does not conform exactly to that obtained from the theoretical plant model derived in section (2.5.2) since the first order response expected has a significant oscillatory mode super-imposed on it. These oscillations can most easily be explained qualitatively in terms of the inter-stage free flow system used in the plant. For example consider a step increase in the pregnant solution flow rate. This will raise the level of the interface between the aqueous and organic phases in settler 4 and hence increase the flow of aqueous phase to stage 3 raising its

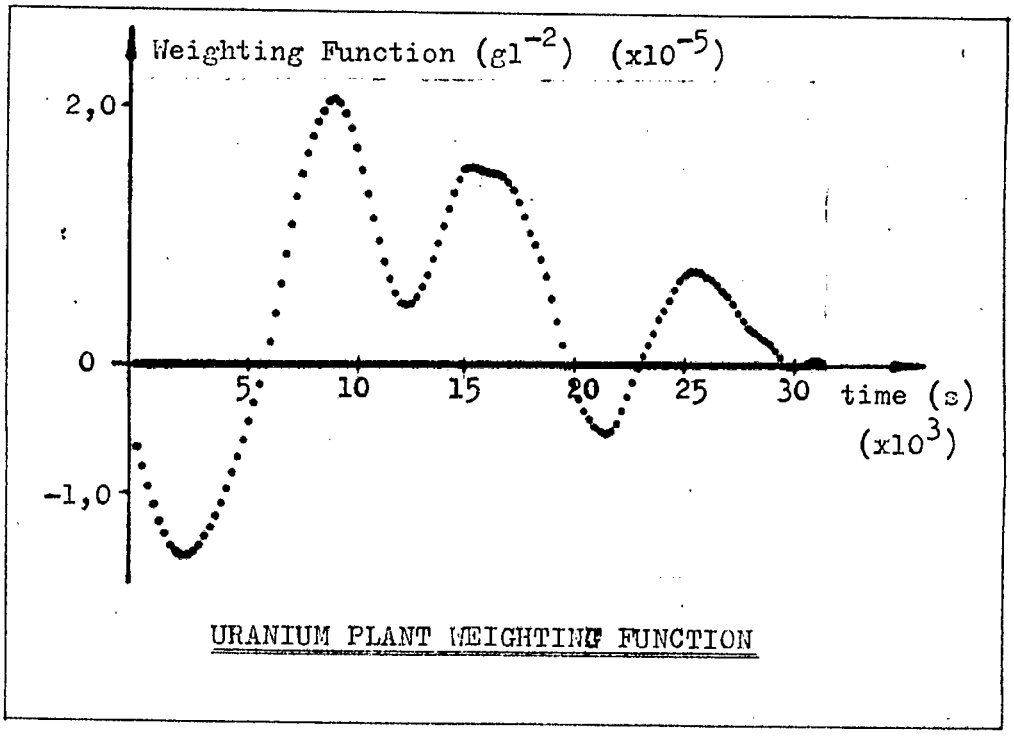

Figure 4.12

interface level which in turn increases the flow of low concentration organic phase from settler 3 to stage 4. Thus the loading of stage 4 will initially be decreased by the organic phase flow from settler 3 but once the levels settle an increase due to the increased pregnant solution flow rate will be observed as predicted by the steady state model - appendix C. It is possible that the settling of levels following a flow perturbation will result in an oscillatory super-position on the theoretical exponential plant behaviour.

CHAPTER 5 THE PLANT MODELS

The mathematical model of the plant describing the transient uranium concentration of the loaded solvent in terms of the pregnant solution flow rate changes is empirically and fully given by the weighting function shown in figure (4.12). Applications of the model in this form are limited to predictions of the plant output concentration variations which result from changes in the input flow rate by using the convolution integral of equation (1.3). Hence two alternative models, the differential equation or analytic model derived from fundamental conservation laws and the empiric frequency response model, are given here. The models are readily handled by classical control theory and hence more suitable for the development of control strategy and analysis of stability. The former model is not as flexible as that of the experimental weighting function, the spline model or any other empiric model since its form is rigidly defined by the order of the differential equation and so its shape can only be altered by changing the co-efficients of the differential equation. However it has the advantage that it is based on fundamental laws [15] and even though the secondary effects - the oscillations present in the experimental response - could not be explained by it, the basic exponential behaviour of the plant is contained in it.

5.1 THE ANALYTIC MODEL

The best available analytic model which is based on fundamental laws is that derived in section (2.5.2). The model parameters (i.e. the components of matices $\underline{A}$ and $\underline{B}$) are more numerous than the constraints imposed by the impulse response of figure (4.12) and hence cannot be uniquely determined from the results of the PRTS noise tests. However by observing that

(i) The theoretical response, y_4, to changes in pregnant solution flow rate, A, is not sensitive to variations of the co-efficients in the first and second rows of matrix $\underline{A}$ - equation (2.14).

(ii) Nor is it sensitive to changes in component a_{32} since variations in y_3 due to pregnant solution flow changes are small compared with those in y_4 - simulation results in section (2.5.2).

(iii) The step response gain is given by b_{32} / a_{33}.

the relevant portion of matrix equation (2.14) which will describe the output concentration in terms of the pregnant solution flow rate is given by

$$\dot{y}_4 = a_{33} y_4 + b_{32} A \qquad (5.1)$$

where y_4 is the uranium concentration of the loaded solvent

A is the pregnant solution flow rate

a_{33} and b_{32} are components of matrices $\underline{A}$ and $\underline{B}$ respectively.

The solution to equation (5.1) when an unit impulse is applied to the pregnant solution flow rate is given by

$$y_4(t) = y_4(0)\ \exp\{-t/T\} \qquad (5.2)$$

where $y_4(0) = b_{32}$
$T = 1 / a_{33}$

Model Parameters

The model parameters, a_{33} and b_{32}, were determined by a trial and error method in which $y_4(t)$ was calculated from equation (5.2) using various values for $y_4(0)$ and T and comparing it with the weighting function of figure (4.12). The parameters chosen were those for which the response $y_4(t)$ appeared to fit the impulse response best. No formal curve fitting technique was used since the accuracy of the model will be poor whatever parameters are chosen because of the oscillations. Incorporation of a time lag, τ, in equation (5.2) produced better results and the values selected for the parameters are given below:

$$\tau = 1{,}5\ \text{h}$$
$$a_{33} = 1{,}09\text{x}10^{-4}\ \text{s}^{-1}$$
$$b_{32} = 1{,}85\text{x}10^{-5}\ \text{ls}^{-1}$$

and the model is given by

$$y_4(t) = 0 \qquad \text{for } 0 < t < \tau$$
$$y_4(t) = y_4(0)\ \exp\{-(t-\tau)/T\} \qquad \text{for } \tau < t < \infty$$

The impulse response of this model and that derived experimentally are shown in figure (5.1).

Discussion

The amplitude of the oscillations in the experimental response are so large that the theoretical model cannot adequately describe the transfer function between the uranium concentration of the loaded solvent and the pregnant solution flow rate. And since analytic modelling of the effects introduced by the free-flow inter-stage connections was not feasible for the plant (levels at the overflows cannot be measured because the mixer-settlers are closed welded units) the empiric model was adopted as the most suitable form for describing the dynamic behaviour of the plant.

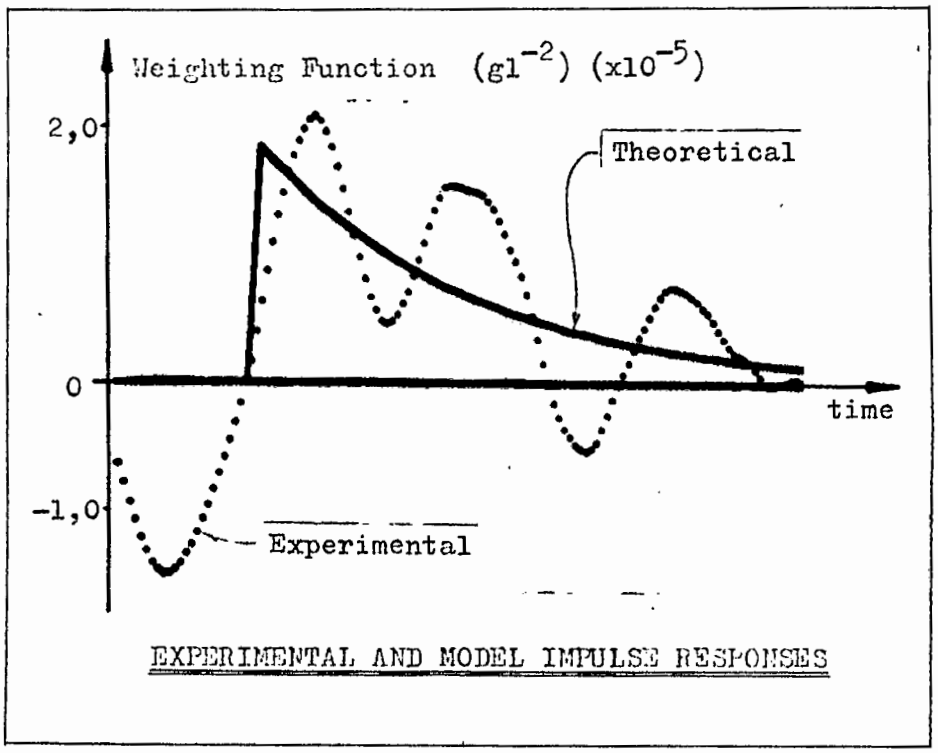

EXPERIMENTAL AND MODEL IMPULSE RESPONSES

Figure 5.1

5.2 THE EMPIRIC MODELS

5.2.1 THE IMPULSE RESPONSE

In general when no analytic model is availabe , the empiric model in the form of an impulse response is regarded as complete.[11] Thus the empiric model is given by the weighting function as shown in figure (4.12) and does not require selection of parameters. The major disadvantage of the impulse response description is that it can only be used to evaluate the uranium concentration of the loaded solvent in terms of the pregnant solution flow rate and not for designing a control system which prefers a frequency response representation of the model. However its validity as a model for the plant can be demonstrated by predicting the uranium loadings which were produced by the PRTS noise variations in the pregnant solution flow rate during the tests performed on the plant. The results are shown in figures (5.2) and (5.3).

Discussion

The discrepancy between the predicted and the measured uranium loadings in the 26 digit test can be attributed to noise introduced in the plant which was not produced by the PRTS noise and hence eliminated by correlation. In the pilot tests the basic shape of the uranium loadings are predicted in both cases but for the second test a DC component proportional to the mean value of the PRTS noise over a half cycle is present in the theoretical response but not in the experimental especially towards the end of the test run. No satisfactory explanation could be found for this although it suggests that

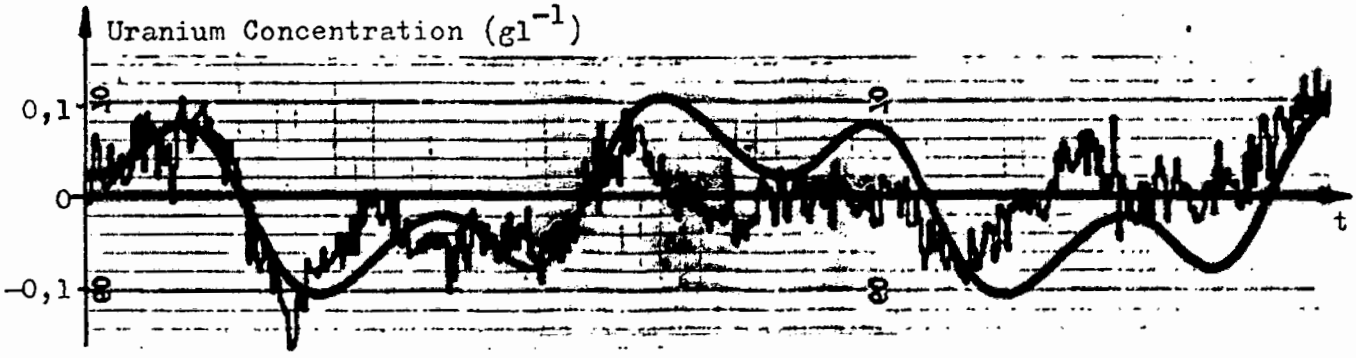

(a) Second Test

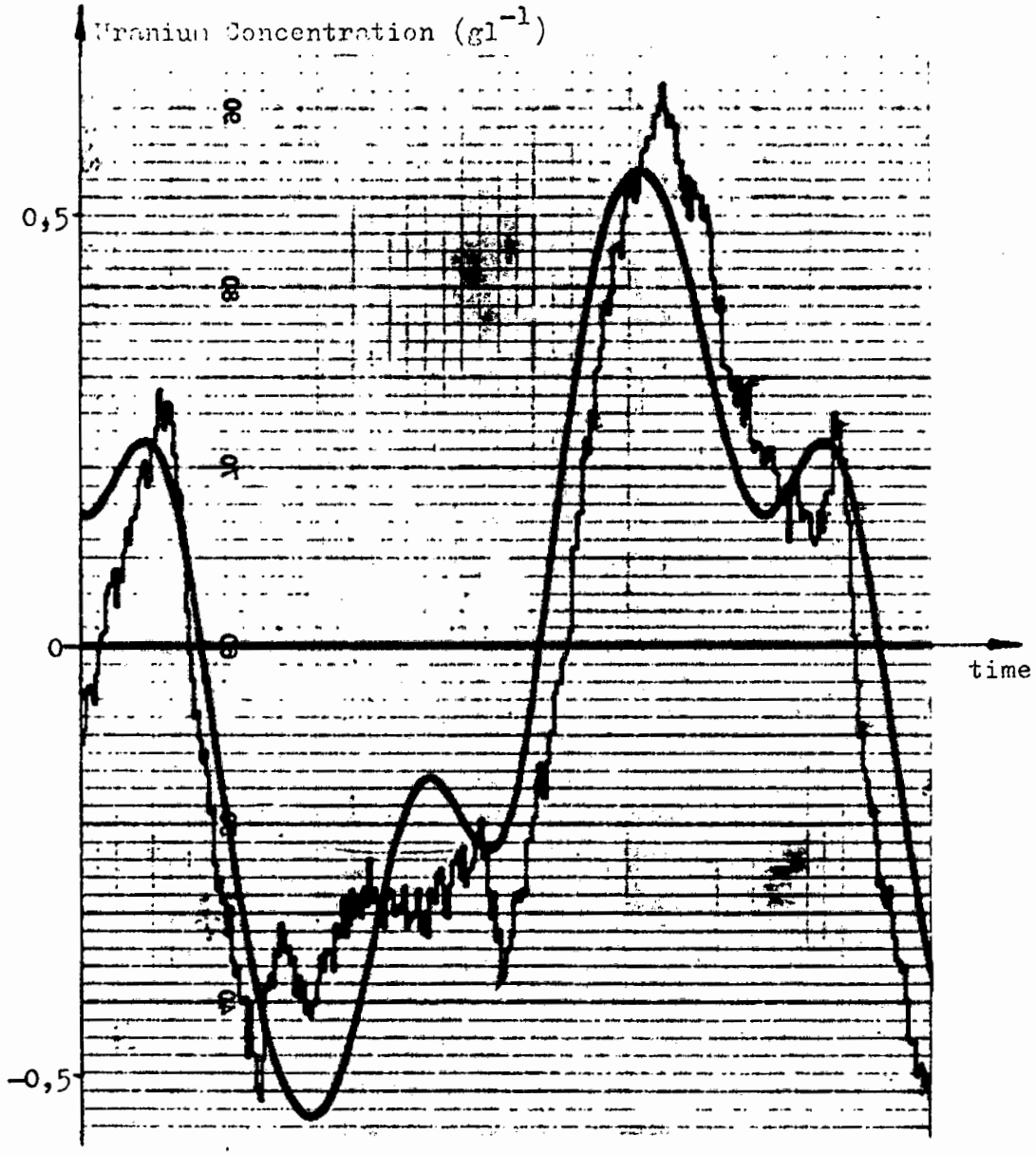

(b) First Test

PILOT TEST EXPERIMENTAL AND PREDICTED EXTRACT SOLVENT LOADING

Figure 5.2

the plant characteristics are time dependent or that the plant is a non-minimal phase system.

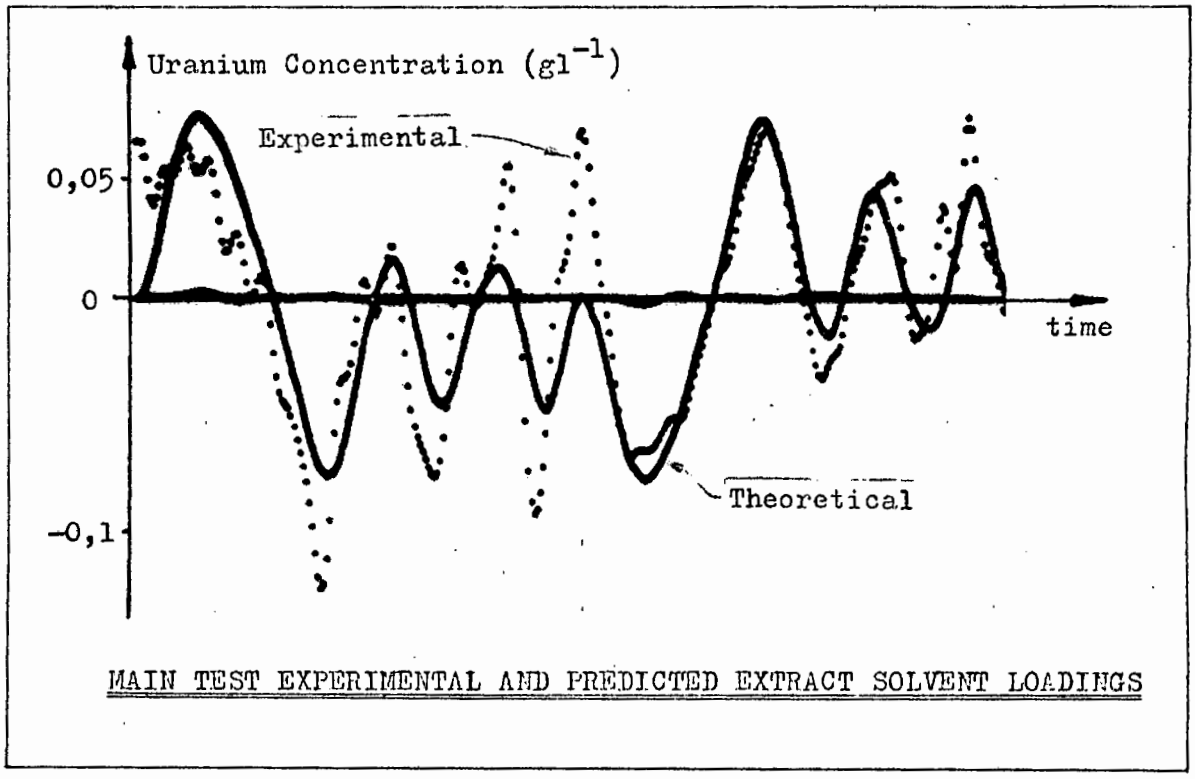

Figure 5.3

5.2.2 THE FREQUENCY RESPONSE

The frequency response for the plant is shown in figure (5.4). No further information is contained in this representation of the impulse response for the plant, but it supports the validity of the analytic model by having an amplitude variation with frequency which is predominantly that of a first order system. The phase angle is however very erratic and again suggests that the plant is a non-minimal phase system.

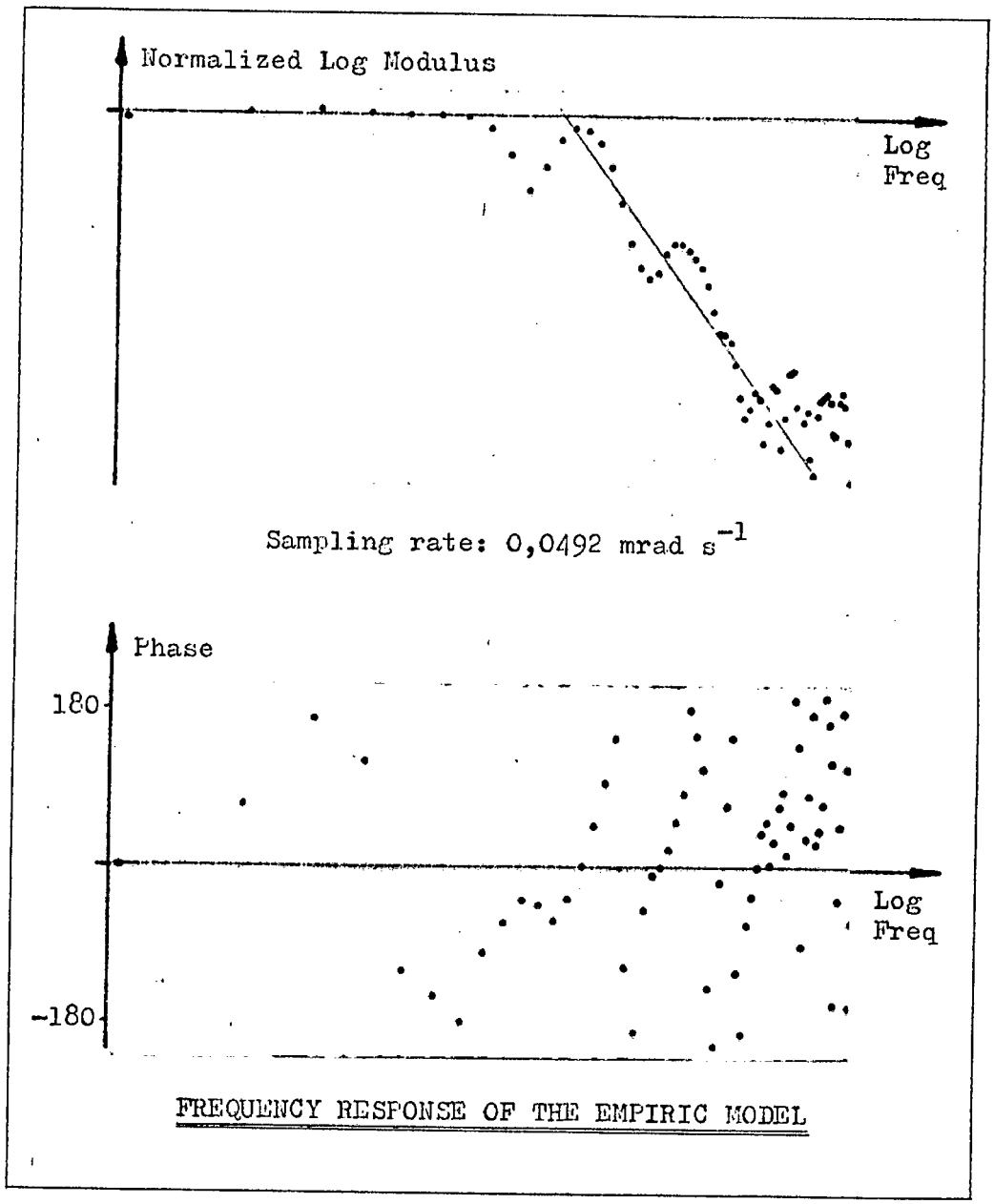

FREQUENCY RESPONSE OF THE EMPIRIC MODEL

Figure 5.4

CONCLUSION

The conclusions drawn from the results of laboratory and field experiments for identifying unknown systems using correlation techniques have been divided into two sections. The first deals with the correlation method as a tool for identification and the second with the actual plant models obtained using the method.

CORRELATION

Failure of the step response analysis to yield consistent results, necessitated the use of another method for identifying the uranium plant. The correlation technique using PRTS noise perturbations of the plant input was selected on the strength of its inherent noise rejection properties. These properties were thoroughly investigated - appendix A - and have shown the method to be superior to the step response test in identifying a simulated 'noisy' system. Thus for the same results, smaller perturbations could be imposed on the input and the system could be validly linearized about a steady state operating point. Results of the predictions making use of the weighting function obtained from the correlation function - figures (5.2) and (5.3) - attest to the effectiveness of the correlation method as a tool for on-line identification of a production-line system for which the step response test was unsuccessful.

However simplicity of the input test signal was compromised in order to achieve the noise rejection: Selection of a step input signal requires specification of one parameter, namely, amplitude whereas the PRTS requires in addition to amplitude, that the digit length and period be specified. These parameters are selected using the criteria discussed in section (1.3.1) which require some apriori knowledge of the unknown system characteristics. Since the parameters are invariably incorrectly selected, pilot tests have to be run before a suitable PRTS noise can be chosen for identifying the system. Apart from studying plant records for which the bandwidth of the input is usually inadequate, or conducting a pilot test which effectively reduces the method to one of trial and error, no technique could be found whereby the characteristics of the unknown system could be estimated. Thus further work on this aspect of system identification would be extremely useful.

PLANT MODELS

Inter-stage free-flow on the plant and the inaccessibility of the weirs and butterfly valves controlling these flow rates result in a system which is essentially non-analytic. It is doubtful whether any analysis would produce a satisfactory model of the process without the model becoming excessively

complex. Hence the empiric model was chosen as that most suited to describing the transfer function between the uranium concentration of the loaded solvent and the pregnant solution flow rate. The simple lumped parameter model was however fitted to the data as it is the most appropriate analytic model available. However it fails to describe the impulse response of the plant satisfactorily and cannot be regarded as a valid approximation to the plant behaviour.

The impulse response of figure (4.12) completely describes the model but, finding application primarily in the convolution integral, it is unsuited to aiding the design of a control strategy. Its frequency response - figure (5.4) - shows the plant to be a non-minimal phase system creating further complications in implementing automatic control of the plant. The free-flow employed between the stages of the plant is the source of the phase peculiarity of the model as was explained qualitatively in section (4.3). Thus control of inter-stage flow rates, as found on most mixer-settler systems, would improve controllability of the plant in a control system which uses a system such as the EPURAN uranium analyser to measure the plant output and the pregnant solution flow rate to control the uranium loading of the output.

Lastly, considerable problems were experienced during execution of the experiments by the presence of aqueous phase (or air bubbles) in the solvent samples pumped through the detector of the EPURAN which affected the readings of the EPURAN analyser. A settler on the sample stream, as suggested by Mr. U.Frischmuth, would be essential prior to its use in an automatic control system for the plant. The delays required to settle the aqueous phase (or to remove the air bubbles from the solvent) would however have to be carefully studied to avoid excessive delays in the feedback loop.

REFERENCES

PRTS Noise and Correlation

1 CHANG,J.A. Generation of Multi-level Maximal Length Sequences and their Application to Process Identification. PhD Thesis, Univ of Wales, 1967.

2 CHURCH,R. Tables of Irreducible Polynomials for the First Four Prime Moduli. Annals of Mathematics, 36, 1, Jan 1935.

3 DAVIES,W.D.T. System Identification for Self-Adaptive Control. John Wiley & Sons, London, 1970.

4 DOUCE,J.L., NG,K.C. & WALKER,A.E.G. System Identification in the Presence of a Ramp Disturbance. Electronics Letters, 2, 7, July 1966.

5 LEE,Y.W. Statistical Theory of Communications. John Wiley & Sons, 1960.

6 MISA-LLORCA,R. Digital Simulation Techniques for the Optimal Design of Multivariable Systems. MSc Thesis, Univ of Wales, 1971.

7 SELWAY,R.E. Correlation Techniques in Adaptive Aircraft Control Systems. PhD Thesis, Univ of Wales, 1967.

8 SELWAY,R.E. & BELL,D. On-line Analysis of a Non-linear Control System using Correlation Methods. Measurement and Control, 1, June 1968.

Mathematical Models

9 ALY,G. & OTTERTUN,H. Dynamic Behaviour of Mixer-Settlers.III.Testing Mathematical Models using Flow Rates as Input Signals. J.Appl. Chem.Biotechnology, 23, 1973.

10 ALY,G. & WITTENMARK,B. Dynamic Behaviour of Mixer-Settlers.II. Mathematical Models and Identification Methods. J.Appl.Chem. Biotechnology, 22, 1972.

11 ANDERSSEN,A.S. & WHITE,E.T. Identification with Pulse Type Inputs having Application to the Mineral Processing Industry. Int.Fed of Autom.Control Symp.on Autom.Control in Min,Miner and Met Process, 2nd, Sydney, Aust, Aug 1973.

12 BURNS,P.E. & HANSON,C. Transient Response of a Multi-stage Mixer-Settler. British Chem.Engng, 12, 1, Jan 1967.

13 CADMAN,T.W. & HSU,C.K. Dynamics and Control of Multi-stage Liquid Extraction. Trans.Instn.Chem.Engrs, 48, 1970.

14 CASTRO,M.G.,HOH,Y-C.,SMUTZ,M. & BAUTISTA,R.G. Some Dynamic Considerations of a Multi-stage Mixer-settler Extractor and Stripper. Ind.Eng.Chem.Process.Des.Develop, 12, 4, 1973.

15 EYKHOFF,P.,VAN DER GRINTEN,P.M.E.M.,KWAKERMAAK,H. & VELTMAN,B.P.Th. Survey: Systems Modelling and Identification. Third Congress of IFAC, London, June1966.

16 POLLOCK,G.G. & JOHNSON,A.I. The Dynamics of Extraction Processes.I. Introduction and Critical Review of Previous Work, Can.J. Chem.Engng, 47, 1969.

17 POLLARD,A. Process Control. Heinemann, London, 1971.

18 VAN DE VUSSE,J.G. A new Model for the Stirred Tank Reactor. Chem.Engng.Sc, 17, 1962.

Miscellaneous

19 BERGLAND,G.D. A Guided Tour of the Fast Fourier Transform. IEEE Spectrum, July 1969.

20 GIBSON,J.E. Non-Linear Automatic Control. McGraw-Hill, 1963.

21 GUPTA,S.C. & HASDORFF,L. Fundamentals of Automatic Control. John Wiley & Sons, 1970.

22 SCHAFER,R.W. & RABINER,L.R. A Digital Signal Processing Approach to Interpolation. IEEE Proc, 61, 6, June 1973.

23 TRUXAL,J.G. Control Engineers' Handbook. McGraw-Hill, 1958.

24 BLACKMAN,R.B. & TUKEY,J.W. The Measurement of Power Spectra. Dover Publications Inc, New York, 1959.

NIM Publications and Reports.

25 CHAIX,R.P. & ZIMMER,C.H.E. EPURAN: An X-Ray Absorption Analyser for the On-line Analysis for Uranium in Purlex Solvents. NIM Report 1473, Proj 68071, Aug 1972.

26 CHAIX,R.P. EPURAN - Economic Purlex Uranium Analyser. NIM Technical Memo, No2, Nov 1972.

27 CHAIX,R.P. EPURAN: The On-line Analysis of Uranium in the Multiple Solvent Streams of Purlex Plants. Atomic Energy Board, Rep No PIN 172.

28 ROBINSON,C.G. A Dynamic Model for the Extraction Bank of Purlex Plants. NIM Report No 1454, Proj 68070, July 1972.

29 FAURE,A. & TUNLEY,T.H. The Purlex Process - A Description of the Pilot Plant that led to the use of the Process in South Africa. NIM ICE 12/69.

APPENDIX A CORRELATION TECHNIQUE NOISE REJECTION

Gaussian white noise does not correlate with any signal and even its ACF rapidly falls off to zero from its zero lag value. Since PRTS noise approximates white noise, the statistical properties of white noise also apply to it, but to a lesser extent. The following simulation of system indentification using step and cross-correlation techniques for obtaining the system weighting function illustrates (i) the limitations of PRTS noise in suppressing noise through its statistical properties and (ii) the advantages of the correlation method over the step response analysis in identifying 'noisy' systems.

THE SYSTEM

Block Diagram

A second order system was chosen for identification in preference to a first order because it has two different time constants associated with it - one is the natural oscillation period and the other is the settling time - thus requiring the PRTS noise digit length and period to be selected independently. The system was simulated on an analog computer and is shown in block diagram form in the figure below.

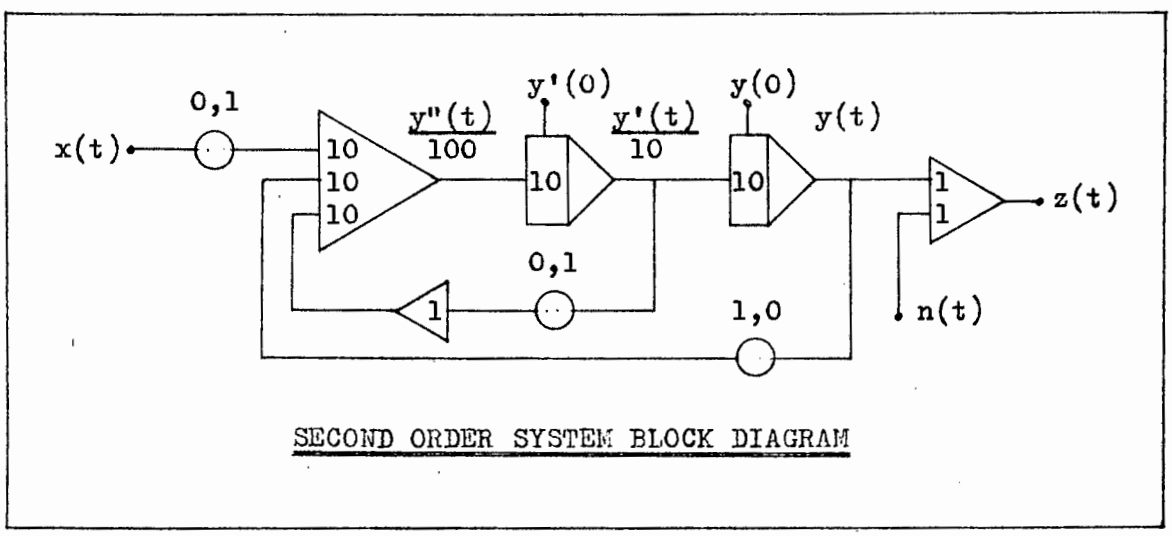

SECOND ORDER SYSTEM BLOCK DIAGRAM

where x(t) is the system input
y(t) is the output due to x(t)
n(t) is the noise added to y(t)
z(t) is the simulated measured output of a noisy system.

Transfer Function

The system transfer function, G(s), is given by

$$G(s) = \frac{Y(s)}{X(s)} = \frac{100}{s^2 + 10\,s + 1000}$$

which has the following characteristics

(i) Poles	$(-\zeta + j\sqrt{1 - \zeta^2})\ \omega_n = (-5{,}0 + j\ 30{,}8)$	
(ii) Damping Factor	$\zeta = 0{,}158$	
(iii) Natural Frequency	$\omega_n = 31{,}6$ rad s^{-1}	so $T_n = 198{,}7$ ms
(iv) Steady State Gain	$K = 10^{-1}$	

Note: All time is given in 'computer time' which is 10^{-1} of real time.

Theoretical Step and Impulse Responses

The theoretical system responses to step and impulse inputs were calculated so that the step and PRTS noise impulse responses obtained experimentally might be checked against theory.

(a) The Step Response

$$y_{step}(t) = A\,K\,\{1 - e^{-\zeta\omega_n t}\ \frac{\sin(\omega_n\sqrt{1 - \zeta^2}\ t + \cos^{-1}\zeta)}{\sqrt{1 - \zeta^2}}\} \qquad (A.1)$$

(b) The Impulse Response

$$y_{imp}(t) = A\,K\,\frac{\omega_n\ e^{-\zeta\omega_n t}}{\sqrt{1 - \zeta^2}}\ \sin(\omega_n\sqrt{1 - \zeta^2}\ t) \qquad (A.2)$$

where A is the step amplitude and the impulse area

$1/(\zeta\omega_n)$ is the time constant

$\sqrt{1 - \zeta^2}\ \omega_n$ is the oscillation frequency

THE EXCITATION, x(t)

The system was perturbed with a 10 V step function and a 5V PRTS noise signal which was chosen using the criteria given in section (1.3.1) and the system characteristics. The excitation details are:

Step Function

Source	General Radio 1340 pulse Generator
Amplitude	10 V
Pulse Duration	1 s
Pulse Period	2 s

PRTS Noise

Polynomial	1021
Digits/Cycle	$N = 26$
Digit Length	$t_o = 80$ ms
Period	$Nt_o = 2{,}08$ s
Amplitude	$a = 5$ V
ACF	$\phi_{xx}(t) = 1{,}39\ \delta(t)$

THE NOISE, n(t)

Two distinctly different noise signals, namely, random and harmonic, were chosen to simulate the noise which might be present in the measurements taken from a real system. The Gaussian white noise tests determined the signal to noise ratio tolerated by each identification method and the sinusoidal

noise illustrated their frequency dependence. The noise details are

Gaussian White Noise

Source	Hewlett-Packhard 3722A Noise Generator
Amplitudes	0,1 0,3 0,5 and 0,8 V_{rms}
Bandwidth	15 Hz
Sequence Length	20
Seq/Gate	1

Harmonic Noise

Source	Hewlett-Packhard 3311A Function Generator
Amplitudes	0,3 V_{rms}
Frequencies	0,1 1 2 4 and 10 Hz
Function	Sine

EXPERIMENTATION

The PRTS noise signal was generated on the Varian computer using the software described in chapter 3 and recorded on one channel of the instrument tape recorder. The step responses were recorded on a second channel of the recorder and in the PRTS test the system output was recorded on a third channel so that the input and output were obtained as synchronous signals. For processing the data the Varian computer was used and the analog signals from the recorder were sampled with the following sampling details

Sampling Time	T = 8 ms
No of Samples	N = 1024 for the PRTS test input and output
	= 224 for the calculated CCF
	= 192 for the step response

RESULTS

The input, the output, the calculated CCF and the step responses obtained are graphed in figures (A.2) to (A.10). On the CCF and the step response plots the 'ideal' case - i.e. n(t) = 0 - are shown as dotted graphs.

Analysis of the step and impulse responses using the peaks of the responses and equations (A.1) and (A.2), the following system characteristics were obtained:

	Step Response	Impulse Response	Block Diagram
ω_n	33,6	33,5	30,8
ζ	0,211	0,218	0,158
K	0,11	0,12	0,10

These parameters were substituted into equations (A.1) and (A.2) and the theoretical responses were calculated using a BASIC program which is listed in appendix E. The experimental points were read in and plotted on the same graphs as the theoretical responses - figure (A.1) - and shows that the experimental and theoretical responses using the above experimental parameters are

in good agreement. The discrepancy between the block diagram and experimental system parameters was attributed to inaccurate potentiometer settings since at values of 0,1 a 10% error was quite feasible on the analog computer used.

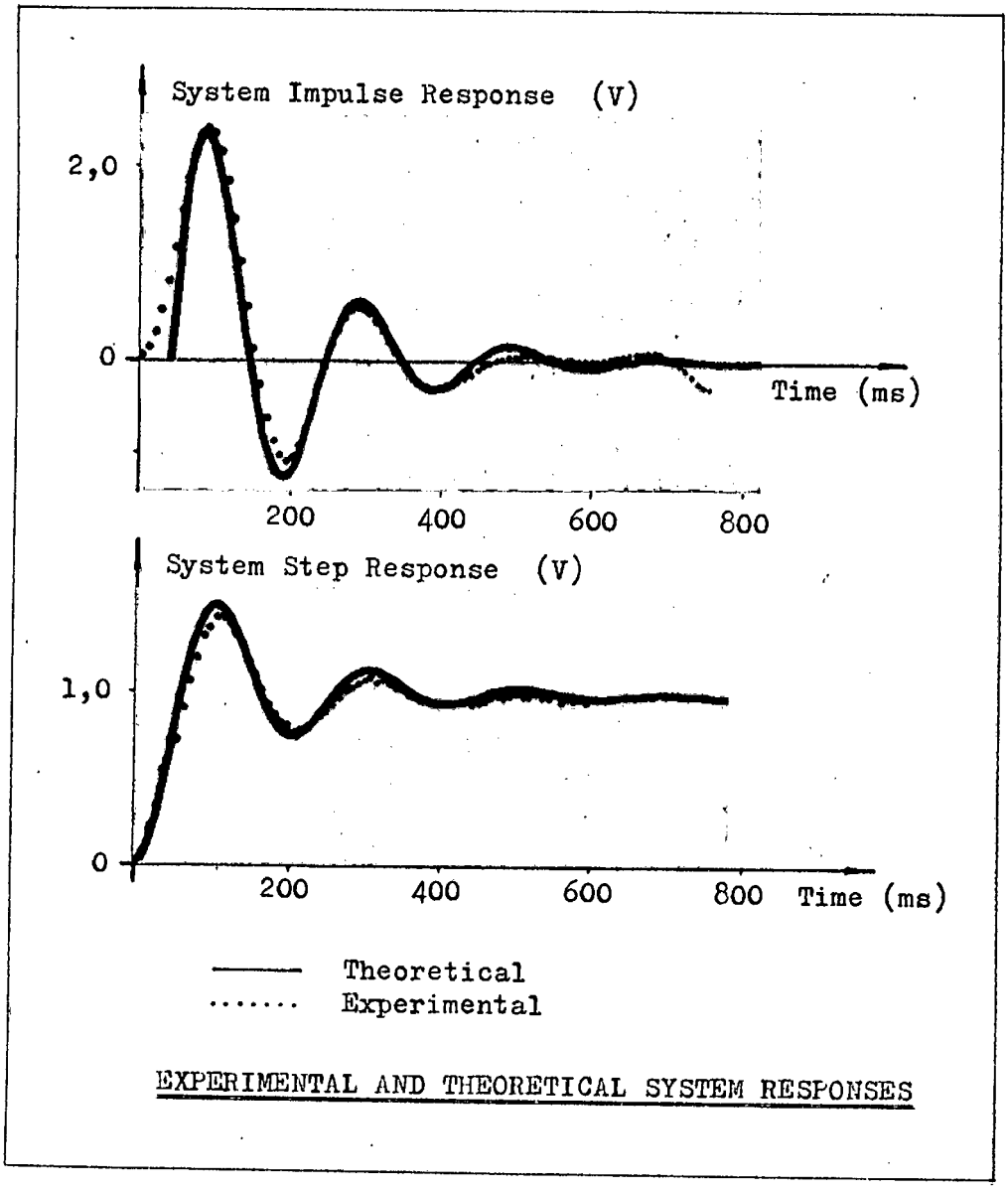

Figure A.1

Note: (i) Two cycles of PRTS noise were applied to the system in the correlation tests. The first cycle is required to allow transients to decay (strictly speaking only half a cycle is needed for a correctly selected code.) It is sometimes held that this 'settling cycle' is applied so that the output can be correlated with the input since correlation involves a shift of the output in time past the input. But since the CCF is calculated from one cycle of the input and output using cyclic correlation, this is not the reason for the first cycle.

(ii) Four correction factors were applied to the CCF to yield the

correct impulse response. These factors are given below:

1/1,39	to adjust for the ACF area of 1,39.
10	to counter-act the tape recorder scaling.
1024/196	since a 196 sample output was used in a 1024 sample correlation - section 3.2.
1024/392	since a 392 sample input was used in a 1024 sample correlation - section 3.2.

DISCUSSION

Trends exhibited by the results are more important than the individual cases given.

The PRTS noise is particularly effective in eliminating random noise as might be expected from the statistical properties of each signal which make them both stochastically independent of other signals. The distortion amplitude should theoretically be linearly dependent on the noise amplitude although this is not clearly illustrated in the cases given.

In the case of harmonic noise, the stochastic independence of the PRTS noise and the harmonic noise is a function of frequency and the distortion due to the noise decreases with increase in frequency as expected from equation (1.2) and the PRTS noise Fourier Transform - figure (B.2).

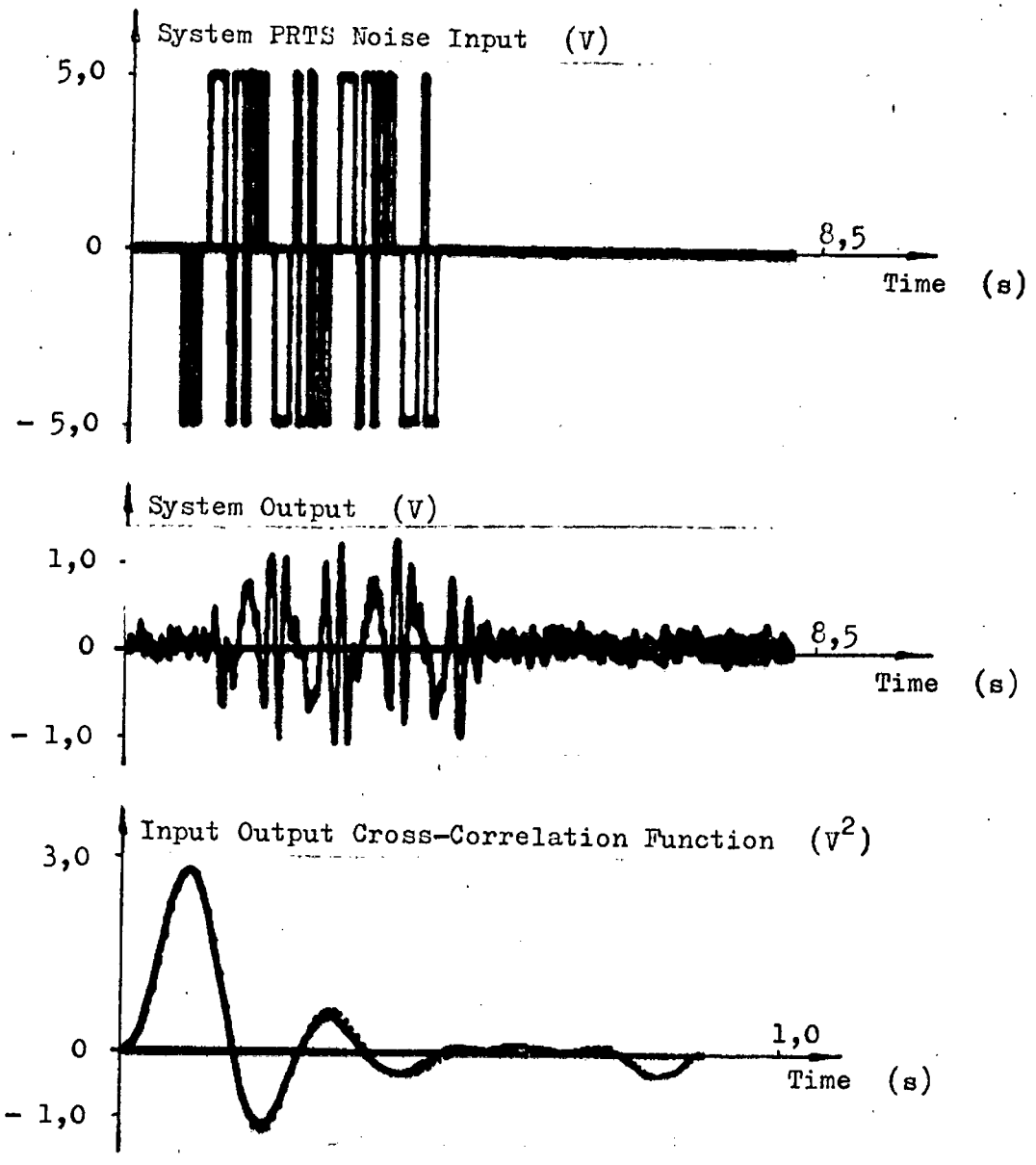

(a) Correlation Impulse Response Analysis

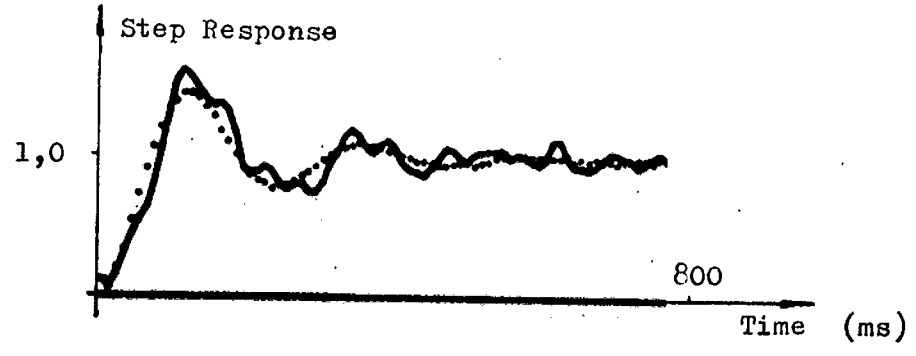

(b) Step Response Analysis

SYSTEM IDENTIFICATION : Noise: 0,1 V_{rms} Gaussian Noise

Figure A.2

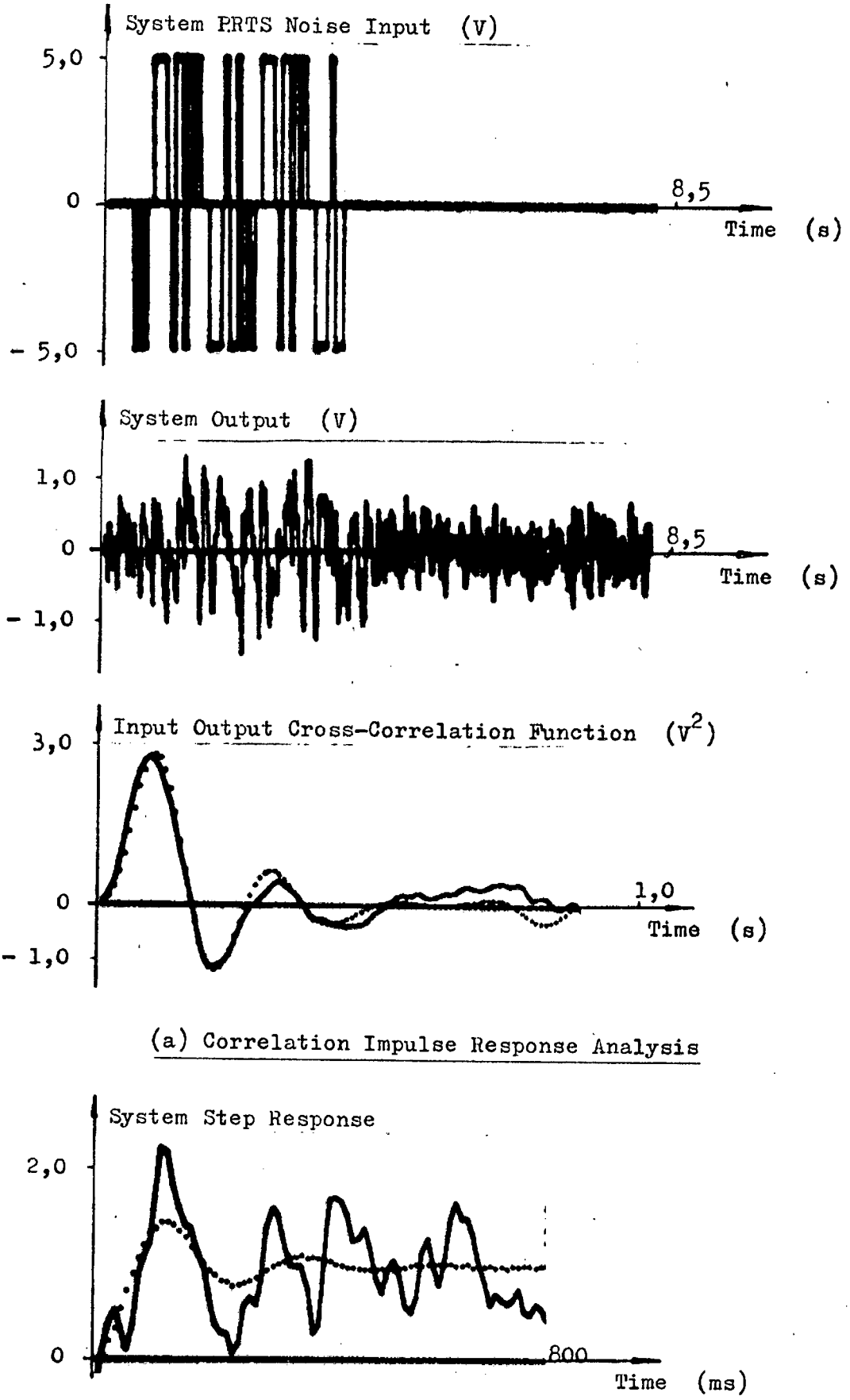

(a) Correlation Impulse Response Analysis

(b) Step Response Analysis

SYSTEM IDENTIFICATION : Noise: 0,3 V_{rms} Gaussian Noise

Figure A.3

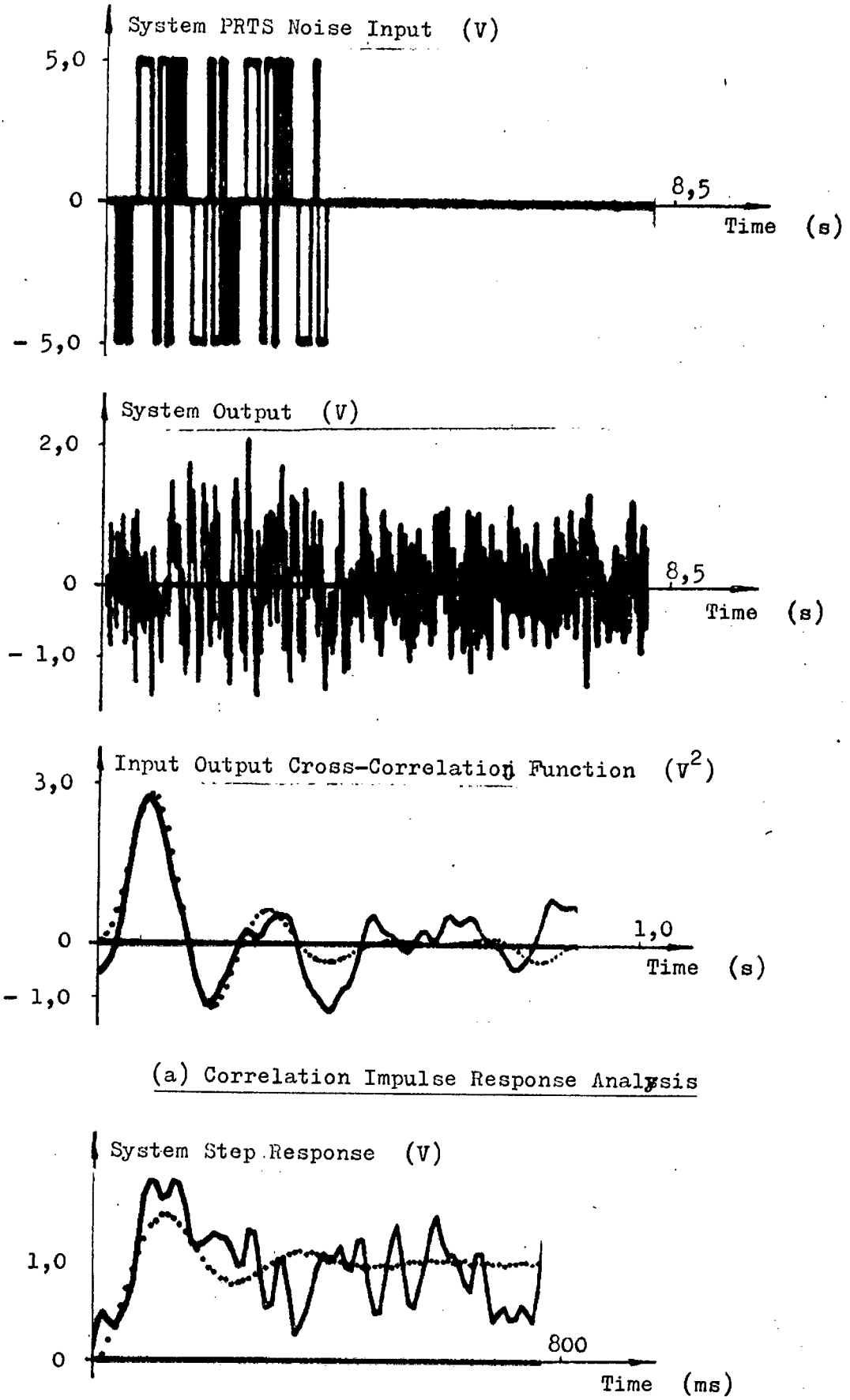

(a) Correlation Impulse Response Analysis

(b) Step Response Analysis

SYSTEM IDENTIFICATION : Noise: 0,5 V_{rms} Gaussian Noise

Figure A.4

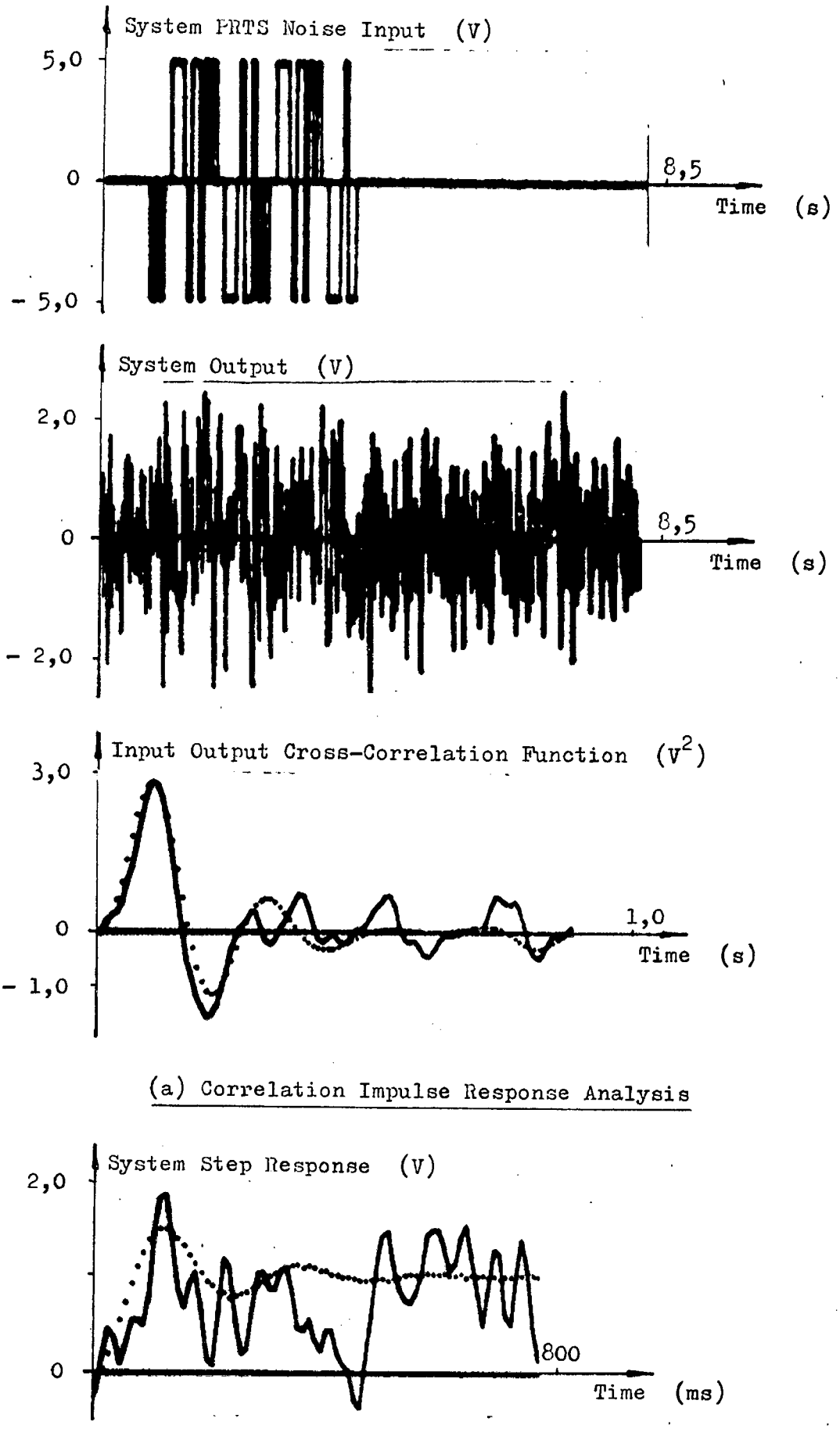

(a) Correlation Impulse Response Analysis

(b) Step Response Analysis

SYSTEM IDENTIFICATION : Noise: 0,8 V_{rms} Gaussian Noise

Figure A.5

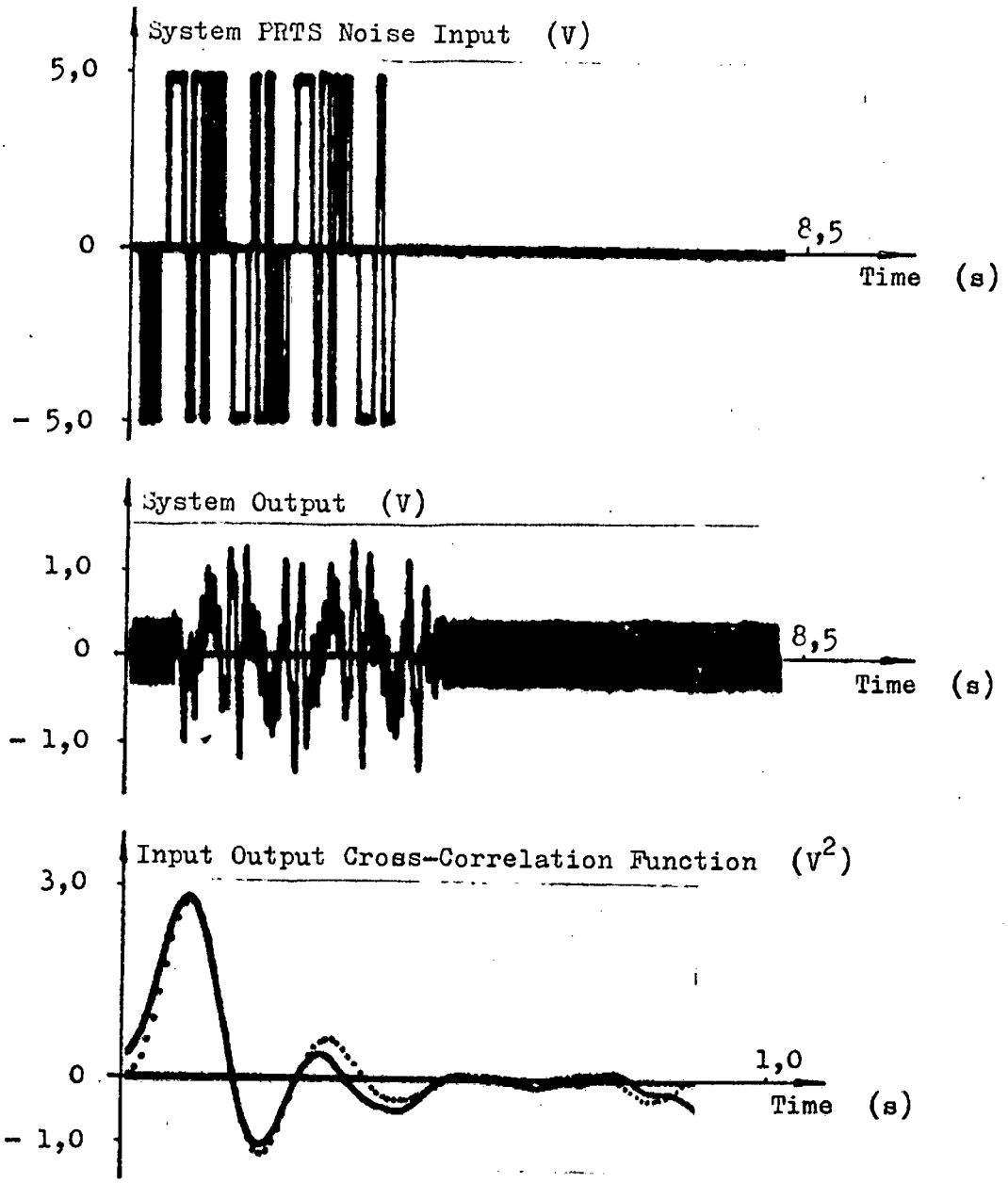

(a) Correlation Impulse Response Analysis

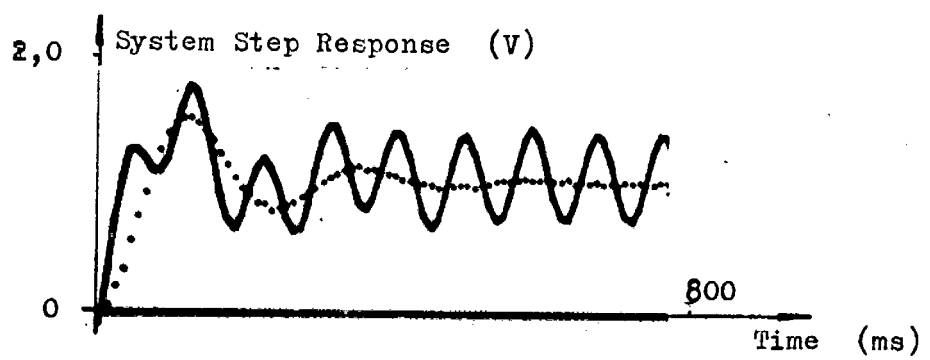

(b) Step Response Analysis

SYSTEM IDENTIFICATION : Noise: 0,3 V 10 Hz Sine Wave

Figure A.6

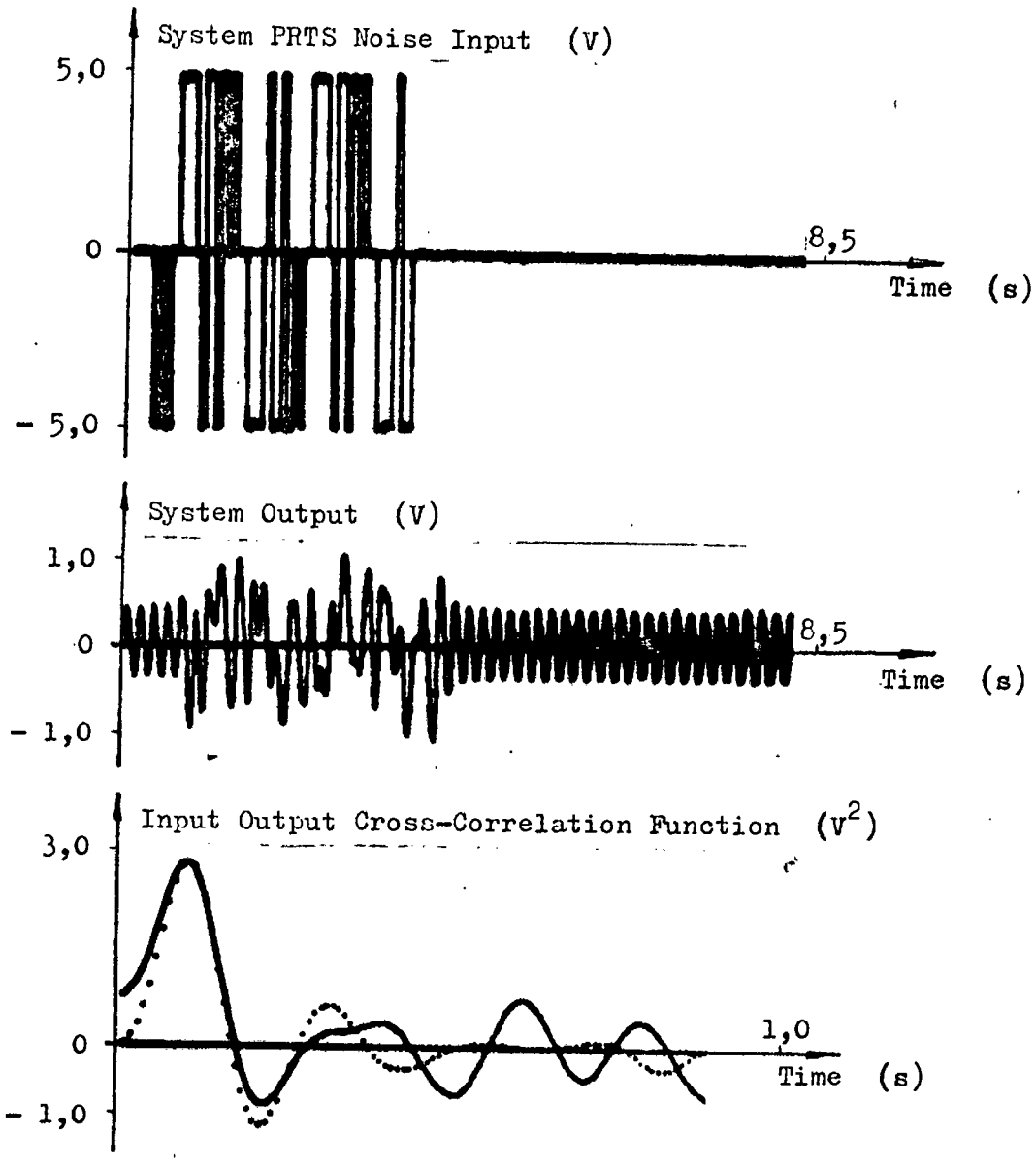

(a) Correlation Impulse Response Analysis

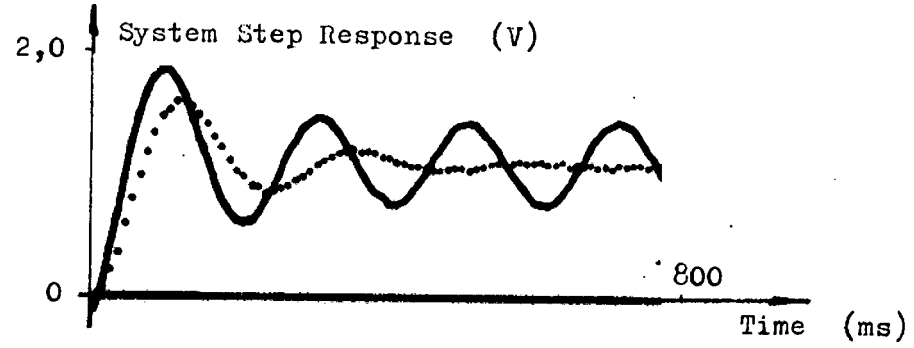

(b) Step Response Analysis

SYSTEM IDENTIFICATION: Noise: 0,3 V_{rms} 4 Hz Sine Wave

Figure A.7

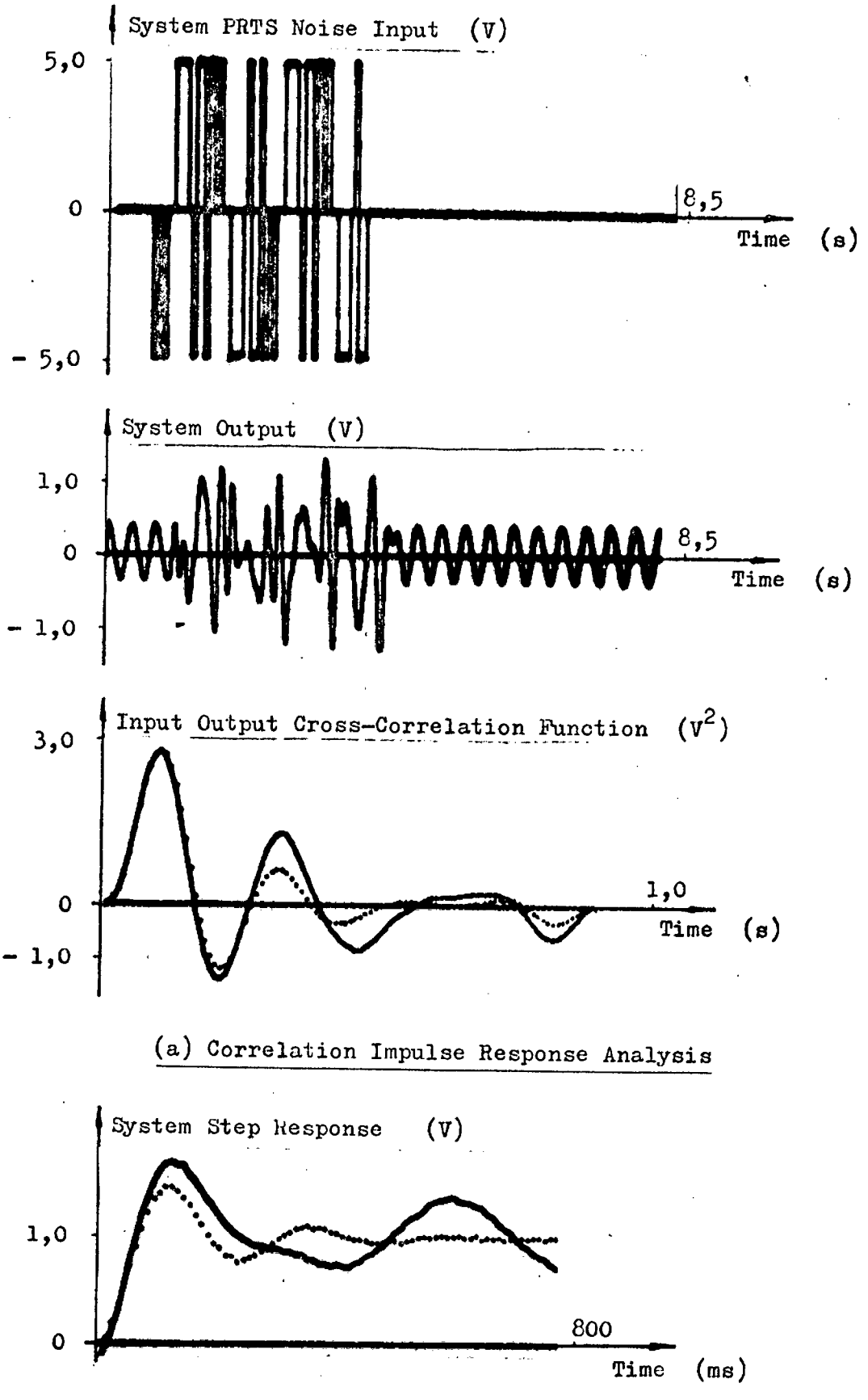

(a) Correlation Impulse Response Analysis

(b) Step Response Analysis

SYSTEM IDENTIFICATION: Noise: 0,3 V_{rms} 2 Hz Sine Wave

Figure A.8

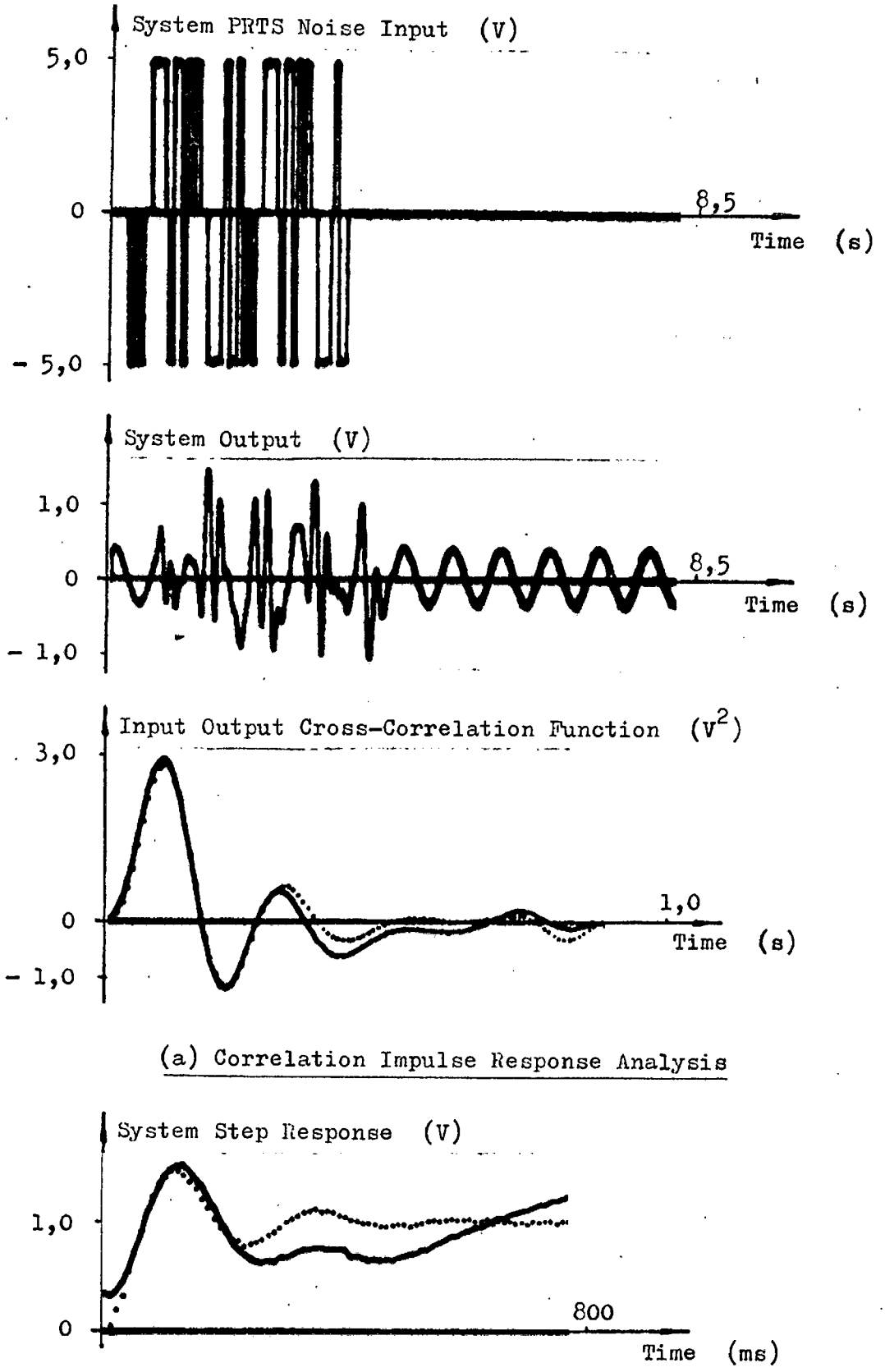

(a) Correlation Impulse Response Analysis

(b) Step Response Analysis

SYSTEM IDENTIFICATION: Noise: 0,3 V_{rms} 1 Hz Sine Wave

Figure A.9

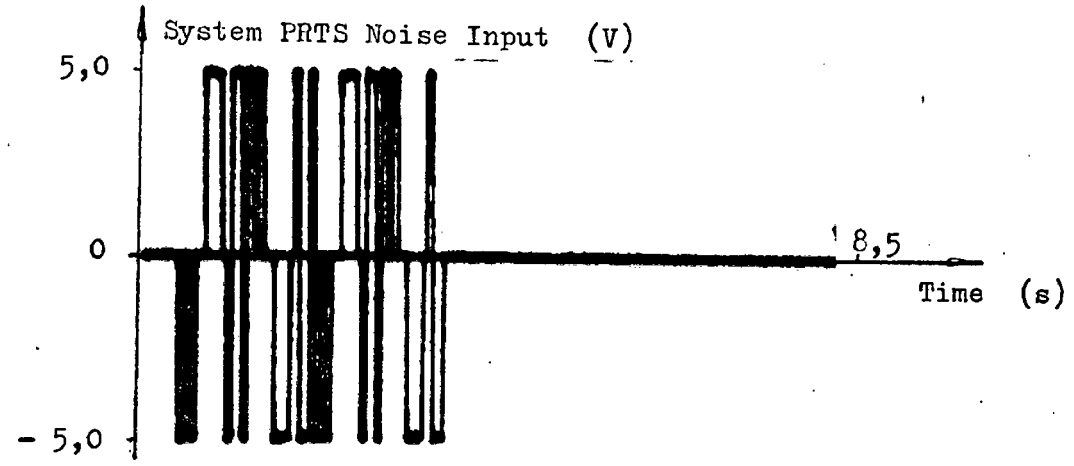

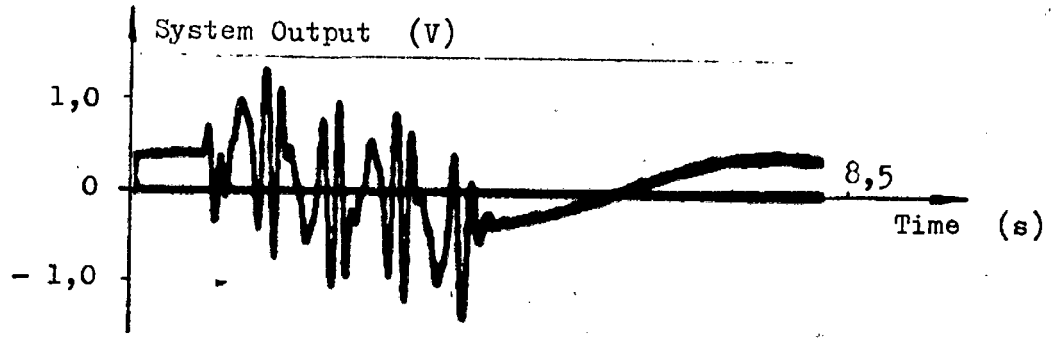

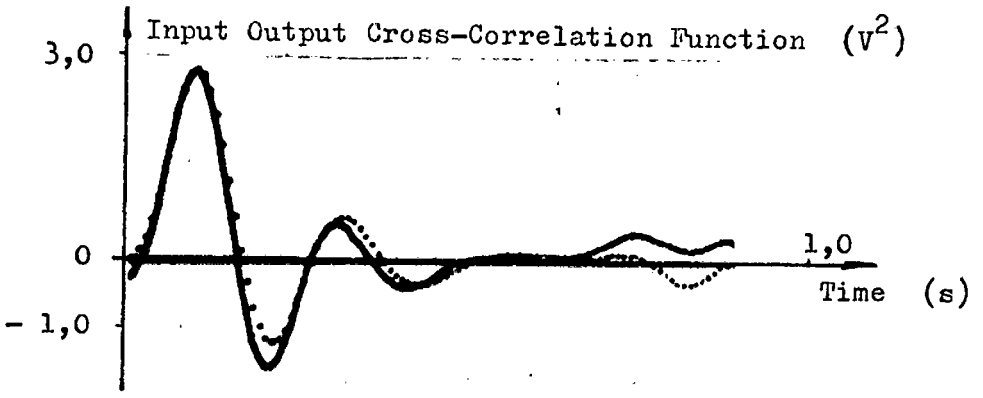

(a) Correlation Impulse Response Analysis

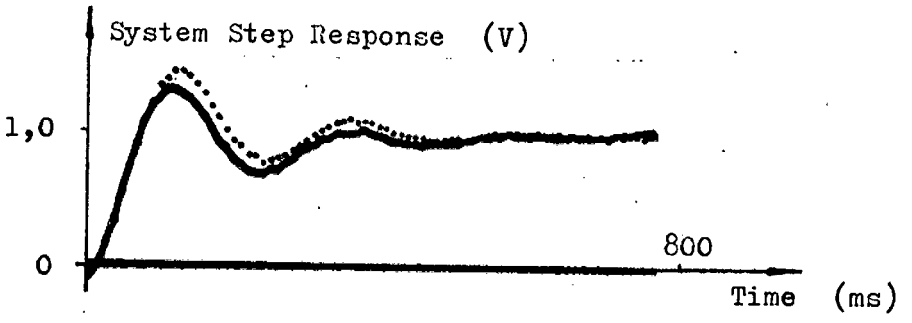

(b) Step Response Analysis

SYSTEM IDENTIFICATION : Noise: 0,3 V_{rms} 0,1 Hz Sine Wave

Figure A.10

APPENDIX B DISCRETE DATA PROCESSING

Continuous signals from the plant were sampled either by the plant instrumentation or by the Varian computer A/D converter before the data could be processed to yield the required correlation functions. Effects that are introduced by the sampling of continuous data and discrete digital data processing - e.g. Fourier Transformation and correlation - can, unless avoided, completely distort the results. The important aspects of digital processing are outlined here to identify these effects.

SAMPLING CONTINUOUS SIGNALS

Sampling rates for equi-spaced data samples must exceed the Nyquist sampling frequency for band-limited signals and wide-band signals require filtering by a low pass filter before sampling to avoid aliasing. Aliasing is readily observed in the Fourier Transform of the signal which will be non-zero at the folding frequency if there is aliasing. Once a signal is incorrectly sampled the samples cannot be processed to eliminate the aliasing.

Further discrepancies between the actual signals and the sampled version could be caused by quantization - i.e. finite number of bits in the A/D converter - finite sampling aperture - i.e. time required for the converter to sample, settle and convert - skew between the channels in multi-channel sampling as used in correlation techniques for synchronously sampling the input and output. But since the resolution and bandwidth of the Varian equipment - table (B.1) - exceed that of the plant instrumentation and the tape recorder, these effects were not of any consequence in processing the plant data.

Table B.1

	Analog/Digital	Digital/Analog
No of Channels	8	2
No of Bits	12	12
Range	-10 to +10 V	-10 to +10 V
Resolution	4,8 mV	4,8 mV
Aperture	<50 ns	-
Conversion Time	<25 µs	<10 µs
Channel Skew	<100 µs	-

DISCRETE FOURIER TRANSFORMATION

The discrete Fourier Transform - DFT - and its high speed computational algorithm, the Fast Fourier Transform - FFT - are only of interest in this section in so far as they approximate the continuous Fourier Transform - CFT. So starting with the definition of the DFT, the method used to improve the

DFT to CFT correspondence is considered and an analysis of the correspondence is given.

Formally no CFT exists for a set of sampled data points, f(nT) where T is the sampling interval. But the DFT, F(kΩ), which is discrete in both time and frequency, and hence suitable for digital computations, can be defined by the pair of summations:

$$f(nT) = \sum_{k=0}^{N-1} F(k\Omega)\, e^{jk\Omega nT}$$
$$F(k\Omega) = \frac{1}{N} \sum_{n=0}^{N-1} f(nT)\, e^{-jk\Omega nT} \qquad \text{(B.1)}$$

where $NT\Omega = 2\pi$.

Note: (i) Both f(nT) and F(kΩ) are cyclic in N samples.

(ii) The similarity between the expressions and the Fourier Series.

For the FFT, the number of samples, N_f, must be a power of 2 to satisfy the requirements of the IBM routine FOUR1. Arrays with less points - as are usually encountered in practice - can be augmented with zeros to give augmented function, $f_a(nT)$. Its FFT, $F_a(k\Omega_f)$, is related to the DFT of f(nT), namely, F(kΩ), by

$$F_a(k\{\tfrac{\Omega}{r}f\}) = \frac{1}{r} F(\{\tfrac{k}{r}\}\Omega_f) \qquad \text{(B.2)}$$

where $r = N_f/N$ and $N_f T\Omega_f = 2\pi$

If k/r is not integer, the value of $F(\{\frac{k}{r}\}\Omega_f)$ is intuitively deduced from F(kΩ).

The degree to which the FFT will approximate the (unknown) CFT can be improved by the use of 'data windows' which reduce the effects of leakage between the CFT samples which is caused by using finite data records and affect the FFT calculated.

It should be noted that the algorithm FOUR1 regards the finite data record as cyclic in time thus yielding discrete Fourier components and since the time function was sampled, the resulting spectrum is cyclic in frequency.

Data Windows

Finite data records of a signal can be regarded as the infinite signal multiplied by a 'hat function' - or zero order data window. The multiplication operation in the time domain is equivalent to convolution in the frequency domain and since the zero order window has a CFT of the form $\frac{\sin x}{x}$, the side-lobes of this function will cause leakage when convolved with the CFT of the infinite record. Obviously this leakage can be reduced by the use of data windows with smaller side-lobes and the resulting convolution will approximate the 'true' CFT of the signal more accurately.

The four main data windows, namely, the zeroth order, $w_o(t)$, the first

order, $w_1(t)$, the Hanning window, $w_n(t)$, and the Hamming window, $w_m(t)$, are shown in figure (B.1). The corresponding Fourier Transform moduli of the zeroth order, $W_o(\omega)$, and the Hanning, $W_n(\omega)$, which is representative of the other two are also given.

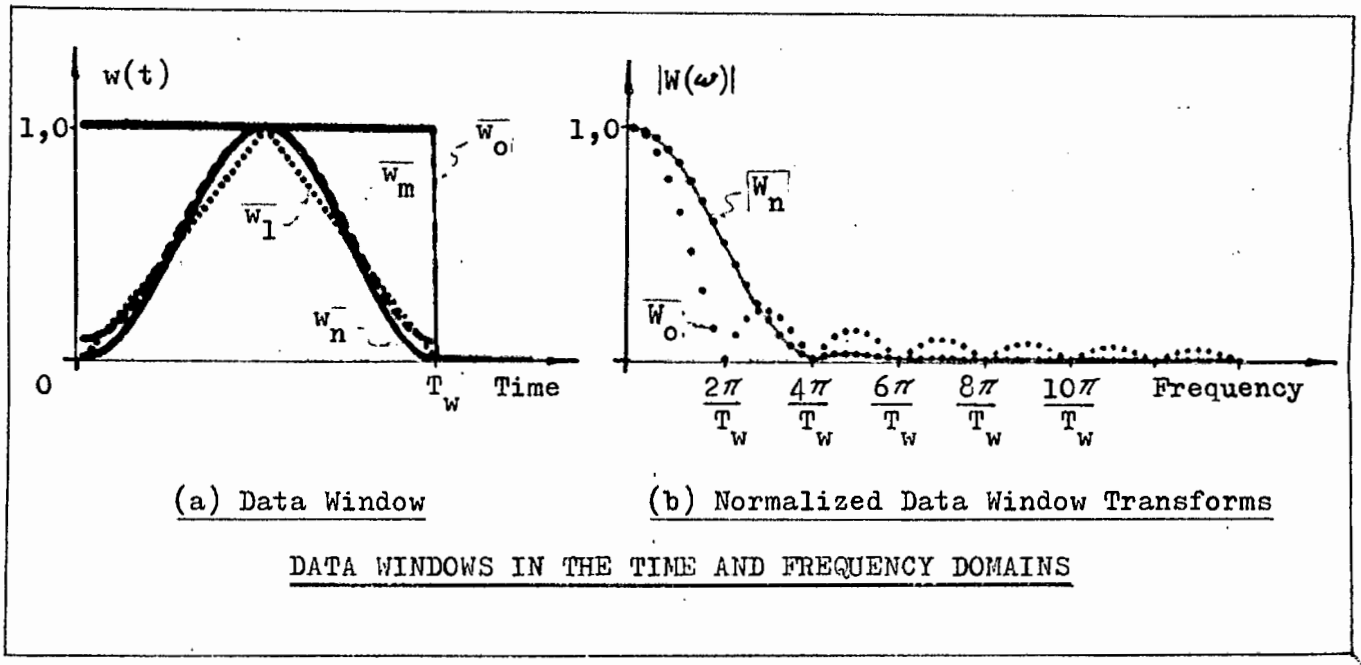

Figure B.1

Figure (B.2) shows the improvements which result in the FFT from the use of a data window, other than a zeroth, which is applied to a 26 digit PRTS noise signal that has a theoretical CFT with a $\frac{\sin x}{x}$ shape. A 260 sample PRTS code was augmented with zeros to form a 1024 sample record suitable for transforming. The reasons for using such a long augmented function are explained later.

Relating the FFT to the CFT.

The effects of sampling a continuous signal to produce a finite discrete data record and then using the FFT to calculate the DFT can most readily be seen mathematically by considering the continuous time function f(t) with CFT; F(ω).

f(t) is sampled to produce a finite data record of N samples which is augmented with zeros to form an L sample array ($L=2^m$, m being integral) that is considered to be cyclic in L samples. These operations can be described by the following

$$f^*(t) = f(t) \times \sum_{n=-\infty}^{\infty} \delta(t-nT) \times w(t) \circledast \sum_{n=-\infty}^{\infty} \delta(t-nLT) \qquad (B.3)$$

where $\times \sum_{n=-\infty}^{\infty} \delta(t-nT)$ is the sampling operator (a Dirac comb) with sampling interval T.

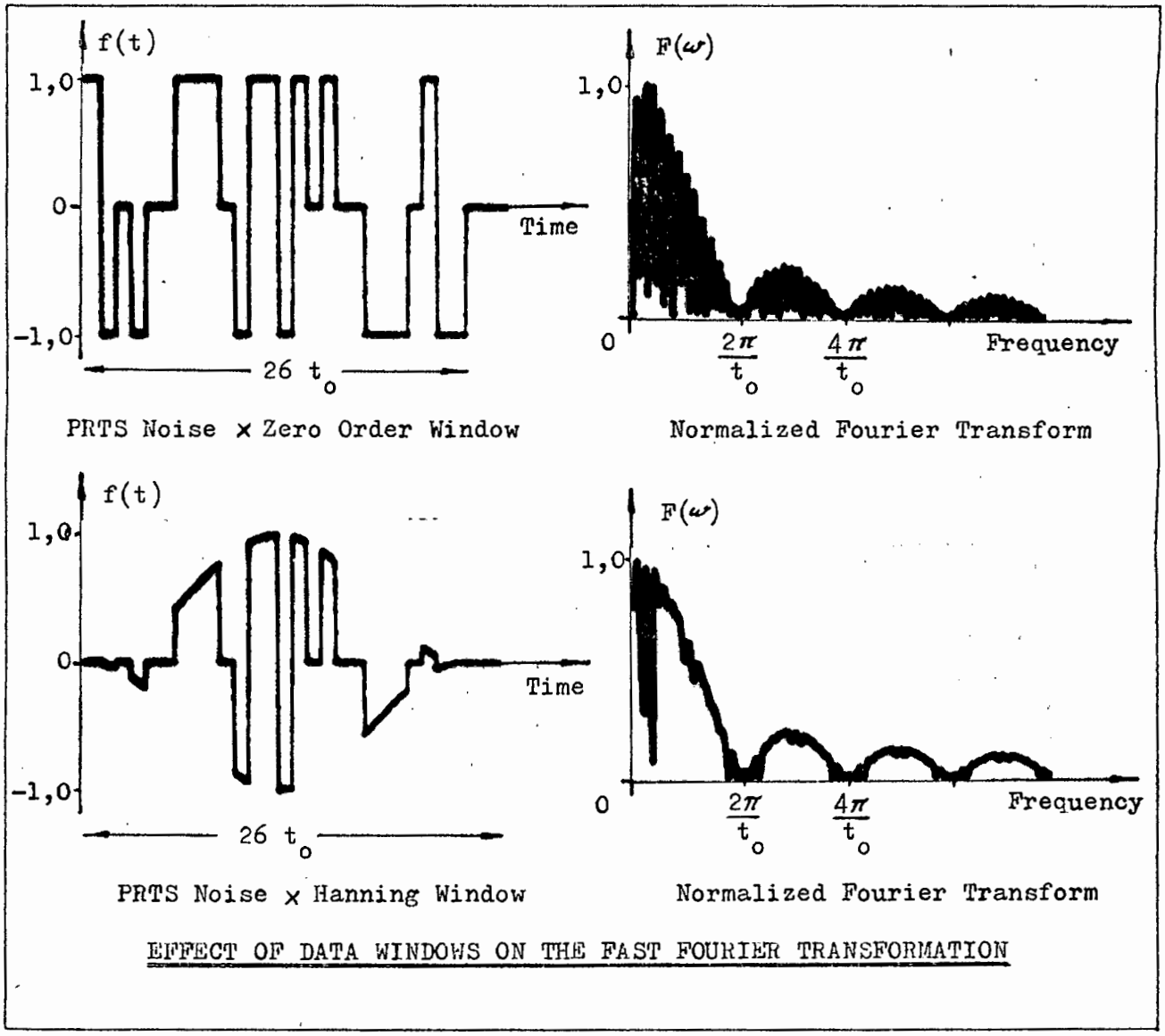

Figure B.2

x w(t) is the application of the data window

$\otimes \sum_{n=-\infty}^{\infty} \delta(t-nLT)$ produces periodicity in the LT samples (Also a Dirac comb)

'$\otimes$' means convolution and 'x' multiplication

The above operations are illustrated in figure (B.3)

Fourier transforming $f^*(t)$ and using the fact that multiplication in the time domain becomes convolution in the frequency domain and vica-versa,

$$F^*(\omega) = a\, F(\omega) \otimes \sum_{k=-\infty}^{\infty} \delta(\omega-kL\Omega) \otimes W(\omega) \times \sum_{k=-\infty}^{\infty} \delta(\omega-k\Omega)$$

where 'a' is a constant produced by Fourier transforming the Dirac combs and $\Omega = \frac{2\pi}{LT}$, the sampling interval in the frequency domain.

Re-arranging the transform it becomes

$$F^*(\omega) = a\, F(\omega) \times \sum_{k=-\infty}^{\infty} \delta(\omega-k\Omega) \otimes W(\omega) \otimes \sum_{k=-\infty}^{\infty} \delta(\omega-kL\Omega) \qquad (B.4)$$

Since $F^*(k\Omega)$ can be related to the FFT by the integral

$$F(k\Omega) = \int_{-\infty}^{\infty} F^*(k\Omega)\, d\omega$$

and by comparison of equation (B.4) with (B.3), it is clear that the result of the FFT algorithm is a sampled version of the continuous function, $F(\omega)$,

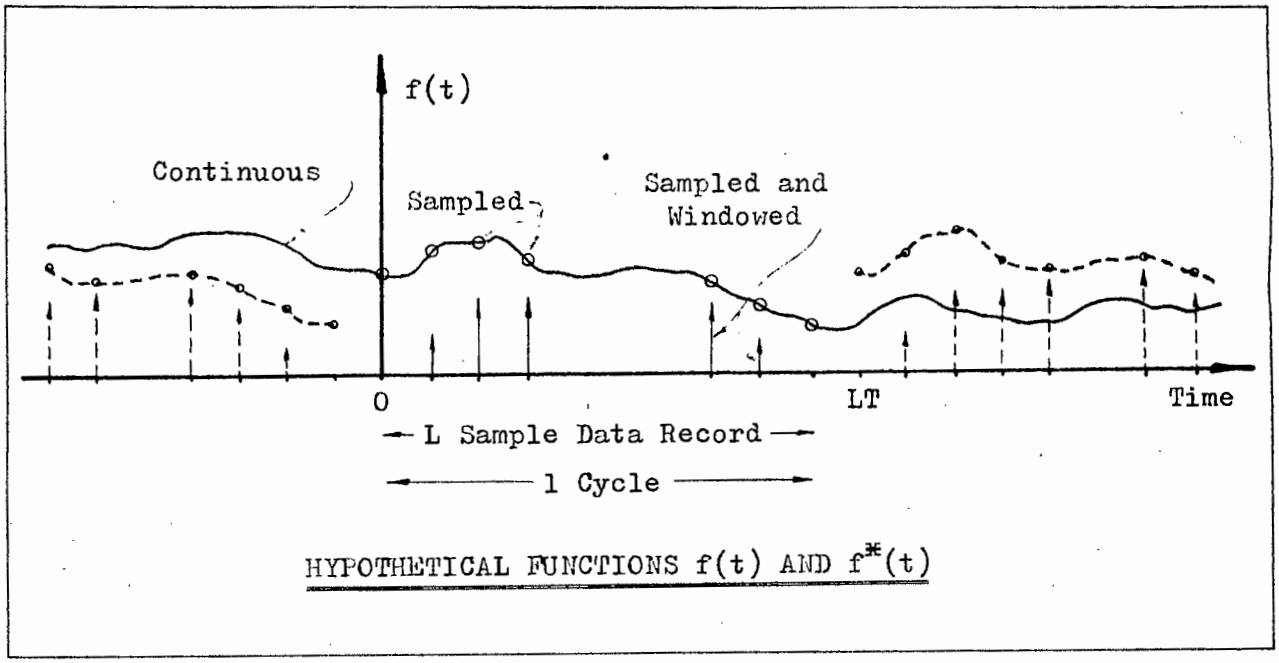

Figure B.3

which is convolved with the CFT of a data window and a dirac comb which produces periodicity in the frequency domain. The latter convolution need not be considered further provided the data is sampled without aliasing - as is assumed here.

Note: (i) The sampling interval, T, determines the periodicity of the FFT.

(ii) The frequency resolution/sampling interval is dependent on the length of data record and is improved with longer arrays.

(iii) The CFT of any data window used will span a minimum of two frequency intervals and it is beneficial to the FFT that it should span more than two since this will reduce ripple in the FFT (the so-called picket fence effect.[19]).

(iv) The frequency components can be emphasized by removal of the DC component of f(t) before transforming.

(v) From a practical point of view, it is beneficial to remove any linear trends in the data as well since these are probably due to drift in the equipment. For an array of sampled data, y(nT), the trend-free data, z(nT), is given by

$$z(kT) = y(kT) - 12 \sum_{n=1}^{N} n\, y(nT)\, (k - \tfrac{N+1}{N}) \,/\, N\,(N^2 - 1)$$

DISCRETE CORRELATION

The discrete CCF - DCCF - of two discrete functions x(nT) and y(nT) of infinite length is defined - analogously with equation (1.1) - by the summation

$$\phi_{xy}(kT) = \lim_{L \to \infty} \frac{1}{2L} \sum_{n=-L}^{L} x(nT)\ y(nT+kT) \qquad (B.5)$$

As with the continuous case, the expression changes for cyclic functions x and y: the limit is dropped and the functions are cyclicly correlated.

Consider two functions x(t) and y(t) which are sampled to produce sampled data records x(nT) and y(mT) of N and M samples respectively and augmented with zeros to form L sample arrays. The cyclic correlation of the augmented functions is then given by

$$^{a}\phi_{xy}(kT) = \frac{1}{L} \sum_{n=0}^{L} x(nT)\ y(\{nT+kT\}) \qquad (B.6)$$

where ({nT+kT}) is T{(n+k)modulo L} thus ensuring periodicity in L samples.

Apart from its use in the fast calculation of the Fourier Transform of signals the FFT is used to give economic and fast computations of the correlation and convolution integrals. The DFT, $^{a}\phi_{xy}(k\Omega)$, of the DCCF, $^{a}\phi_{xy}(nT)$, is given by the following equation - see section 1.1.1

$$^{a}\phi_{xy}(k\Omega) = X_a^*(k\Omega)\ Y_a(k\Omega) \qquad (B.7)$$

where $X_a(k\Omega)$ and $Y_a(k\Omega)$ are the DFT of the augmented versions of x(nT) and y(mT) using an L sample FFT. The relationship between the DCCF of the augmented functions and the true DCCF of the functions which are cyclic in, say, M samples is given by

$$\phi_{xy}(kT) = \frac{L}{M}\ ^{a}\phi_{xy}(kT) \qquad (B.8)$$

since the DFT of an augmented function is given by equation (B.2).

DIGITAL INTERPOLATION OF DISCRETE DATA

For discrete data processing the use of linear interpolation or some other form of interpolation is usually not suitable and introduces spurious frequency components into the signal. The method used for interpolation here is described in detail elsewhere [22] but is outlined below.

The data is first transformed to the frequency domain using the FFT. Then provided there is no aliasing, the transform can be augmented by the addition of zeros about the folding frequency until the desired number of samples is obtained - must be a power of 2 when using FOUR1. Inverse transformation of the resulting DFT then yields the desired interpolated

function. The entire process involved is illustrated by figure (B.4).

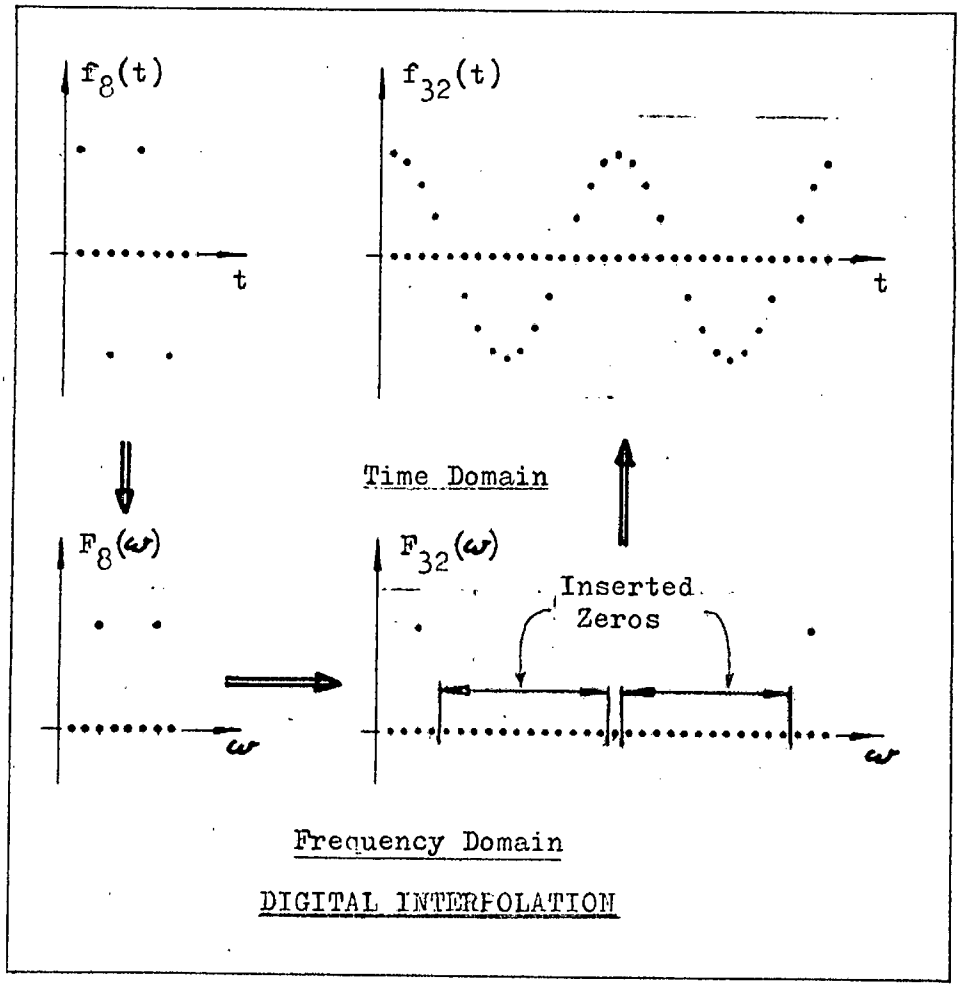

Figure B.4

APPENDIX C THE PROCESS EQUILIBRIUM CURVE

For mathematical modelling of mixer-settler units in series some relationship is required for the ratio of uranium concentration in the two phases leaving a settler to provide a unique solution to the mixer-settler behaviour. It is usual to assume that the phases are in equilibrium when leaving the settler. For the plant considered this assumption is valid.

The equilibrium curve for paraffin, water and uranium oxide can be derived by a dilution technique in the laboratory and also from samples taken on the plant. The difference between the two curves represents a decrease in the uranium maximum loading of the solvent in the plant which is due to the presence of impurities. Curves for the laboratory and pilot plant as well as the operating points of the plant units are shown in figure (C.1) and the differences are clearly seen.

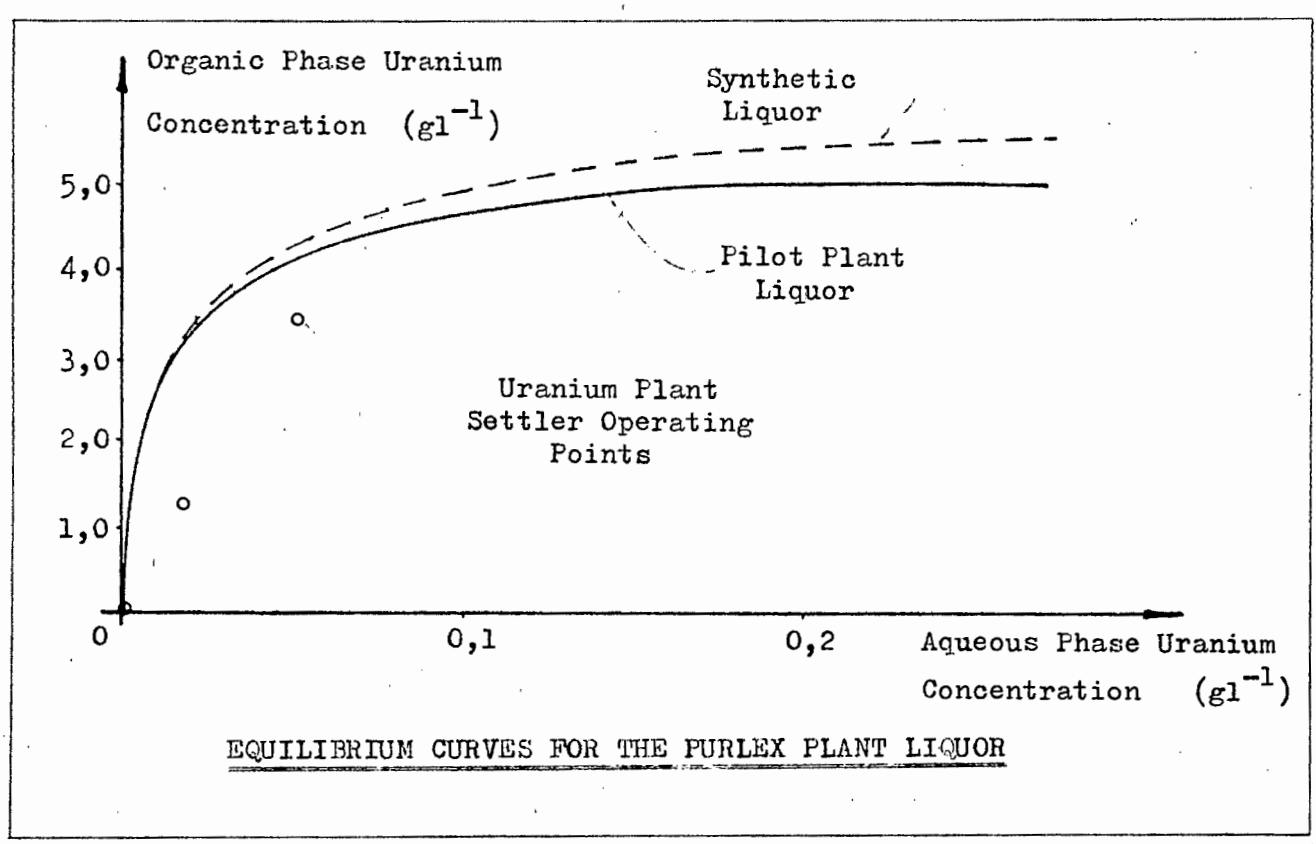

EQUILIBRIUM CURVES FOR THE PURLEX PLANT LIQUOR

Figure C.1

Plant Operating Line at steady State Operation

Steady state modelling of plant behaviour can be done successfully using the equilibrium curve and the plant operating line which will be derived below.

Consider stage 'n' of a three stage system. 'n' = 2, 3, and 4

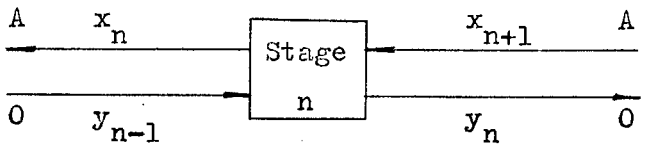

where A and O are the aqueous and organic phase flow rates respectively.

x_n and x_{n+1} are the aqueous phase uranium loadings.

y_{n-1} and y_n are the organic phase urnaium loadings.

Writing mass balance equations for the stage at steady state and re-arranging the following equation is obtained

$$\frac{x_{n+1} - x_n}{y_n - y_{n-1}} = \frac{O}{A} \qquad (C.1)$$

This is the 'operating line' for the stage and is shown in figure (C.2). The transient cross-phase relationship which is the slope, k_n, of the equilibrium curve at the point (x_n, y_n) is also graphed to show the difference between it and the absolute cross-phase relationship, $K_n = y_n/x_n$.

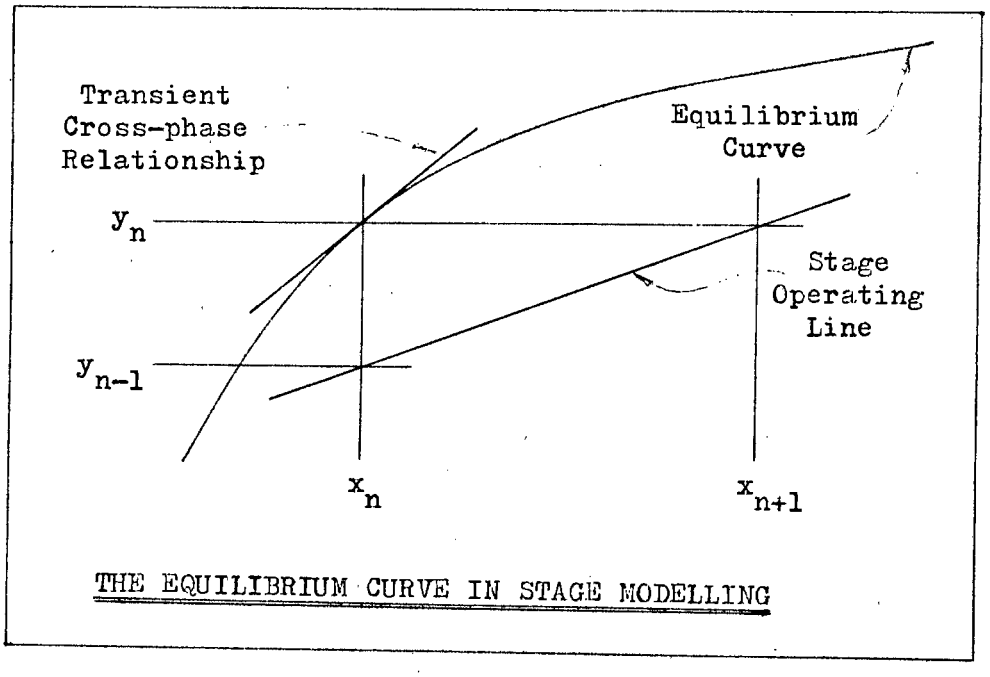

Figure C.2

Equation (C.1) can be generalized to describe a multi-stage plant and the operating line for the plant in which the stage flow rates are independent of the stage number is graphed in figure (C.3). The loadings of all streams are defined by this line whose slope is given by the flow rate ratios and intercept by shifting the line with slope O/A to give the correct feed concentrations.

The model is valid for the steady state conditions only [10] and so can be used to predict the long term conditions which will result from any control

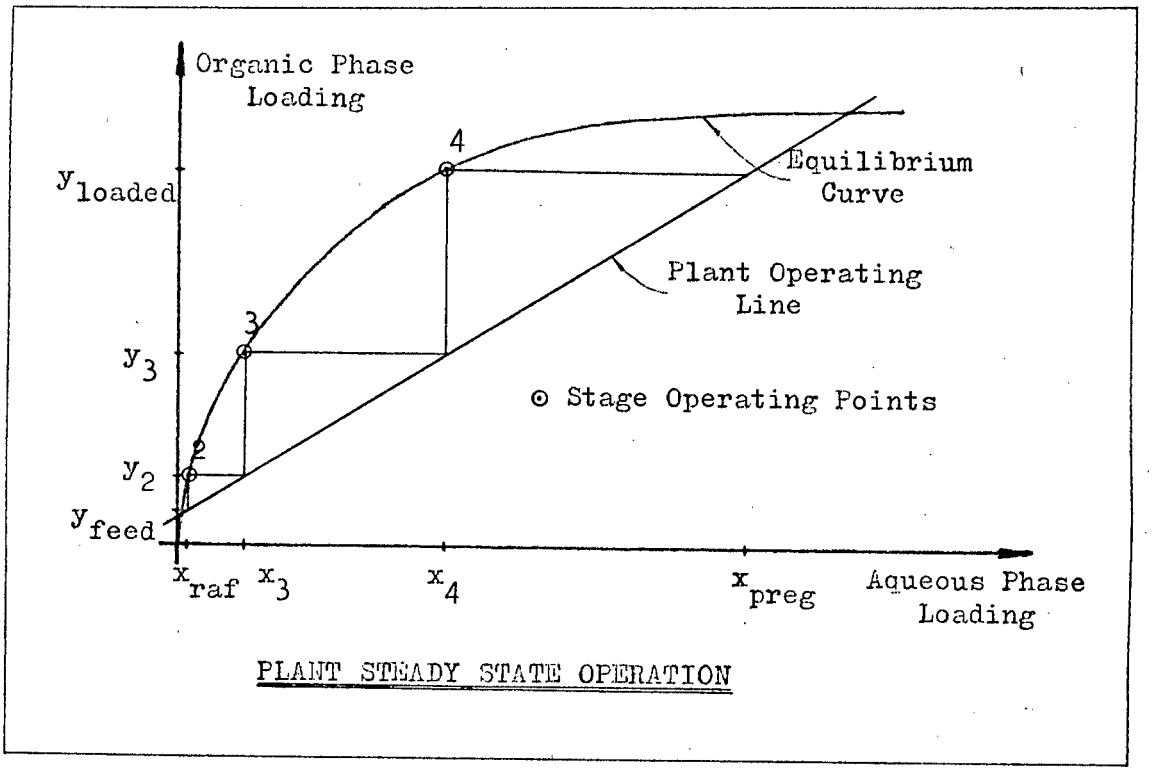

Figure C.3

action. For example a large value for the flow ratio O/A will result in less uranium being extracted by the solvent and represents in-efficient plant operation. On the other hand a small value will result in loss of uranium through the raffinate stream. These effects are illustrated in figure (C.4) below.

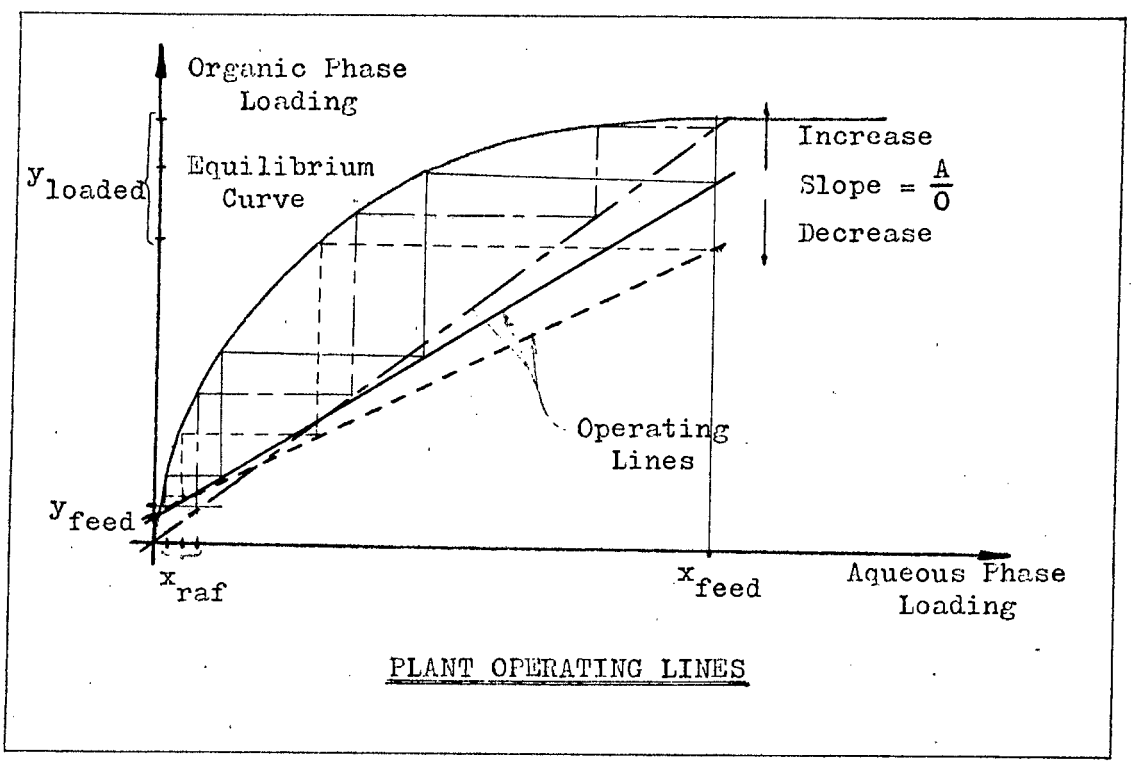

Figure C.4

APPENDIX D PLANT HARDWARE CHARACTERISTICS

The characteristics of all plant hardware were linearized for the purposes of obtaining simple transfer functions for the equipment used in the perturbation experiments. For completeness all the characteristic curves and the linearized versions are given in the following sections. The graphs also serve to give visual indications of the errors likely to be introduced by the linearization.

D.1 EXISTING PLANT EQUIPMENT

(a) EPURAN Calibration Lines

The experimental points and the least squares lines - equation (2.2) - for the EPURAN uranium analysers on settlers 3 and 4 are shown in figure (D.1). Theoretically the points should lie randomly distributed about an exponential absorption curve which has been shown to be linearized with minimal error.[27]

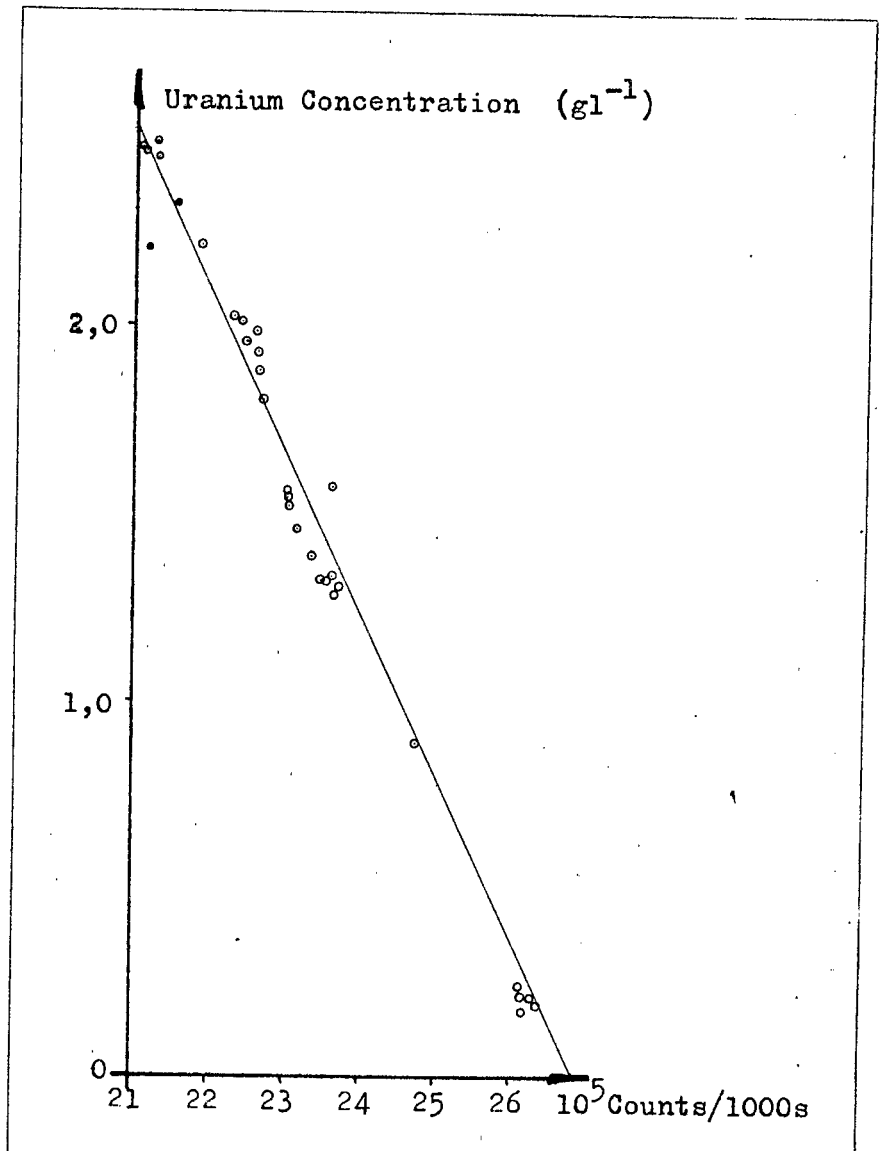

EPURAN 3 CALIBRATION LINE

Figure D.1 (a)

The spread in the sample points can be attributed to the decay rate of the radio-isotope.

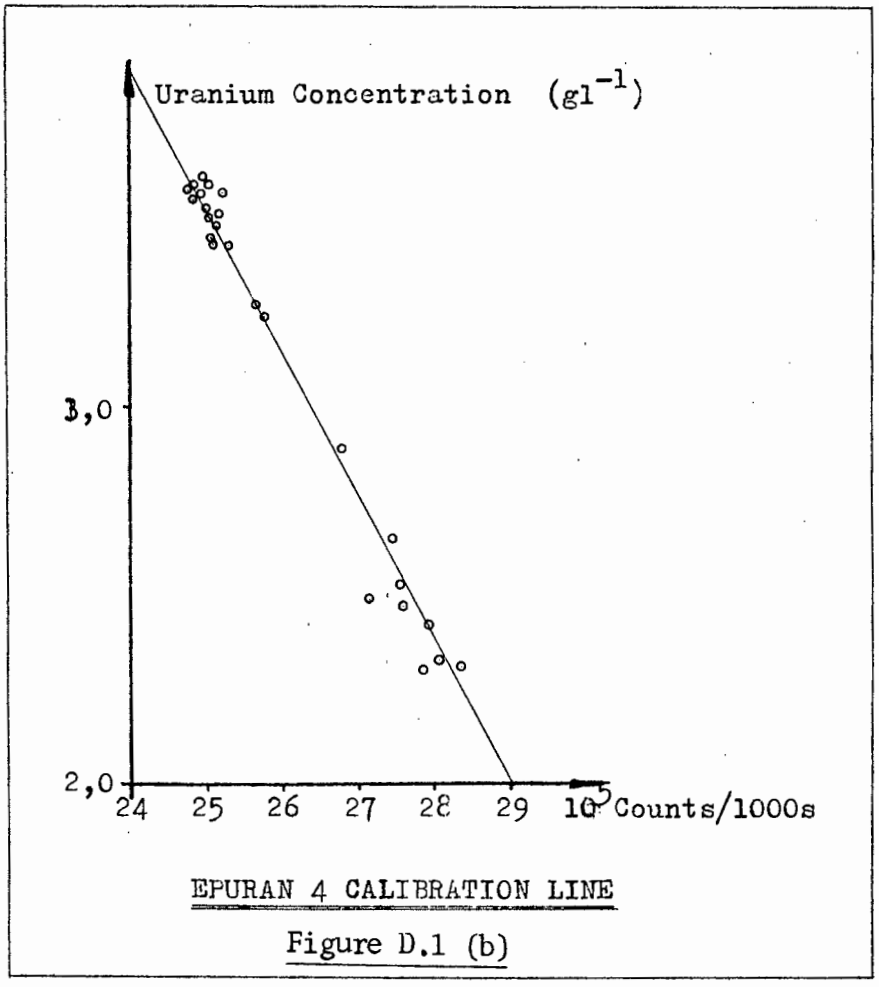

EPURAN 4 CALIBRATION LINE

Figure D.1 (b)

(b) Pregnant Solution Valve Characteristics

Plant steady state operation is at a linear section of the valve transfer

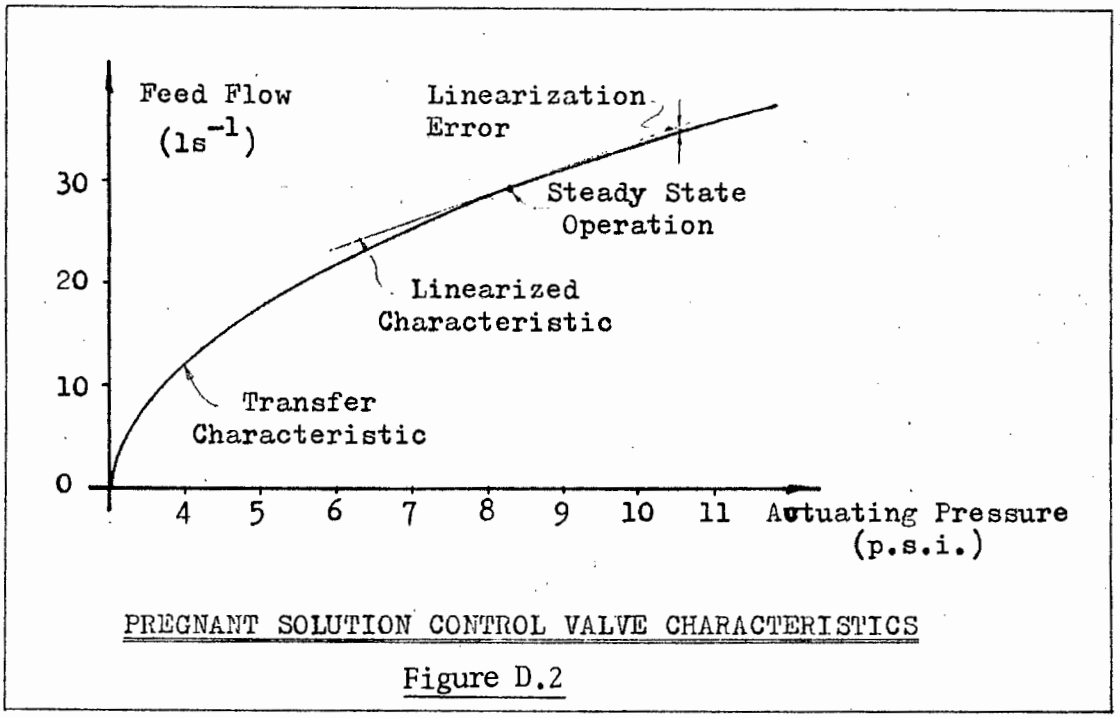

PREGNANT SOLUTION CONTROL VALVE CHARACTERISTICS

Figure D.2

characteristics and the error introduced is minimal. The theoretical transfer function is parabolic as are those for the D.P.Cells used to monitor flow rates.

(c) Pregnant Solution D.P.Cell Characteristic

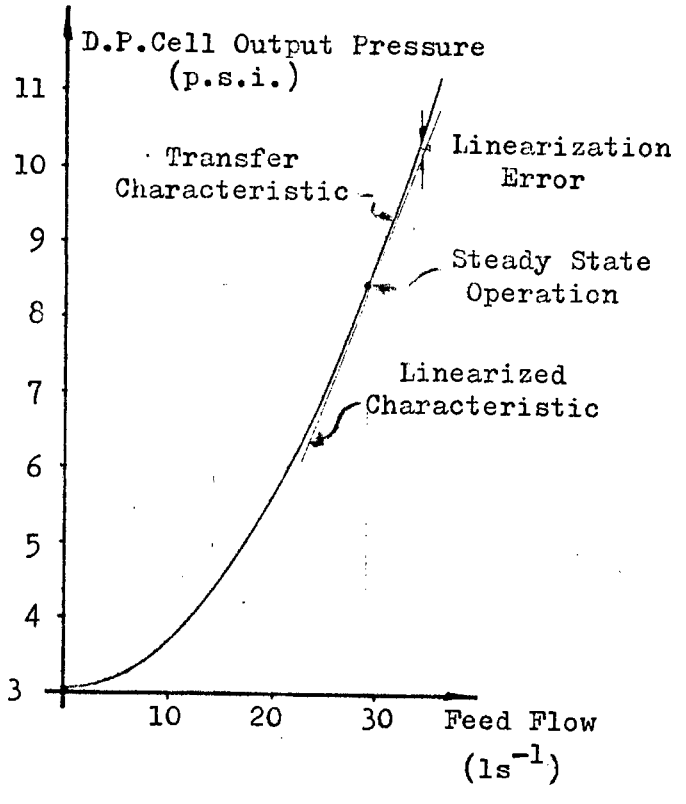

PREGNANT SOLUTION D.P.CELL CHARACTERISTICS

Figure D.3

(d) Loaded Solvent D.P.Cell Characteristics

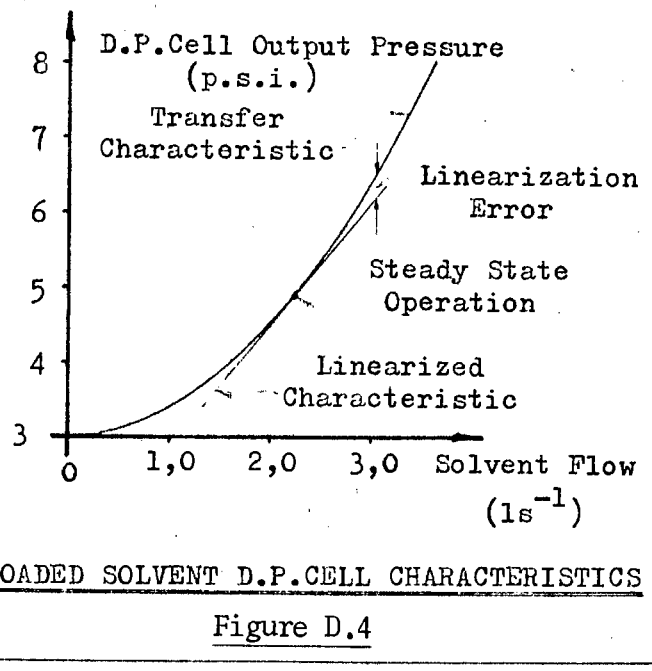

LOADED SOLVENT D.P.CELL CHARACTERISTICS

Figure D.4

D.2 EXPERIMENTAL EQUIPMENT

The experimental points were obtained from off-line tests performed after the installation of the equipment on the plant and the lines are the least squares fits to the data.

(a) Voltage-to-Pressure Transducer

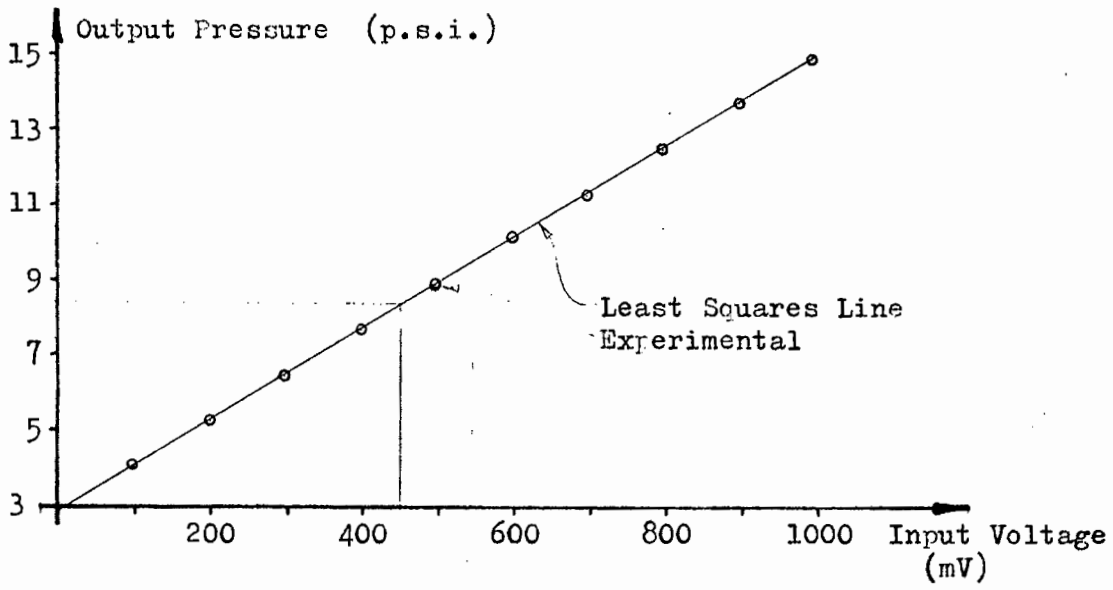

VALVE-ACTUATOR TRANSDUCER CHARACTERISTICS

Figure D.5

(b) Pressure-to-Voltage Transducers

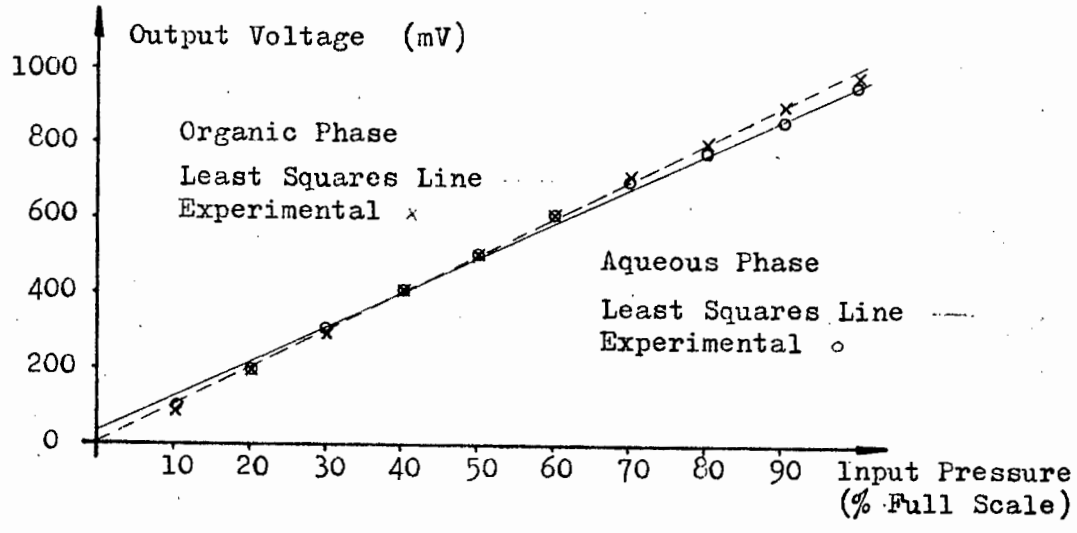

FLOW RATE MONITORING TRANSDUCER CHARACTERISTICS

Figure D.6